SYNTHESIS AND CHARACTERIZATION OF POLYAMPHOLYTE MICROGELS

By

KENNETH WAYNE HAMPTON JR.

Bachelor of Science

Northeastern State University

Tahlequah, Oklahoma

1993

Submitted to the Faculty of the
Graduate College of the
Oklahoma State University
in partial fulfillment of
the requirements for
the Degree of
DOCTOR OF PHILOSOPHY
July, 1999

SYNTHESIS AND CHARACTERIZATION

OF POLYAMPHOLYTE MICROGELS

Thesis approved:

Warren T Ford

Thesis Advisor

Roger Tang

Vinod D Ras

K D Berlin

Wayne B. Powell

Dean of the Graduate College

PREFACE

The principal objective of this project was to synthesize novel polyampholyte latexes, which are stable in high salt concentrations. Latexes are submicroscopic organic particles suspended in an aqueous phase (paints), and polyampholytes are polymers that contain positive (+) and negative (-) charges on the same polymer chain. Latexes are synthesized using different functional monomers. A monomer is the simplest unit used to form polymers. Initially, sulfonate monomers were used to synthesize polyampholyte latexes, but the solubility and reactivity of the sulfonate monomers resulted in poor latexes (the latexes precipitated from solution). Therefore, a carboxylate monomer was successfully employed to form polyampholyte latexes that contained 60/40 and 50/50 positive and negative charges. The latexes are stable in water at high salt concentrations (4 M sodium chloride and 1.2 M barium chloride). The size measurements showed polyampholyte latexes swelled with increasing salt content. Since, the polyampholyte latexes are stable in high salt concentrations, they can be used in any application involving seawater.

ACKNOWLEDGMENTS

I would like to offer my sincere gratitude to my research advisor, Dr. Warren T. Ford for giving me the opportunity to benefit from his guidance. Thank you, for your patience and endless knowledge of polymer/organic chemistry. My tenure at OSU has had many ups and downs, but Dr. Ford was always a constant throughout. I would also like to thank my graduate committee namely Dr. Darrell Berlin, Dr. Ziad ElRassi, Dr. Andrew Mort, and Dr. Penger Tong, several of whom I have extracted valuable knowledge. In addition, I would like to thank Dr. Penger Tong for use of the DLS and Dr. Alan Apblett for use of the DRIFTS instrument. Without their generousity, my project would be incomplete. I would also like to thank the ones that served with me for their friendship and keeping an eye out for the mockingbird: Jag, Amanda, Roy, Paul, Jason, Spence, Ed, Alanta, Yijun and all the undergraduates and post docs that have passed through the group during my stint at OSU.

Finally, I would like to acknowledge those that provided financial support; the Chemistry Department, Dr. Ford and U.S. Army Research Office.

I wish to thank my family, many of whom have had a profound influence on my life. They include Jessica, Stacey, Serena, Brock, the in-laws, Jo, Darrell, Darrin and Dustin. Our frequent visits has supplied me with a great getaway from the science grind; this means more to me than you know. Special thanks goes to my parents, Jana and Dale Wood, who always let me know that I could accomplish anything and did everything in

their power to see that I had that opportunity. My dad's, great friendship was vital to my success. My mom's ability to overcome gave me the strength to battle through all obstacles. You both deserve as much credit for this degree as I do. I am known as a family man, and that comes from growing up in a supportive family environment. Thank you Nana, Dad, Mama Ceal, Grandma Josie, and Papaw.

I would like to take this opportunity to express in writing the deep debt I owe my wife Kristy. She has endured the hardships of graduate school without ever attending one class. Her support, understanding, assurance, stability and love has enable me to accomplish everything I have to date. I owe you big time (farm?).

Finally, I would like to dedicate this thesis to the two lights of my life, Faith Dalynn and Augusta Helene, my girls. They are my inspiration to succeed, my escape from a terrible day, and my reason to get out of bed. Thank you both for the extreme joy you have brought into my life. Our family comes from a long line of great accomplishments and my greatest accomplishment will be to do everything in my power to see that my girls will have the opportunity to accomplish their dreams as I have.

"You have to lose something to gain something,
but smile you need something to go in your
memoirs."

-KWH

TABLE OF CONTENTS

LIST OF TABLES

Chapter II

Chapter III

Chapter IV

LIST OF FIGURES

Chapter I

Chapter II

Chapter III

Chapter IV

LIST OF SCHEMES

Chapter I

Chapter II

Chapter III

Chapter IV

APPENDIX

Figure Page

Table

CHAPTER I

INTRODUCTION

Microgels

Definition of Microgel. A microgel particle is a cross-linked latex particle that is swollen by a good solvent. Figure 1 shows a microgel particle swollen in a good solvent (A) and collapsed in a poor solvent (B).[1] The microgels are cross-linked linear polymer chains having a narrow range of particle sizes without a discrete core, which can be visualized as flawlessly spherical sponges.

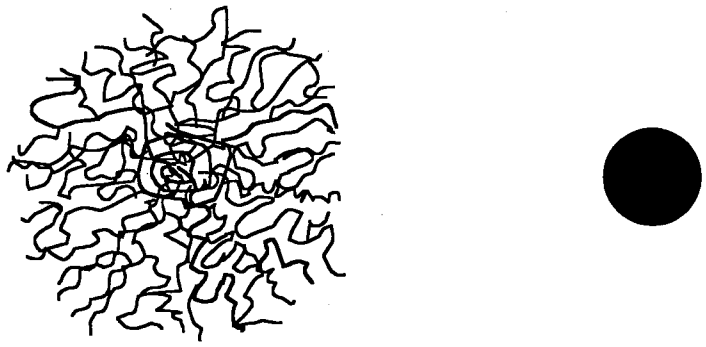

(A) (B)

Figure 1. Microgel particle in a good (A) and poor (B) solvent.

Microgel Synthesis. Microgels are conveniently prepared by emulsion polymerization. Emulsion polymerization is a versatile technique, which yields narrow particle size distributions. Emulsion polymerization can be conducted in the presence of added surfactant (conventional emulsion polymerization) or in the absence of added surfactant (surfactant-free emulsion polymerization). Both polymerizations enable preparation of very small microgel particles (particle diameters less than 150 nm); however, the conventional technique has a problem with the complete removal of residual surfactant.

A typical synthesis of a cross-linked quaternized microgel, via surfactant-free emulsion polymerization, is depicted in Scheme 1. Initially, the polymerization is a heterogeneous mixture of monomers, water, and charged monomer (surfactant) with monomers forming a discrete phase as monomer droplets. A water-soluble initiator is used to begin polymerization followed by aqueous phase propagation of charged monomer. Particle nucleation occurs via either micellar (conventional) and/or homogeneous (surfactant-free) mechanisms. Further propagation occurs inside polymer particles via monomer diffusion from monomer droplets resulting in particle growth. Polymerization is complete when all monomer is converted to polymer. The resulting particles are submicron, dispersed in an aqueous phase, and stabilized by converted charged monomer (polymeric surfactant). There are three excellent recent books devoted to better understanding the emulsion polymerization technique.[2,3,4]

Scheme 1. Synthesis of Cross-linked Quaternized Microgels.

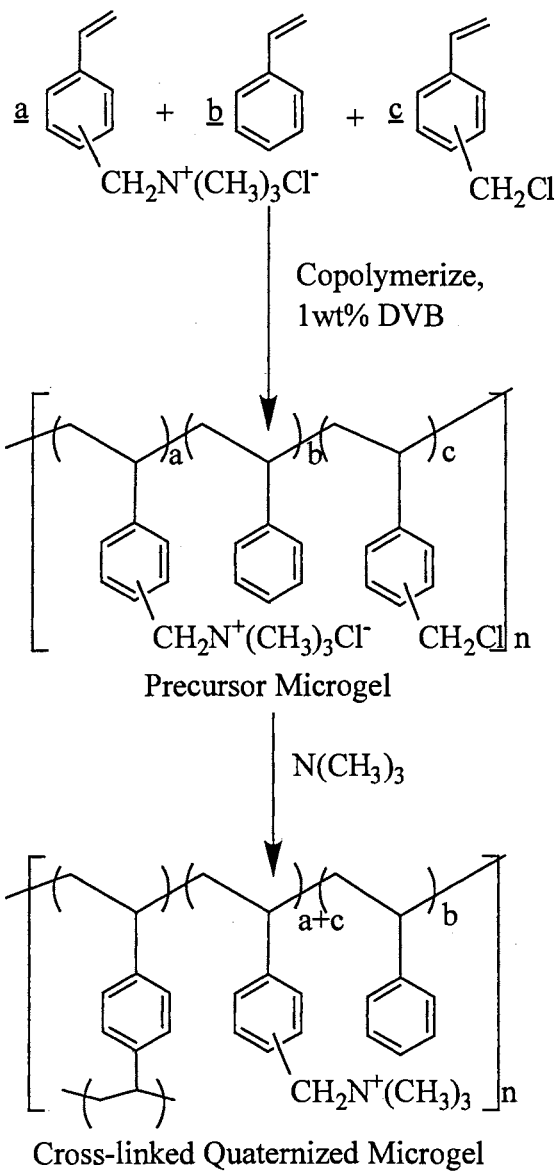

Applications Involving Microgels. High volume applications of copolymer latexes include synthetic rubber, paints, adhesives, paper coatings, carpet backing, and toughened plastics.[5] Other applications involve microgel particles used as surface coatings, and water soluble polymers prepared via inverse emulsion polymerization have found uses in waste water treatment and enhanced oil recovery. Microgels that have a stable, well-defined volume (monodisperse) find applications in opacifying agents, model colloids, calibration standards and pharmaceutical applications.[5]

Microgels are used as colloidal catalysis in our lab. Colloidal catalysis combines two general terms: catalyst and phase transfer catalysis (PTC). A catalyst increases the rate of a reaction without being consumed or appearing in the products and normally is used in small amounts.[6] PTC is a technique where substances located in different phases are brought together to react faster.[7] Colloidal catalysis can consist of micelles, bilayer membranes, or latexes. Colloidal particles provide high surface area and can be prepared with a variety of sizes and functional group compositions. These particles provide a small volume fraction of an aqueous mixture where the rate of a reaction can be much faster than in water. The reactive species are counter ions of the particles and an organic compound that is more soluble in the particle than in the water. Reactions in these heterogeneous systems have produced greater rates (10^3-10^4 accelerated) than in water alone. Latexes used in our lab can be termed anionic phase transfer catalysts because the cationic (quaternary ammonium groups) latex provides a water swollen polymer phase that the substrate prefers, and the counterions (HO^-) of the latex are the reactant. Hence, both reactants are concentrated which leads to rate enhancement. Polymer latexes have

been used as catalyst for hydrolysis of carboxylic and phosphoric esters and decarboxylations.[8]

Stabilities of Microgels. Charged-stabilized latexes maintain a charge balance on the latex surface with small ions of opposite sign in the solution phase (counter-ion cloud). This forms the electrical double layer in which the latex particle surface has an electrostatic potential that can be either positive or negative depending on surface groups (Figure 2, A). In the event that charge no longer provides a practical means of stabilization, a 'hairy particle' can be employed. A typical example is the use of poly(ethylene glycol) chains to stabilize particles.[9] This leads to noncharged 'hairs' extending into the solvent giving a sterically stabilized system (Figure 2, B).

The latex particles formed from emulsion polymerization are likely not as smooth as those in Figure 2 (A). Furthermore, in practice one should view the microgel particles as the combination of charged groups and 'microhairs'. From this qualitative description of a microgel particle, the effects of microgel stabilization can be broken down into: (1) *electrostatic effects*, caused by repulsive interactions between charges of the same sign, (2) *steric effects*, arising from the unfavorable entropy of mixing of chains from the surfaces of more than one particle, (3) *solvating effects*, arising from organization of solvent molecules near an interface or between polymer chains, and (4) *attractive effects*, or van-der Waals interactions.[10]

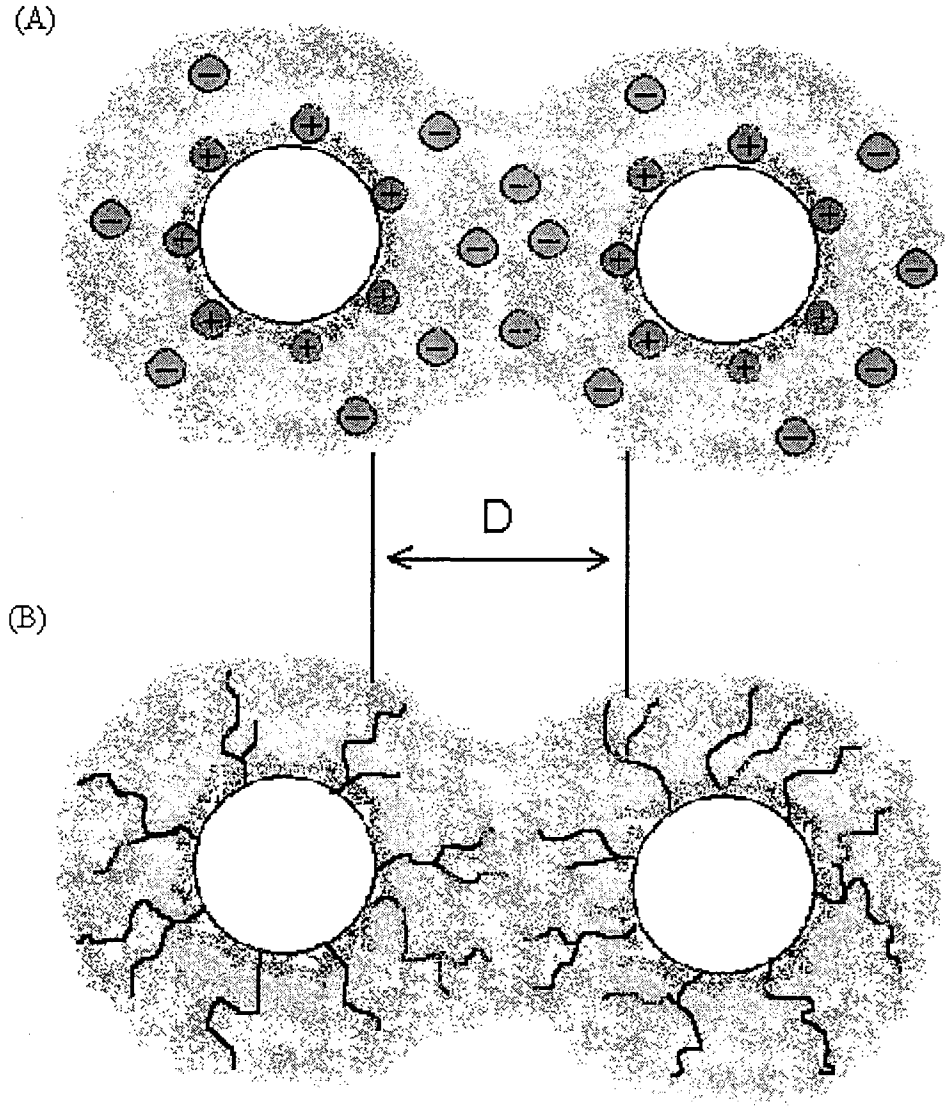

Figure 2. Stability of microgel particles (A) charge stabilized and (B) steric stabilized.

When charged-stabilized latexes are in dispersions of high electrolyte concentrations, the electrical double layer is disturbed due to shielding of surface groups. The electrostatic repulsions are shielded causing the distance (D, Figure 2) between particles to decrease. Concurrently, the increase in electrolyte concentration in the medium causes an osmotic effect resulting in reduction of solvent (water) in the counter-ion cloud. The polymer chains contract due to loss of water. This also results in decreasing the distance (D) between microgel particles. The deswelling of the microgel particles in salt solutions results in van-der Waals attractions causing aggregates. Once the aggregates reach a certain weight, they precipitate.

Statement of Problem

Previously in this lab, monodisperse charged latexes containing quaternary ammonium ions (N^+) were synthesized[11] and used as catalyst supports in aqueous solutions.[12] In those studies, one of the main factors influencing rates of reaction was electrolyte or salt content in the reaction. The microgel's effectiveness as a catalyst is reduced by increased salt concentrations. The rates of reactions could not be measured by UV-vis spectra at concentrations of NaCl higher than 0.1 M. The problem was two-fold (1) the anion of the salt competes with substrate for cationic sites (ion exchange), and (2) the microgel aggregates due to shielding of electrostatic replusions (unstable). In order to study rates of reactions in high salt concentrations, a microgel that is stable in greater than 1 M NaCl is needed.

Polyampholytes

Definition of Polyampholyte. A polyampholyte is a polymer that contains positively and negatively charged repeat units randomly dispersed within the same linear chain. This polymer may be either neutral, having the same number of negative as positive monomers, or have a net charge of one sign. If the net charge is large, the polymer will behave as conventional polyelectrolytes. However, a polymer with close to neutral charge will demonstrate an anti-polyelectrolyte behavior. Polyampholytes expand and remain stable in salt solutions (Figure 3).[13] This is a unique property that could find many useful applications for polymers in high electrolyte solutions, considering the majority of the earth's surface is seawater.

Polyampholytes have been synthesized by polymerization of water-soluble monomers forming statistical and block polyampholytes, zwitterionic, hydrogels and inverse microemulsions. Besides possessing unique molecular composition, polyampholytes exhibit interesting solution properties. In pure water most polyampholytes, having from about 40/60 to 60/40 N^+/SO_3^- (ammonium/sulfonate) functional groups, are insoluble due to intrapolymer electrostatic attractions.[13] Moreover, copolymers exhibit increased solubility, and the solution has enhanced viscosity upon adding salt due to expansion of the polymer coil.[13] In other words, negative and positive charges attract each other and form a tight coil and possibly form aggregates in aqueous solution leading to low solubility. However, when an electrolyte is introduced into the polyampholyte, its anion and cation act as counter ions to the polymer. The anionic and

cationic groups of the polymer are now separated and are no longer held together by the strong intrapolymer electrostatic interactions. Therefore, a solution of copolymer has increased viscosity in salt solutions due to expansion of the polymer coil conformation (Figure 3).

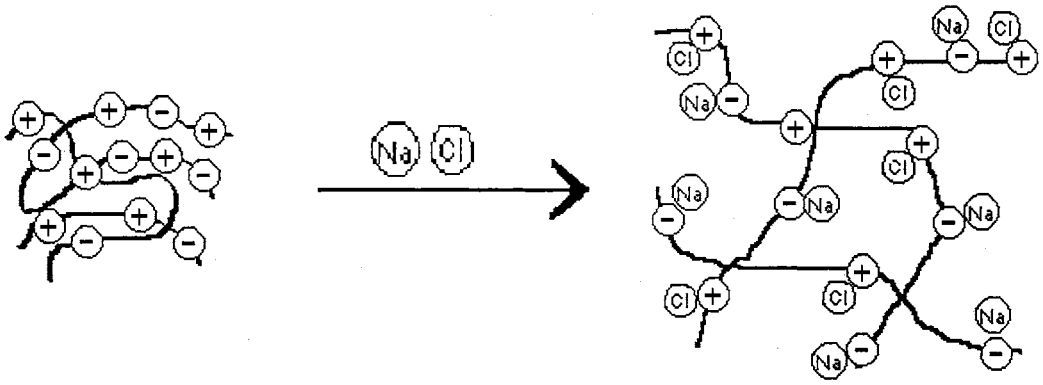

Figure 3. Solution behavior of a water-soluble polyampholyte.

Scheme 2. Statistical Polyampholytes Containing (A) Carboxylate Ions and (B) Sulfonate Ions.

(A)

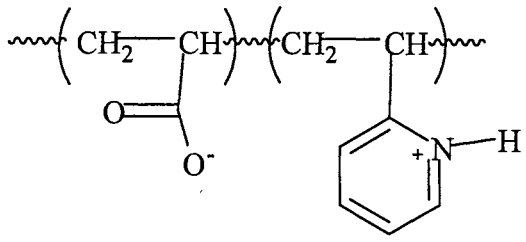

(B)

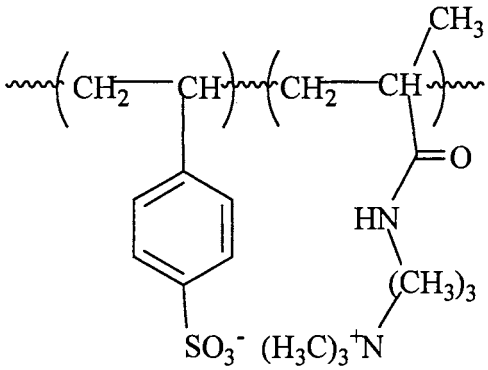

Statistical Polyampholytes. The first synthetic polyampholytes were produced by radical polymerization of methacrylic acid (MAA) and 2-vinylpyridine (2VP) (Scheme 2, A).[14-15] This statistical linear copolymer showed very different solution properties when compared to the corresponding homopolyelectroytes: poly(MAA) and poly(2VP). The copolymer was insoluble in water in the range $3.8 < pH < 6.8$ but became soluble outside this range. A study of viscosities of the copolymer showed a minimum at the isoelectric point (i.e.p.) which is defined as the pH of zero charge. Several other investigations with MAA followed with cationic repeat units *N,N*-diethylaminoethyl methacrylate[16] and 2-dimethylaminoethyl methacrylate.[17-18]

Spontaneous free radical copolymerization of polymerizable sodium styrenesulfonate (NaSS) and 2-dimethylaminoethyl methacrylate was also investigated (Scheme 2, B).[19-20] The polyampholyte proved insoluble in water at any pH value due to the low pK_a of the sulfonate moiety. Addition of a neutral salt solubilized the ampholyte at all pH values. These early investigations on the statistical carboxylate and sulfonate quaternary ammonium polyampholytes describe the general solution behavior that has enticed researchers.

Block Polyampholytes. In contrast to conventional free-radical copolymerization, polyampholytes with block copolymer architectures can be synthesized under living polymerization conditions (anionic, cationic, or group transfer polymerizations). Initial investigations using sequential addition of protected monomers via anionic or cationic polymerization conditions resulted in broad molecular weight distributions and similar solution properties similar to those of statistical polyampholytes.[21-23] However, using group transfer polymerization of 2-(dimethylamino)ethyl methacrylate (DMAEMA) and an anionic precursor [2-tetrahydropyranyl methacrylate (THPMA) or *tert*-butyl methacrylate (tBMA)] control of molecular weight and copolymer composition was achieved.[24-26] Precursor blocks were quantitatively deprotected via hydrolysis. The i.e.p.'s of the DMAEMA-MAA were determined by pH/precipitation titrations. Furthermore, the block copolymers formed micelles in alkaline solutions at elevated temperatures with the cationic block in the core and the MAA block forming a solvated corona (Figure 4). The temperature-induced

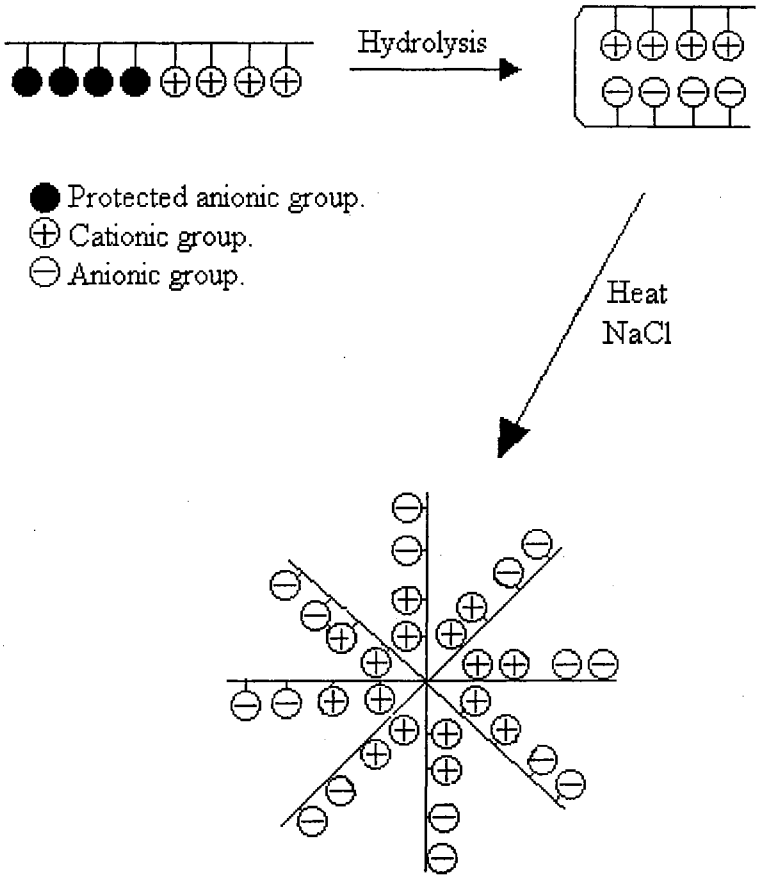

Figure 4. Micellization of block polyampholytes.

micellization is fully reversible. The presence of NaCl produced smaller, more well defined micelles.[24]

Zwitterions. Zwitterions are homopolymers that contain opposite charges on the same monomer unit (Scheme 3). A homopolymer prepared by free-radical polymerization of 1-vinyl-3-(3-sulphopropyl)imidazolium hydroxide was the first reported sulfobetaine polyampholyte to have increased viscosity with increasing salt concentrations an "anti-polyelectrolyte" behavior (Scheme 3, A).[27] A series of investigations with polysulfobetaines followed that corroborated the initial observation of polymer expansion with increasing salt concentrations.[28-31] Another class of zwitterionic polymers are carboxybetaines, in which the anionic group is a carboxylate functionality (Scheme 3, B).[32-34] At low pH values, the carboxylate moiety can be protonated, allowing behavior as polycations or polyampholytes depending on the pH of the aqueous medium. These homopolymers have similar polyampholyte behavior at high pH values as the sulfobetaines.[27-31]

Scheme 3. Zwitterionic Polymers.

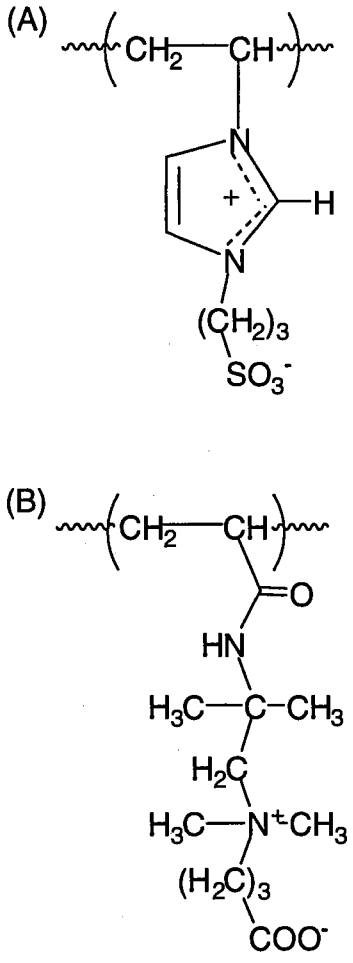

Polyampholyte Hydrogels. Hydrogels are H-bonded ampholytes that swell and deswell on salt and pH changes. Vinyl polymers having hydroxyl groups such as poly (vinylalcohol) (PVA) are easily cross-linked to form gels in aqueous solutions. Accordingly, an acrylamide-based polyampholyte gel with 10% sulfonic and quaternary ammonium groups, respectively, swells by 40% with increasing NaCl concentration from 10^{-2} to 1.0 M. This swelling is in contrast to the deswelling observed for common polyion gels in high salt concentrations.[35] Polyampholytic hydrogels swell, shrink, or

bend when a DC electric field is applied.[36] A polyampholyte gel, having weakly acidic groups depending on the pH, acts either as a cation or anionic gel. Near the cathode and anode the concentration of anions (cathode) and cations (anode) are increased. This causes disturbances in osmotic pressure due to swelling at the cathode and shrinking at the anode or the reverse. These materials are currently being investigated in order to construct an "intelligent" device.[36]

Inverse Microemulsions. Distribution of charges along a chain strongly depends on the chemical synthetic method. Copolymerization of water-soluble monomers, sodium 2-acrylamido-2-methylpropanesulphonate (NaAMPS) and 2-(methacryloyloxy)-ethyltrimethylammonium chloride (MADQUAT) or similar cationic monomers (Scheme 4) have been investigated in homogeneous aqueous solution. These NaAMPS-MADQUAT copolymerization lead to alternating polyampholytes,[37-40] whereas copolymerizations in inverse microemulsions produce random polyampholytes.[41-43] Random copolymers are more homogeneous in composition than those prepared in solution. In these experimental studies it was revealed that the distribution of the charges influenced the polyampholyte properties. The alternating polyampholytes (solution polymerization) are usually soluble over the entire range of pH even at the i.e.p. In contrast, random polyampholytes (inverse microemulsions) are insoluble at the i.e.p. and in pure water. A recent theoretical study explains these results.[44] The inverse microemulsion copolymerization of NaAMPS and MADQUAT using a cross-linking monomer *N,N*-methylenebisacrylamide (BA) resulted in a series of colloidal microgels.

These microgels were not monodisperse and were only stable between 0.4 and 1.0 M $MgCl_2$.[45]

Objective of the Research

The objective of this research was to synthesize a new class of latexes: polyampholytes. The synthesis of covalently cross-linked polyampholytes proceeds through an emulsion copolymerization of vinylbenzyl chloride (VBC), an anionic precursor monomer, divinylbenzene, and styrene to produce a precursor latex. Reaction of the precursor latex with trimethylamine (TMA) and deprotection of the anionic monomer produces a polyampholyte latex containing quaternary ammonium ions (N^+) and sulfonate (SO_3^-) or carboxylate (COO^-) ions. Compositions of polyampholyte latexes are controlled by the amounts of functional monomers used in the copolymerization. Figure 5 depicts what is expected to occur when an aqueous dispersion of a cross-linked polyampholyte latex is introduced to a salt solution. Particles should swell in salt solutions due to screening of intrapolymer electrostatic interactions. Ongoing studies in our lab to produce a cross-linked polyampholyte latex will not only advance the fundamental science of colloids but should provide a latex that is stable in high salt dispersions and will find many uses.

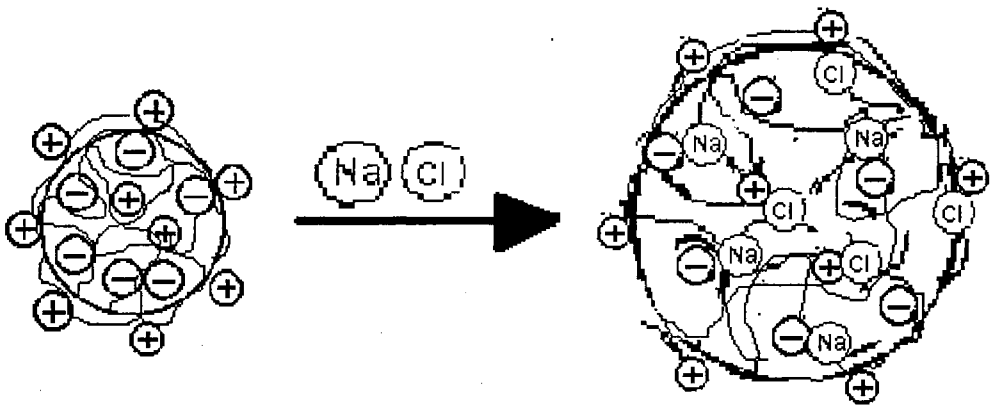

Figure 5. Expected behavior of a polyampholyte microgel.

References

1. Saunders, B. R.; Vincent, B. *Adv. Colloid Interface Sci.* **1999**, *80*, 1-25.

2. Gilbert, R. G. *Emulsion Polymerization*; Ottewill, R. H.; Rowell, R. L., Eds. Academic Press: London, 1995, pp 1-73.

3. Fitch, R. M. *Polymer Colloids: A Comprehensive Introduction*; Ottewill, R. H.; Rowell, R. L., Eds. Academic Press: San Diego, 1997, pp 6-46.

4. El-Aasser, M. S.; Sudol, E.D. *Emulsion Polymerization and Emulsion Polymers*; Lovell, P. A.; El-Aasser, M. S., Eds. Wiley: New York, 1997, pp 38-55.

5. Sudol, E. O.; Daniels, E. S.; El-Aasser, M. S. *Polymer Latexes: Preparation, Characterization, and Applications;* ACS Symposium Series 492: Washington D.C., 1992, pp 1-11.

6. Dehmlow, E. V. *Concise Encyclopedia of Chemical Technology*; Kirk-Othmer, Eds. Wiley: New York, 1985, pp 224-225.

7. Tomoi, M.; Ford, W. T. *Syntheses and Separations using Functional Polymers*; Sherrington, D. C.; Hodge, P., Eds. Wiley: New York, 1988, pp 181-207.

8. Ford, W. T. *React. Funct. Polymers* **1997**, *33*, 147-158.

9. Ottewill, R. H.; Satgurunathan, R. *Colloid Polym. Sci.* **1987**, *265*, 845-853.

10. Ottewill, R. H. *Emulsion Polymerization* Piirma, I., Ed. Academic Press: New York, 1982, pp 1-47.

11. Ford, W. T.; Yu, H.; Lee, J. J.; El-Hamshary, H. *Langmuir* **1993**, *9*, 1698.

12. Ford, W. T.; Lee, J. J. *J. Org. Chem.* **1993**, *58*, 4070.

13. Bekturov, E. A.; Kudaibergenov, S. E.; Rafikov, S. R. *Rev. Macromol. Chem. Phys.* **1990**, *30*, 233-303.

14. Lorawetz, H. M.; Fitzgerald, E. B.; Fuoss, R. M. *J. Am. Chem. Soc.* **1950**, *72*, 1864.

15. Alfrey, T., Jr.; Morawetz, H. M. *J. Am. Chem. Soc.* **1952**, *74*, 436-438.

16. Alfrey, T., Jr.; Fuoss, R. M.; Morawetz, H. M.; Pinner, H. *J. Am. Chem. Soc.* **1952**, *74*, 438-441.

17. Ehrich, G.; Doty, P. *J. Am. Chem. Soc.* **1954**, *76*, 3746-3777.

18. Merle, Y.; Merle, L. *Macromolecules* **1982**, *15*, 360-366.

19. Salamone, J. C.; Tsai, C. C.; Watterson, A. C. *J. Macromol. Sci.-Chem.* **1979**, *A13*, 665.

20. Peiffer, D. G.; Lundberg, R. D. *Polymer* **1985**, *26*, 1058-1068.

21. Varoqui, R.; Tran, Q.; Pefferkorn, E. *Macromolecules* **1979**, *12*, 831-835.

22. Bekturov, E. A.; Frolova, V. A.; Kudaibergenov, S. E.; Schulz, R. C.; Zoller, J. *Makromol. Chem.* **1990**, *191*, 457-463.

23. Bekturov, E. A.; Frolova, V. A.; Kudaibergenov, S. E.; Khamzamulina, R. E.; Nurgalieva, D. E.; Schulz, R. C.; Zoller, J. *Makromol. Chem., Rapid Commun.* **1992**, *13*, 225-229.

24. Patrickios, C. S.; Hertler, W. R.; Abbott, N. L.; Hatton, T. A. *Macromolecules* **1994**, *27*, 930-937.

25. Lowe, A. B.; Billingham, N. C.; Armes, S. P. *Chem. Commun.* **1997**, 1035-1036.

26. Lowe, A. B.; Billingham, N. C.; Armes, S. P. *Macromolecules* **1998**, *31*, 5991-5998.

27. Salamone, J. C.; Volksen, W.; Olson, A. P.; Israel, S. C. *Polymer* **1978**, *19*, 1157-1162.

28. Monroy Soto, V. M.; Galin, J. C. *Polymer* **1984**, *25*, 121-128.

29. Schulz, D. N.; Peiffer, D. G.; Agarwal, P. K.; Larabee, J.; Kaladas, J. J.; Soni, L.; Handwerker, B.; Garner, R. T. *Polymer* **1986**, *27*, 1734-1742.

30. Lee, W.; Hwong, G. *J. Appl. Polymer Sci.* **1996**, *59*, 599-608.

31. Lowe, A. B.; Billingham, N. C.; Armes, S. P. *Chem. Commun.* **1996**, 1555-1556.

32. Kathmann, E. E.; White, L. A.; McCormick, C. L. *Polymer* **1997**, *38*, 871-878.

33. Kathmann, E. E.; White, L. A.; McCormick, C. L. *Polymer* **1997**, *38*, 879-886.

34. Kathmann, E. E.; McCormick, C. L. *J. Polym. Sci., Part A: Polym. Chem.* **1997**, *35*, 231-242.

35. Okazaki, Y.; Ishizuki, K.; Kawauchi, S.; Satoh, M.; Komiyama, J. *Macromolecules* **1996**, *29*, 8391-8397.

36. Kudaibergenov, S. E. *Ber. Bunsenges. Phys. Chem.* **1996**, *100*, 1079-1082.

37. McCormick, C. L.; Johnson, C. B. *Macromolecules* **1988**, *21*, 686-693.

38. McCormick, C. L.; Johnson, C. B. *Polymer* **1990**, *31*, 1100-1107.

39. McCormick, C. L.; Salazar, L. C. *Macromolecules* **1992**, *25*, 1896-1900.

40. McCormick, C. L.; Salazar, L. C. *Polymer* **1992**, *33*, 4617-4624.

41. Corpart, J.; Selb, J.; Candau, F. *Polymer* **1993**, *34*, 3873-3886.

42. Corpart, J.; Candau, F. *Macromolecules* **1993**, *26*, 1333-1343.

43. Skouri, M.; Munch, J. P.; Candau, S. J.; Neyret, S.; Candau, F. *Macromolecules* **1994**, *27*, 69-76.

44. Higgs, P. G.; Joanny, J. F. *J. Chem. Phys.* **1991**, *94*, 1543-1554.

45. Neyret, S.; Vincent, B. *Polymer* **1997**, *38*, 6129-6134.

CHAPTER II

SYNTHESIS AND CHARACTERIZATION OF SULFONATE CONTAINING CROSS-LINKED POLYAMPHOLYTE LATEXES

Abstract

Three types of sulfonate monomers have been prepared for the synthesis of cross-linked polyampholyte latexes: *p*-styrenesulfonyl chloride (SSC, 79.5%), methyl *p*-styrenesulfonate (MSS, 67%), and methyl *m,p*-vinylbenzylsulfonate (MVBS, 44%). These sulfonate monomers were copolymerized in surfactant-free emulsions with styrene, vinylbenzyl chloride (VBC), divinylbenzene, and either vinylbenzyl(trimethyl) ammonium chloride (VBTMAC) or sodium *p*-styrenesulfonate (NaSS) for charge stabilization. Treatment of the latexes with trimethylamine converted the VBC to quaternary ammonium cations and the sulfonyl chloride or methyl sulfonates to sulfonate anions. *m,p*-Vinylbenzyl methoxy poly(ethylene gycol) (VBMPEG) improved the colloidal stabilities of the latexes. All latexes containing a styrene sulfonate monomer were polydisperse due to low solubility or unfavorable copolymerization reactivity of the monomers.

Introduction

Water soluble sulfonate containing polyampholytes have been synthesized by copolymerization of both anionic and cationic monomers into the polymer backbone[1-3] or by incorporating into polymer zwitterionic (sulfobetaine) monomer units.[4-6] Synthesis of latexes using a lipophilic sulfonate monomer has not been reported to date; however, several sulfonate functionalized latexes have been published.[7-9] In those studies, amounts of sodium styrene sulfonate (NaSS) exceeding 2% of monomers generated secondary particles, making preparation of highly sulfonated polystyrene latexes by batch or seeded emulsion copolymerization impossible. Hence, a lipophilic monomer that is freely miscible with styrene and VBC must be employed in order to achieve a high-charge density cross-linked polyampholyte latex.

The synthesis of covalently cross-linked quaternary ammonium sulfonate polyampholytes proceeds through an emulsion copolymerization of vinylbenzyl chloride (VBC), sulfonate monomer [*p*-styrenesulfonyl chloride (SSC), methyl *p*-styrenesulfonate (MSS) or methyl *m,p*-vinylbenzylsulfonate (MVBS)], divinylbenzene, and styrene to produce a precursor latex. Reaction of the precursor latex with trimethylamine (TMA) and other tertiary amines in one step produces a polyampholyte latex containing quaternary ammonium ions (N^+) and sulfonate ions (SO_3^-) as outlined in Scheme 1. The compositions of the polyampholyte latexes are controlled by the amounts of functional monomers used in the copolymerization.

Scheme 1. Synthesis of Cross-linked Polyampholyte Latexes.

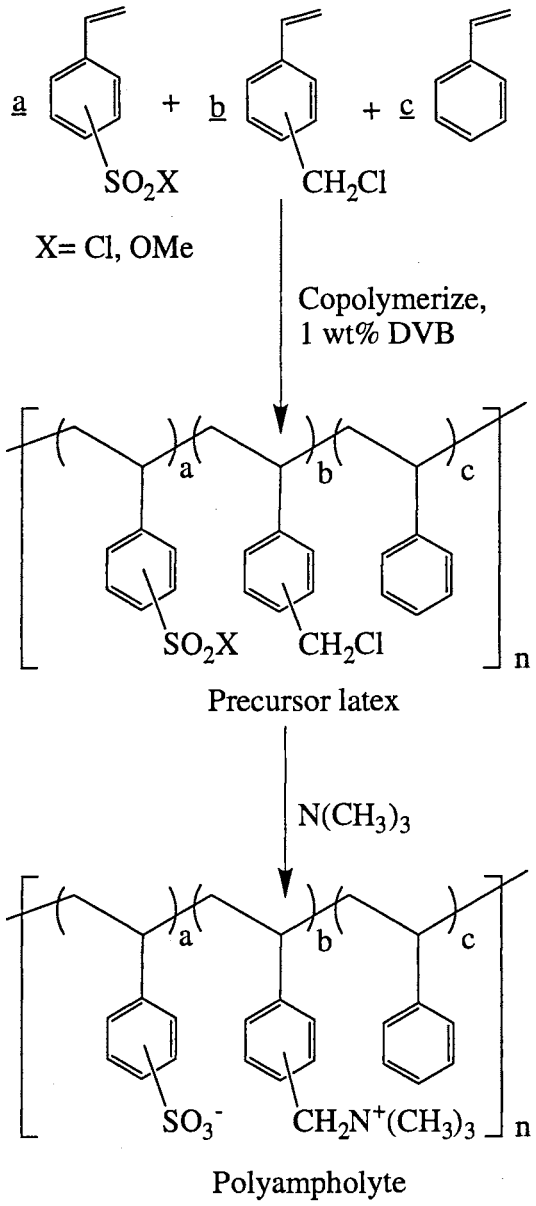

Experimental

Materials. Iraganox 1010 (CIBA GEIGY Corporation), sodium *p*-styrenesulfonate (NaSS, Polysciences), thionyl chloride (Aldrich), sodium iodide (J.T. Baker), sodium sulfite (Fisher), and 25 wt% trimethylamine in water (Eastman) were used as received. The monomers vinylbenzyl chloride, styrene, and divinylbenzene (Aldrich) were distilled under vacuum, and filtered through alumina prior to use. (*m,p*-Vinylbenzyl)trimethylammonium chloride (VBTMAC) was prepared previously[10] and used as a 0.0302 M aqueous solution (as measured with a chloride selective electrode). The initiator, VA-044 [2,2'-azobis(*N,N'*-dimethyleneisobutyramidine) dihydrochloride, Wako] was used as received. *N,N*-dimethylformamide (DMF, Aldrich) was dried with CaH, and distilled onto 5Å molecular sieves. THF (Aldrich) was distilled over sodium. MPEG-OH (Aldrich, MW 2000) was initially dried by azeotropic distillation with toluene and further under vacuum at 50 °C overnight and stored under nitrogen. Water was deionized by an E-pure (Barnstead) 3-module system to a conductivity of 0.65 μmhos.

***p*-Styrenesulfonyl Chloride (2).** A 1000 mL 4-neck flask equipped with a mechanical stirrer, thermometer, and nitrogen inlet was placed into a 40 °C oil bath. Iraganox 1010 (1.0 g) was added with 210 mL of anhydrous DMF. NaSS (70 g, dried in vacuum at 40 °C) was added in small amounts. The NaSS was only slightly soluble and remained suspended in DMF. The contents of the flask were chilled in a ice bath for at least 10 min. Chilled thionyl chloride (175 mL) was added dropwise over a 1 h period through an ice-jacketed addition funnel while the stirred mixture was held at <5 °C, and

the mixture was stirred for 1 h. The mixture was kept under nitrogen for 12 h at 5 °C, poured into 600 mL of ice water, and extracted 2x 400 mL of toluene. The extract was washed 2x 400 mL of water, dried over anhydrous sodium sulfate, and concentrated on a rotary evaporator at <40 °C to leave 43.9 g (79.5%) of a straw-colored oil. ^{1}H NMR (400 MHz, $CDCl_3$) δ 5.55 [d, 1H, J = 10.3 Hz], 5.95 [d, 1H, J = 17.5 Hz], 6.8 [q, 1H, alpha H], 7.6-8.0 [dd (para), 4H, C_6H_4]. (Appendix, Figure 1)

Methyl *p*-Styrenesulfonate (3). In 185 mL of dichloromethane and 75 mL of methanol, 37.3 g of SSC (**2**) was dissolved. Iraganox 1010 (3 mg) was added, and the mixture was allowed to stir in an ice bath for 30 min. A solution of 27.5 g of potassium hydroxide in 31 mL of water was cooled in an ice-jacketed addition funnel and added dropwise to the organic solution over 45 min. The temperature was raised to 25 °C, and the mixture was stirred for 1 h. Ice water (300 g) was added, and the mixture was neutralized with dilute sulfuric acid and extracted with 3x 100 mL portions of dichloromethane. The extracts were combined, dried over anhydrous sodium sulfate, filtered, and rotary evaporated at <40 °C. The residue was dissolved in 5 mL of dichloromethane and filtered through 10 g of silica gel. Rotary evaporation of the solvent <40 °C, gave 24.1 g (67%) of a yellow oil. ^{1}H NMR (400 MHz, $CDCl_3$) δ 3.8 [s, 3H, CH_3], 5.45 [d, 1H, J = 10.9 Hz], 5.95 [d, 1H, J = 17.7 Hz], 6.9 [dd, 1H, alpha H], 7.6-7.9 [dd , 4H, C_6H_4]. (Appendix, Figure 2)

***m,p*-Vinylbenzyl Methoxy Poly(ethylene gycol) (5).** Into a 100 mL three-necked flask were added 7.0g (3.5 mmol) of dry MPEG-OH (**4**) and 35 mL of THF. The

mixture was heated to reflux under nitrogen, and 0.420 g (17.5 mmol) of sodium hydride (60% dispersion in mineral oil) was added. The mixture was allowed to reflux for 20 h, and cooled to 25 °C under nitrogen. VBC (**6**, 2.67g, 17.5 mmol) was added, and the mixture stirred under nitrogen for 48 h. The mixture was poured into 250 mL of ice-cold acetone under nitrogen and centrifuged. The supernatant fluid was decanted, the acetone was removed with rotary evaporation, and the residue was extracted with 100 mL of water and 3x 50 mL of dichloromethane. The organic extracts were combined, dried over anhydrous $MgSO_4$, filtered, concentrated by rotary evaporation to 30 mL, and poured into ice-cold diethyl ether under nitrogen. The product was collected by vacuum filtration and dried to vacuum to give 5.56 g (81.3%) of white solid. ^{1}H NMR (400 MHz, DMSO-d_6) δ 3.25 [s, 3H, CH_3O-], 3.51 [bs, -CH_2CH_2O-], 4.49 [d, 2H, Ar-CH_2O-], 5.25 [dd, 1H, J = 11.8 Hz], 5.82 [dd, 1H, J = 17.2 Hz], 6.55 [m, 1H, alpha H], 7.2-7.5 [m, 4H, C_6H_4]. (Appendix, Figure 3)

Sodium *m,p*-Vinylbenzylsulfonate (7). A solution of VBC (**6**, 30 g, 0.20 mole) and sodium sulfite (Na_2SO_3•$7H_20$, 31.5g, 0.22 mole) in acetone/water (2:1, 600 mL) was stirred magnetically for several minutes. The reaction was started by the addition of 1.525 g of sodium iodide. After stirring in an oil bath at 45 °C for 24 h, the mixture was filtered, and the retained sodium chloride was washed with acetone. The acetone/water was removed under reduced pressure to yield white crystals, which were rinsed with 100 mL of dichloromethane and dried to give 35.7 g (82.6%) of a white solid. ^{1}H NMR (400 MHz, DMSO-d_6) δ 3.7 [d, 2H, CH_2], 5.2 [t, 1H, J = 10.0 Hz], 5.75 [d, 1H, J = 17.7 Hz], 6.7 [dd, 1H, alpha H], 7.2-7.4 [m, 4H, C_6H_4]. (Appendix, Figure 4) The mixture was

42% *meta* and 58% *para* by ^{1}H NMR integration of the CH_2 region at 3.7 ppm and analysis of the multiplets at 7.2-7.4 ppm.

Methyl *m,p*-Vinylbenzylsulfonate (9). NaVBS (**7**, 38 g, dried over night in the vacuum dessicator at 40 °C) was treated with thionyl chloride in DMF as in the synthesis of SSC (**2**). The resulting VBSC (**8**) was not isolated, but after removal of the toluene by rotary evaporation, was converted directly into MVBS (**9**) by potassium hydroxide in dichloromethane/methanol as in the synthesis of MSS (**3**). A yellow oil was recovered in 44.1% yield (16.2 g). ^{1}H NMR (300 MHz, $CDCl_3$) δ 3.76 [d, 3H, CH_3], 4.35 [d, 2H, CH_2], 5.3 [d, 1H, J = 10.9 Hz], 5.76 [d, 1H, J = 17.6 Hz], 6.73 [q, 1H, alpha H], 7.3-7.5 [m , 4H, C_6H_4]. (Appendix, Figure 5)

General One Shot Latex Synthesis. A 100-mL three-neck round-bottom flask equipped with an overhead stirrer with a Teflon blade, a condenser, and a nitrogen inlet was charged with 70 mL of water and either 0.060 g of VBTMAC in water or NaSS (**1**). The mixture was stirred, and purged with nitrogen for 20 min. A mixture of styrene, VBC, SSC and DVB was added. The mixture was stirred and heated for 20 min in a 60 °C oil bath. The reaction was initiated by adding 1 wt% of VA-044 or the amounts of potassium persulfate and sodium bisulfite required to make the aqueous phase 4.0 mM in each was added, and the mixture was stirred at 60 °C for 10 h. The latex was filtered through a cotton plug to remove a small amount of coagulum.

Semibatch Emulsion Polymerization. A 100 mL 3-neck round bottom flask was equipped with a nitrogen inlet, Teflon blade stirrer, and condenser with syringe pump inlet. A typical recipe is shown in Table III. All water and initial monomers were charged to the flask at room temperature and purged with nitrogen for 10 min while heating at 60 °C and with stirring at 500 rpm. The reaction was then initiated by adding VA-044. After 20 min, the second mixture of monomers was fed to the flask over 70 min by a syringe pump. Heating and stirring were continued for 2 h. The latex was then filtered through a cotton plug to collect the filterable solids.

Quaternization and Cleaning of the Latexes. A mixture of 50 mL of latex (about 5.0 g solid), 25 mL of H_2O, and 17.0 g of 25 wt% trimethylamine in a water solution was added to a 150 mL beaker and sealed in a stainless steel reactor. The mixture was held under pressure with magnetic stirring for 48 h with the reactor half immersed in a 60 °C oil bath. The excess trimethylamine was evaporated by bubbling nitrogen through the mixture. A Spectra/Por® dialysis membrane with a molecular weight cutoff of 50,000 was washed with deionized water several times to remove sodium azide. The latex was dialyzed against deionized water for a week with frequent changing of the water and was ultrafiltered in a stirred filtration cell through a 0.1 μm cellulose acetate/nitrate membrane (Millipore) under 20 psi of nitrogen. Deionized water was added repeatedly for several days until approximately 800 mL of filtrate was collected and the filtrate had a constant conductivity of 1.5 μmhos. The percent solids (w/v) of each latex was measured by evaporating 3 x 1 mL of the dispersion at >100 °C to constant weight.

Measurement of Latex Particle Sizes by TEM. Transmission electron micrographs were obtained with a JEOL 100-CX2 instrument at a magnification ranging from 10,000 to 14,000 with 100-μA filament current and 80-kV accelerating voltage. Samples were prepared by placing a drop of latex that had been diluted to 1% solids on a Formvar-coated Cu grid, removed excess latex by touching a piece of filter paper to the drop, and dried in air. Subsequently, one drop of a 1% solution of uranyl acetate was placed on the grid for 1 min, the excess solution was removed again with filter paper, and the grid was air dried. Diameters of 75 nonaggregated particles were measured directly from micrograph negatives using an optical microscope equipped with a calibrated stage and a 10-fold objective lens. The arithmetic mean, number average diameter, weight average diameter, and polydispersity were calculated from the following equations and were reported in the text.

$$\text{Arithmetic Mean} = \text{Mean} = \sum D_i / \sum n \quad (1)$$

$$\text{Number average diameter} = D_n = (\sum D_i^3 / \sum n)^{1/3} \quad (2)$$

$$\text{Weight average diameter} = D_w = (\sum D_i^6 / \sum D_i^3)^{1/3} \quad (3)$$

$$\text{Polydispersity} = D_w / D_n \quad (4)$$

Results and Discussion

Synthesis of SSC. Several groups have been successful in using *p*-styrenesulfonyl chloride (SSC, **2**) in polymerizations of ion exchange membranes[11] and microspheres.[12] In both cases, hydrolysis of the sulfonyl chloride to the corresponding acid during polymerization was not an issue. If the rate of hydrolysis of the sulfonyl chloride was slower than the rate of polymerization, then the sulfonyl chloride group in the resulting polymer can be converted into a strong acid center. In the procedure we have chosen, SSC is hydrolytically stable enough to be purified during preparation by washing with water.

Scheme 2. Synthesis of SSC and MSS.

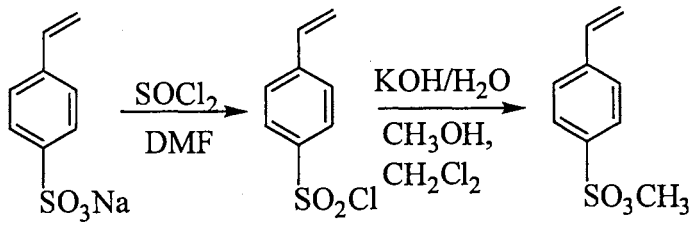

NaSS (1) **SSC (2)** **MSS (3)**

Accordingly, SSC (**2**) was prepared from reaction of sodium *p*-styrenesulfonate (NaSS, **1**) with thionyl chloride in anhydrous DMF in the presence of the inhibitor Iraganox 1010 as outlined in Scheme 2. Initially, two synthetic routes were explored for production of SSC. The first, as described above, is from a modified literature procedure,[13] and an increased yield as well as lighter color of the sample (due to the

purity of the thionyl chloride) was the basis of choosing these conditions over the second route of phosphorous pentachloride in chloroform.[14-15] Like other researchers, when we used phosphorous pentachloride, low yields were obtained along with a product that polymerized readily even when kept at low temperatures.

Polymerizations with SSC. Freshly prepared SSC was used in a series of one shot polymerizations using both cationic and anionic initiation as shown in Table 1. The first entry, C50N, was a control experiment that demonstrated formation of a stable latex from the cationic monomer, styrene, and VBC, with no sulfonate monomer. The next two entries were designed to give approximately equal amounts of (+) and (-) charges after quaternization, but both latexes were unstable at the precursor stage. Hydrolysis of the sulfonyl chloride group either before or after polymerization resulted in neutralizing charge stabilization of the particles. When potassium persulfate was employed with surface stabilized by NaSS units (A25N,25S), a stable precursor latex was synthesized. However, after quaternization the amount of SO_3^- units and N^+ units were theoretically equal, producing a neutral latex that was not stabilized by electrostatic repulsions and coagulated. Thus, our goal was to use excess VBC and obtain a latex with excess N^+ units to stabilize the particles. However, an intriguing question arises: Will polymer chain motions allow an anionic stabilized latex to migrate TMA treated positive charge sites to the surface for stabilization?

The anionic emulsion polymerization (A37.5N/12.5S, Table 1) was designed in the same manner as previous experiments [theoretical 3:1 (N^+/SO_3^-) charged latex]. Using excess VBC units, a stable precursor and polyampholyte latex were produced.

Thus, polymer chain motions do allow an anionic stabilized latex to switch surface charges. Yet, TEM of A37.5N/12.5S indicated a polydisperse latex with particle diameters ranging from 60-210 nm (Figure 1). Moreover, when the polymerization was designed to give a theoretical 1:3 (N^+/SO_3^-) charged latex (A12.5N/37.5S, Table 1), the resulting precursor and quaternized latex were unstable. Therefore, a series of charged-stabilized polyampholyte latexes seems unattainable, and adapting a *m,p*-vinylbenzyl methoxy poly(ethylene glycol) monomer seems appropriate as a steric stabilizing agent.

Table 1. Compositions of the Charged Stabilized Copolymer Latexes Synthesized by a One Shot Polymerization Technique.

Sample[a]	Weight of monomers, g			Precursor	After Quat.
	Styrene	VBC	SSC		
C50N[b]	4	4	--	Stable	Stable
C25N/25S[b]	4	2	2	Coagulated	Unstable
C50N/50S[b]	--	4	4	Coagulated	Unstable
A25N/25S[c]	4	2	2	Stable	Unstable
A37.5N/12.5S[c]	3.2	3.2	1.6	Stable	Stable
A12.5N/37.5S[c]	3.2	1.6	3.2	Stable	Unstable

[a] C, A = cationic, anionic stabilized latexes; 25N/25S = wt% of monomer precursors to N^+ and SO_3^- repeat units. [b] The sample contained 60 mg of VBTMAC, 200 mg of DVB and 70 mL of water at 60 °C, and was initiated with 1 wt% of VA-044 (80 mg). [c] The sample contained 80 mg of NaSS, 100 mg of DVB and 65 mL of water at 50 °C, and was initiated by 4 mM of $K_2S_2O_8$ (70 mg) and $NaHSO_3$ (27 mg) and 8 mM of $NaHCO_3$ (45 mg).

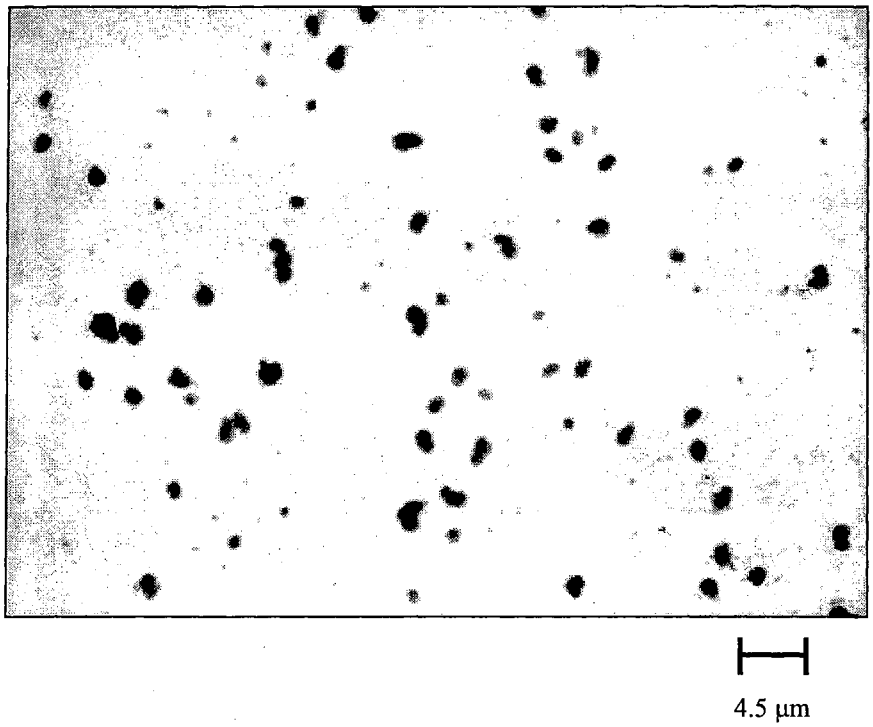

Figure 1. TEM of A37.5/S12.5 latex.

Sterically Stabilized Particles. Synthesis of *m,p*-vinylbenzyl methoxy poly(ethylene glycol) (VBMPEG, **8**, Scheme 3) was achieved, and the resulting monomer was used in terpolymerization of styrene, VBC, and SSC (Table 2). Resulting latexes are colloidally stable after dialysis and stirred ultrafiltration.

Scheme 3. Synthesis of VBMPEG

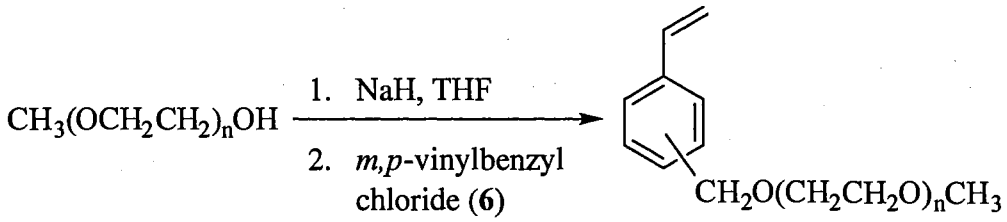

MPEG-OH (4) **VBMPEG (5)**

Their visual appearance during dialysis was informative. Ideally, the distribution of particles sizes should be very narrow (monodisperse). During dialysis, the electrolyte concentration was reduced, which increased the electrostatic repulsive forces (concentration of particles was increased). The latex inside the dialysis membrane became iridescent due to ordering of the particles into 'colloidal crystals'. This has been observed previously with monodisperse latexes, which, in the right size and concentration range, show brilliant colors. Latex SS50N was iridescent during dialysis, but sulfonate containing latexes (SS25N/25S and SS25S) were not. This observation was confirmed when TEM analysis revealed that SS50N was monodisperse with a diameter of 166 nm and SS25N/25S was polydisperse with diameters ranging from 25-235 nm (Figure 2). Thus, sulfonate containing latexes are polydisperse, which could be related to sulfonyl chloride hydrolysis or monomer reactivity.

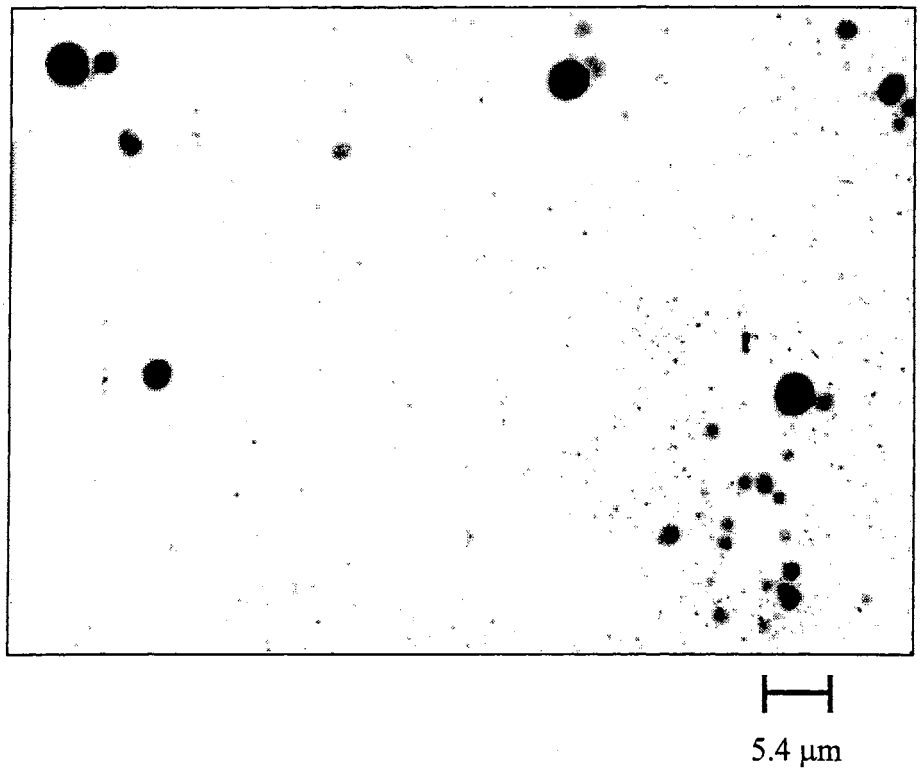

Figure 2. TEM of SS25N/25S latex.

Table 2. Compositions of the Steric Stabilized Copolymer Latexes.

Sample[a]	Styrene (g)	VBC (g)	SSC (g)	VBMPEG (g)
SS50N	3.6	4.0	-	0.4
SS25N/25S	3.6	2.0	2.0	0.4
SS50S	3.6	-	4.0	0.4

[a] SS = steric stabilized latexes. All samples contained 1 wt% of initiator VA-044 , 0.10 g of DVB, 0.06 g of VBTMAC and 70 mL of water.

Hydrolysis of SSC. An experiment was designed to test the hydrolysis rate of SSC at room temperature and at 60 °C (reaction temperature of emulsion polymerization). D_2O was added to a solution of acetone/SSC and the vinyl hydrogen integration's monitored every 15 min by ^{1}H-NMR. Results are presented in Figure 3. D_2O addition produced an insoluble product: SSC. Figure 3 depicts complete conversion of the sulfonyl chloride to the sulfonic acid at 60 °C in 75 min and 40% conversion at room temperature in 90 min. Moreover, the resulting sulfonic acid was completely soluble at the end of the analysis. Conditions were not identical to the emulsion polymerization but do indicate that hydrolysis does occur over the time frame of the polymerization procedure, and that the hydrolysis product is water soluble. The *p*-styrenesulfonic acid would cause formation of water soluble polymer resulting in unstable latexes and/or secondary particle nucleation resulting in polydisperse latexes with varied compositions that were observed in the SSC emulsion polymerizations.

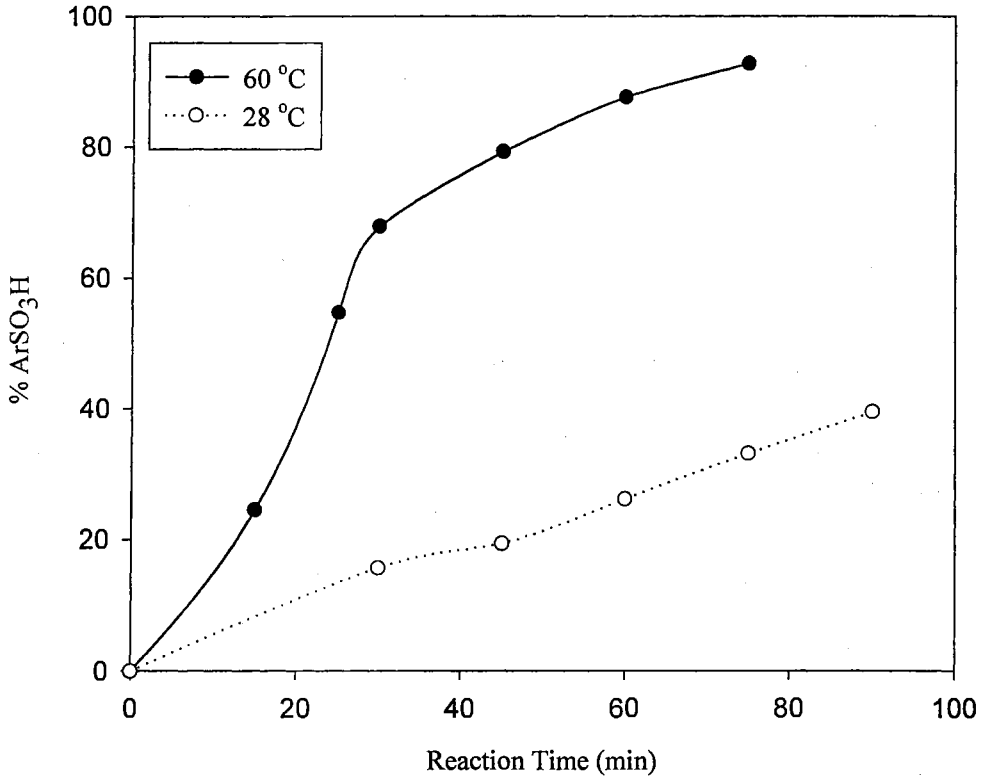

Figure 3. Hydrolysis of SSC.

Synthesis of MSS. A non-hydrolyzing monomer must be used in latex synthesis. Methyl *p*-styrenesulfonate (MSS, **3**) was synthesized by a modified literature procedure as outlined in Scheme 2.[16] The resulting MSS was used in a one shot emulsifier-free polymerization. The latex was very viscous and would not pass through a cotton plug. The precursor latex was unstable, and subjecting the latex to quaternization with TMA did not alleviate the instability. This would suggest that MSS was slightly water soluble, and water soluble polymer was being formed.

Semibatch Polymerizations with SSC and MSS. All latexes synthesized by a batch method resulted in unstable and/or polydisperse particles. These problems can be related to low solubilties and differences in reactivity of monomers. A semi-continuous addition of monomers by a semibatch emulsion polymerization would control these problems. In doing so, a defined particle seed will be produced and swell with addition of monomer. If all monomers are soluble in a polystyrene latex then polymerization of all new polymer formed will be in the seed particles. Furthermore, by using a slow addition of monomers the seed should be starved for monomers, and reactivity of monomers can be controlled. Hence, controlling composition and particle size is key in guaranteeing the quality of the latex products.

Freshly prepared MSS and SSC were used in a series of semibatch polymerizations using both cationic initiation and steric stabilization as shown in Table 3. The first entry SS50N was a controlled experiment revealing stabilization without a sulfonate monomer added, whereas the next two entries containing SSC and MSS,

respectively, resulted in fairly monodisperse latexes which coagulated after two weeks of storage.

Table 3. Compositions of the Semibatch Copolymer Latexes.

Sample[a]	Styrene (g)	VBC (g)	MSS (g)	SSC (g)
SS25N	1.0	1.0	-	-
SS25N/25S	1.0	1.0	-	1.0
SS3N/1S	1.0	1.5	0.5	-

[a] SS = steric stabilized latexes. The initial reactor charge contained 1 wt% of initiator VA-044 (40 mg), 50 mL of water, 0.0076 g of VBTMAC, 0.051 g VBMPEG, and 1g styrene. The monomer feed mixture also contained 0.15 g of VBMPEG and 0.05 g of DVB.

Synthesis of MVBS. Because a stable latex with theoretically equal charge was not obtained with either SSC or MSS, incorporation of methyl *m,p*-vinylbenzylsulfonate (MVBS, **9**) monomer into latex synthesis was investigated. A monomer with a benzyl functionality should give random reactivity, because of removal of the sulfonate functionality from the para position, and the ring system, should effectively cause the reactivity of the vinyl group to be similar to those of VBC and styrene.

Hence, NaVBS (**7**, Scheme 4) was prepared by reacting *m,p*-vinylbenzyl chloride (VBC, **6**) with a catalytic amount of sodium iodide and sodium sulfite. During the first attempts, white crystals were collected after vacuum filtration and a dichloromethane rinse. These white crystals, *para*-rich NaVBS, were collected (25.4 %). Solvent was removed from the dichloromethane/water filtrate giving a yellow powder, *meta*-rich

NaVBS (59.6%). Separation of the *meta* isomer is likely due to incomplete removal of water during the solvent removal step. A higher conversion was obtained by complete removal of the water/acetone (82.6%).

Initial attempts at treating NaVBS with thionyl chloride (as used with NaSS) resulted in two compounds being formed (two CH_2 groups in the ^{1}H-NMR). The second compound was believed to be the hydrolyzed product of the sulfonyl chloride, but attempts at using freshly distilled DMF and sodium bicarbonate washes (base) did not remove a possible sulfonic acid. Therefore, the time the monomer remained in the sulfonyl chloride state was limited. After the thionyl chloride treatment of NaVBS, workup and methylation were conducted as quickly as possible. The resulting products revealed two CH_2 groups in the ^{1}H-NMR. After several chromatographic separations, a pure methyl *m,p*-vinylbenzylsulfonate (MVBS, **9**) was obtained in very low yields. The chromatographic separations were in a mixture of dichloromethane/hexane, and white crystals precipitated as pure product. So, a recrystalization procedure could separate the two compounds which result from the above procedure.

Scheme 4. Synthesis of MVBS.

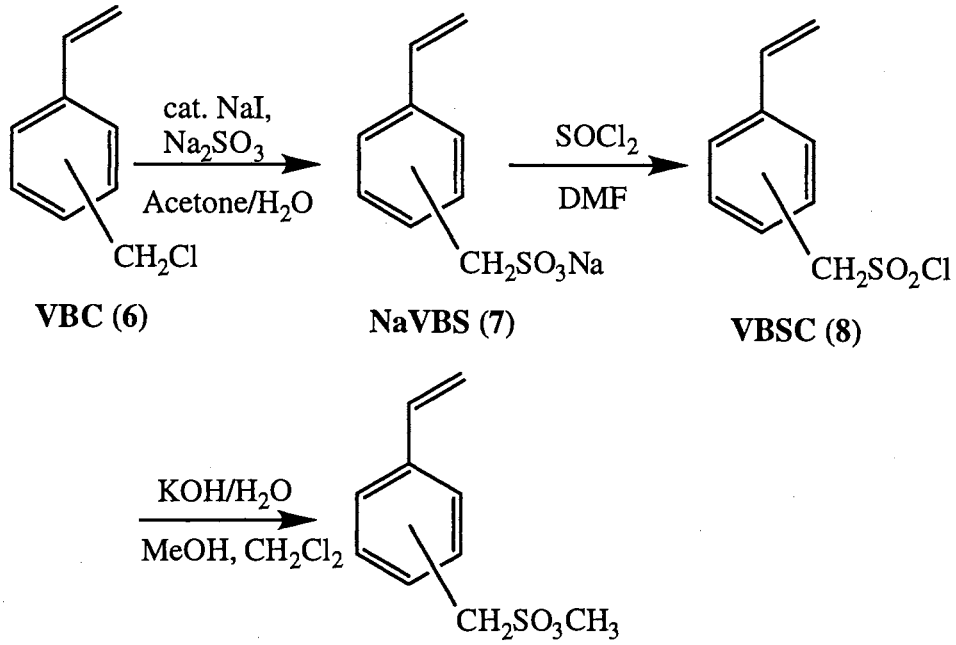

VBC (6) **NaVBS (7)** **VBSC (8)**

MVBS (9)

Vilsmeier-Haack Reagent. Observation of an unknown CH_2 peak in the ^{1}H-NMR having the same chemical shift as VBC, led to spiking the products of the MVBS reaction with VBC. The resulting ^{1}H-NMR spectrum indicate that the compound at 4.5 ppm was VBC . Therefore, the two compounds present after the methylation are MVBS and VBC. Rationalizing the production of VBC led to a better understanding of the mechanism of methylation. A literature search revealed that thionyl chloride can combine with DMF to form an intermediate complex known as a Vilsmeier-Haack reagent.[17] Since NaVBS contains a reactive benzyl carbon that can undergo an S_N2 reaction, production of VBC is rationalized by substitution of a free chlorine anion onto the benzyl carbon as outlined in Scheme 5. The formation of VBC can be minimized by reducing the reaction temperature to -5 °C without loss of the MVBS yield.

Scheme 5. Mechanism for Production of VBC Byproduct in MVBS Synthesis.

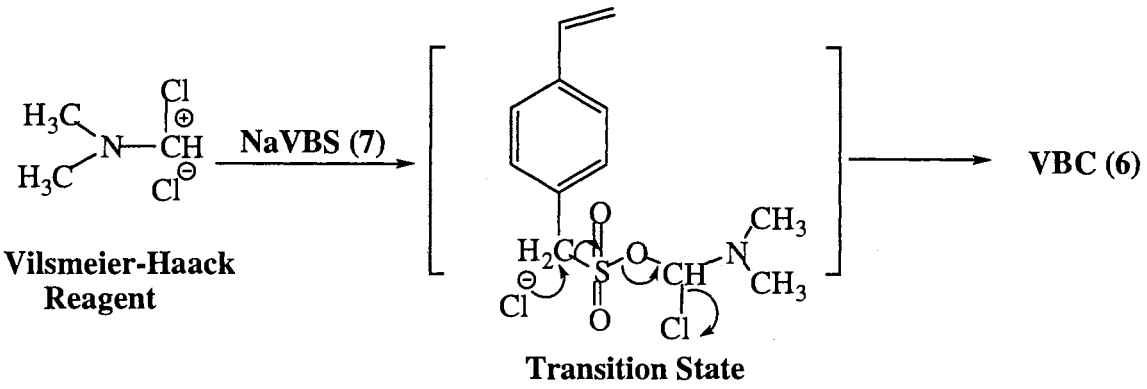

Polymerizations with MVBS. MVBS was purified by successive washes with cold hexane resulting in > 98 % pure MVBS. During the hexane washes, the *meta* isomer was slightly soluble. Initial attempts using the 50:50 *meta/para* mixture of MVBS in a semibatch emulsifier-free polymerization by cationic initiation resulted in coagulated latexes.

During storage of MVBS at 4 °C, white crystals of the *para* isomer formed. The supernatant, yellow oil enriched in the *meta* isomer was removed by washing with cold hexane, but recovery of each purified monomer was low. Because of noticeable differences in solubilities of the isomers of MVBS, separation of NaVBS isomers was pursued. The *meta* isomer was the first objective, since the *meta* isomer appeared to have similar solubilities as VBC. Using ethanol as the washing solvent during the workup of the NaVBS synthesis, a 85:15 *meta/para* mixture of NaVBS was obtained. This sodium salt was further reacted as described previously to give 23% yield of 75% *meta* enriched

MVBS. This monomer was used in two different, buffered one shot polymerizations of an anionically stabilized cross-linked latexes (compositions are given in Table 4).

Table 4. Compositions of MVBS Copolymer Latexes.

Sample[a]	Styrene (g)	VBC (g)	MVBS (g)	VBMPEG (g)
SS10N/10S	1.5	0.2	0.2	0.1
SS20N/20S	1.1	0.4	0.4	0.1

[a] The sample contained 15 mg of NaSS, 20 mg of DVB and 20 mL of water at 50 °C, and was initiated by 4 mM of $K_2S_2O_8$ (17.7 mg) and $NaHSO_3$ (12 mg) and 8 mM of $NaHCO_3$ (17.8 mg).

Precursor latexes (before quaternization) of both entries appeared stable with no coagulum collected after polymerization. SS10N/10S contain 10 wt% each of VBC and MVBS and SS20N/20S contained 20 wt% each of VBC and MVBS. The latter began to coagulate during dialysis. This would indicate that the increase in MVBS caused coagulation. However, TEM analysis of the first entry revealed a bimodal particle size distribution with small 150 nm and larger 3 μm particles (Figure 4). Thus, as MVBS content increased, the number of larger particles increased and fell out during dialysis. Two possibilities can be examined: (1) over time smaller particles coagulate forming larger uniform particles, or (2) MVBS copolymer was insoluble in a polystyrene latex; hence, formed discrete larger particles containing MVBS and smaller styrene/VBC particles. Then, the content of larger particles increased with MVBS concentration, and coagulation is observed due to particle size and not actual coagulation.

As a result, *para* rich MVBS was synthesized in order to explore solubility variances. An 83% *para*-MVBS was synthesized in 44% yield from isolated *para* NaVBS from the above procedure. After removing 7% VBC with several cold hexane washes, a semibatch emulsifier-free polymerization was conducted with 10 wt% each of MVBS and VBC. *para*-MVBS monomer was not miscible in styrene/VBC; therefore, an acetone/H_2O solution was used. The resulting latex after quaternization was completely coagulated.

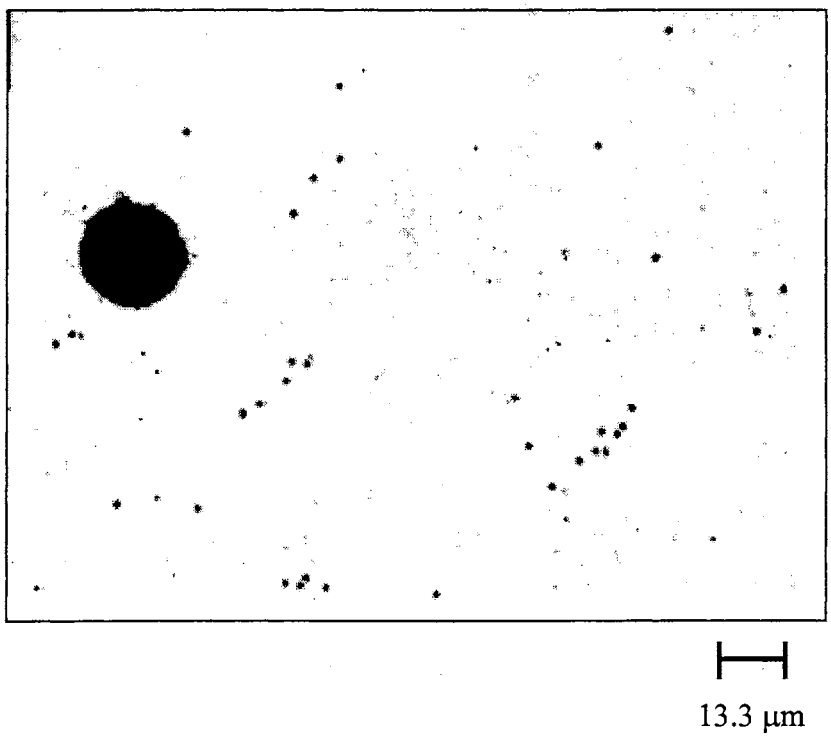

Figure 4. TEM of SS10N/10S latex.

Conclusions

None of the three styrenesulfonate monomers produced monodisperse colloidally stable latexes. SSC hydrolyzed competitively with emulsion polymerization, and the resulting *p*-styrenesulfonic acid caused secondary particle formation. MSS and *meta*-rich MVBS gave unstable and/or polydisperse latexes due to either low solubility in VBC/styrene latexes or too high reactivity during copolymerization. *para*-rich MVBS was incompletely miscible even with VBC and styrene monomers. A shorter form of the chapter is in press.[18]

References

1. Candau, F.; Selb, J.; Corpart, J. *Polymer* **1993**, *34*, 3873.
2. Candau, F.; Neyret, S.; Candau, S. J.; Munch, J. P.; Skouri, M. *Macromolecules* **1994**, *27*, 69.
3. Candau, F.; Corpart, J. *Macromolecules* **1993**, *26*, 1333.
4. McCormick, C. L.; Kathmann, E. E.; *J. Polym. Sci: Part A* **1997**, *35*, 231.
5. McCormick, C. L.; Kathmann, E. E.; *J. Polym. Sci: Part A* **1997**, *35*, 243.
6. McCormick, C. L.; Salazar, L. C.; Welch, P. M.; Mumick, P. S. *Macromolecules* **1994**, *27*, 323.
7. Kim, J.H.; Chainey, M. D.; El-Aasser, M. S.; Vanderhoff, J. W. *J. Polym. Sci. Part A: Polym. Chem.* **1992**, *30*, 171.
8. Juang, M. S.; Krieger, I. M. *J. Polym. Sci. Polym. Chem. Ed.* **1976**, *14*, 2089.
9. Sunkara, H.; Jethmalani, J. M.; Ford, W. T. *J. Polym. Sci. Part A: Polym. Chem.* **1994**, *32*, 1431.
10. Ford, W. T.; Yu, H.; Lee, J. J.; El-Hamshary, H. *Langmuir* **1993**, *9*, 1698.
11. Takata, K.; Ihara, H.; Sata, T. *Angew. Makromol. Chem.* **1996**, *236*, 67.
12. Shahar, M.; Meshuham, H.; Margel, S. *J. Polym. Sci. Polym. Chem. Ed.* **1986**, *24*, 203.
13. Kamogawa, H.; Kanzawa, A.; Kadoya, M.; Naito, T.; Nanasawa, M. *Bull. Chem. Soc. Jpn.* **1983**, *56*, 762.
14. Yoda, N.; Marvel, C.S. *J. Polm. Sci. Part A* **1965**, *3*, 229.
15. Chang, W.; Nakabayashi, N.; Uno, K.; Iwakura, Y. *J. Polm. Sci. Part A* **1967**, *5*, 3193.
16. Upson, D. A. *Macromolecular Syntheses* **1986**, *10*, 8.
17. Busshard, H. H.; Mory, A.; Schmid, M.; Zollinger, H. *Helv. Chim. Acta*, **1959**, *42*, 1653.
18. Hampton, K. W.; Ford, W. T. *ACS Symposium Series*, **1999**, in press.

CHAPTER III

SYNTHESIS AND CHARACTERIZATION OF CARBOXYLATE CONTAINING CROSS-LINKED POLYAMPHOLYTE LATEXES

Abstract

We have synthesized novel high charge density quaternary ammonium carboxylate polyampholyte microgels. The synthesis of covalently cross-linked polyampholytes proceeds through an emulsion copolymerization of vinylbenzyl chloride (VBC), *tert*-butyl methacrylate (tBMA) or methacrylic acid (MAA), divinylbenzene, and styrene to produce a precursor latex. Reaction of the precursor latex with trimethylamine (TMA) and deprotection of the carboxylate by acid hydrolysis in two steps produces a polyampholyte microgel. The compositions of polyampholyte microgels are controlled by the amounts of functional monomers used in copolymerization. Turbidity and coagulation kinetic experiments reveal microgels that are stable in high salt concentrations (4 M NaCl and 1.2 M $BaCl_2$). Light scattering studies show a "polyampholyte effect": swelling and stability in salt solutions.

Introduction

Synthesized linear carboxylate containing polyampholytes date back a half-century and are likely the first synthesized polyampholytes.[1] The focus of this research was to better understand and mimic proteins which can contain COO^-, N^+, or SO_3^- repeat units, making them natural polyampholytes. Linear polyampholytes can comprise chains with strong and weak acid or strong and weak base groups in various combinations. Carboxylic acid containing polyampholytes have been conventionally prepared by direct, free-radical polymerization of acrylic or methacrylic acid (MAA) with various vinyl cationic comonomers (**1**).[2]

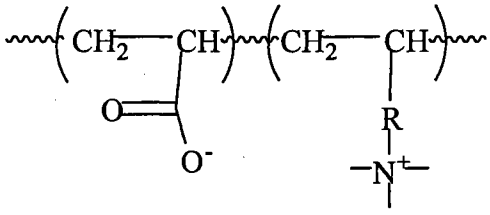

1

These synthetic routes can result in statistical (**2**) or alternating (**3**) placement of ionic groups along polymer backbones. Living polymerizations (anionic, cationic, or group transfer polymerizations) enable one to synthesize block polyampholyte copolymers (**4**) with controlled compositions and architecture.[3] Linear polyampholytes have also been synthesized as polymeric betaines whose acidic (A) and basic (B) groups are situated within the same monomer unit (**5**).[4]

-ABAABABBAABBA- (2)

-ABABABABABABA- (3)

-AAAAAAABBBBBB- (4)

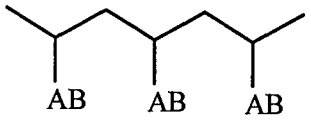

(5)

Depending on the pH of the medium, quaternary ammonium carboxylate polyampholytes can exhibit properties of either polyacids or polybases. The net charge of the macromolecule assumes a negative or positive value, respectively. The pH value, at which a polyampholyte is electroneutral, is called the isoelectric point (i.e.p.) (**6**).

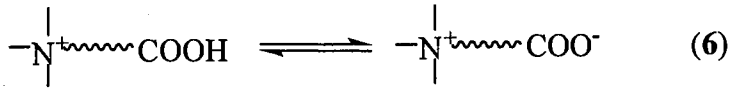

(6)

At the i.e.p., polyampholytes have unique hydrodynamic properties. Carboxylate containing polyampholytes are affected more by pH than the corresponding sulfonate containing polyampholytes due to higher pK_a values of the carboxylic acid units. Copolymers containing nearly equalmolar amounts of the cationic and anionic monomers display a minimum in viscosity in pure water and a maximum in viscosity in concentrated salt solutions. This behavior is due to shielding of ionic charges along the polymer chain, which results in disruption of positive-negative charge interactions that allow coil expansion by enhanced solvations.

Several examples of MAA-styrene copolymer latexes have been synthesized.[5] Conventional emulsion polymer systems employ monomers that are relatively water insoluble such as styrene. The primary reaction locus is inside polymer particles, and

aqueous-phase polymerization is usually negligible. However, carboxylic acid monomers are often completely soluble in water. Yet, MAA will still distribute to varying extents into the organic phase depending on its relative hydrophobicity. Significant amounts of polymerization can occur in both particle and aqueous phases. So, emulsion polymerizations with MAA must be conducted at high monomer content to maximize the fraction of MAA in organic phase.

We have attempted the synthesis of cross-linked sulfonate containing polyampholyte latexes, but long-term stability of these latexes is not satisfactory (Chapter II). This chapter describes the synthesis of cross-linked carboxylate containing latexes by surfactant emulsion polymerization of styrene, vinylbenzyl chloride (VBC), carboxylate monomer [methacrylic acid (MAA), trimethylsilyl methacrylate (TMSMA), tetrahydropyranyl methacrylate (THPMA) or *tert*-butyl methacrylate (tBMA)], and divinylbenzene (DVB). Chloride selective titrations, elemental analysis, diffuse reflectance infrared fourier transform spectroscopy (DRIFTS), conductimetric titrations, turbidity, coagulation kinetics, transmission electron microscopy (TEM), and dynamic light scattering (DLS) were used to characterize the synthesized microgels.

Scheme 1. Synthesis of Carboxylate Containing Polyampholyte Microgels.

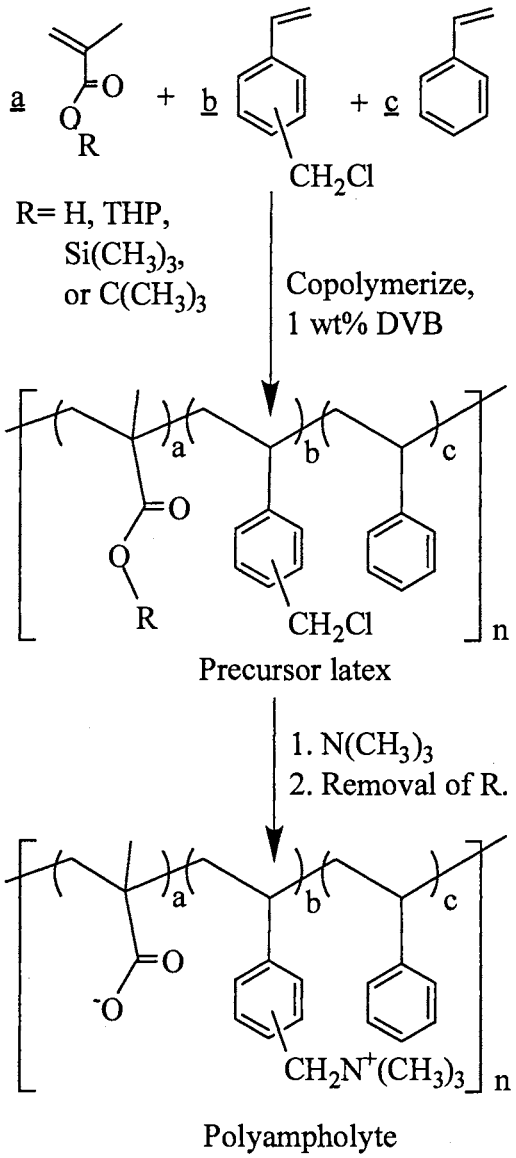

Experimental Section

Materials. Sodium dodecyl sulfate, sodium bisulfite, potassium persulfate, *p*-toluenesulfonic acid (PTSA), 1,4-dioxane, and trimethylamine (25 wt% in water, Eastman) were all used as received. Monomers *m,p*-vinylbenzyl chloride, styrene, divinylbenzene, methacrylic acid, tetrahydropyranyl methacrylate, trimethylsilyl methacrylate, and *tert*-butyl methacrylate (Aldrich) were distilled under vacuum and filtered through alumina prior to use. Water was deionized and treated with active carbon using an E-pure (Barnstead) 3-module system resulting in water with conductivity of 0.65 μmhos.

Semibatch Emulsion Polymerization Containing Carboxylated Monomers. In a 100 mL 3-neck round bottom flask equipped with a nitrogen inlet, Teflon blade stirrer, and condenser/addition funnel was placed sodium dodecyl sulfate (0.060 g) and water (20.0 mL). The addition funnel was equipped with a mechanical stirrer. The mixture was heated to 60 °C with constant stirring under a gentle flow of nitrogen for 15 min. The monomer charge was prepared separately by mixing sodium dodecyl sulfate (0.12 g), sodium bisulfite (0.015 g), water (5 mL), and 5 g of monomers consisting of styrene, VBC, [MAA, THPMA, TMSMA, or tBMA], and DVB in a predetermined mole ratio. The monomer mixture was transferred to the addition funnel and stirred to form a pre-emulsion.

Initially 0.50 g of pre-emulsion was weighed out and transferred to the reaction flask. Potassium persulfate (0.04 g) and sodium bisulfite (0.005 g) were added to the reaction flask to initiate polymerization. An opaque polymer latex formed within 30 min, and the monomer mixture was added continuously over a period of 1 h. After addition of the monomer charge, the addition funnel was removed and replaced by a condenser. The mixture was stirred at 60 °C for 3 h. Theoretical total solids content after polymerization was 20%. The polymer was allowed to cool to room temperature and was filtered through a cotton plug to collect solid coagulum. Most latexes did not contain coagulum.

Quaternization and Cleaning of Latexes . The procedures are in Chapter II.

Chloride Selective Electrode Titration of Quaternized Microgels. A small portion of the quaternized sample was purified by dialysis and ultrafiltration as described later. The concentration of quaternary sites was determined by titrating chloride counterions with a chloride ion selective electrode (Orion Research Inc.). Sensitivity of the electrode was checked daily with a volumetric standard NaCl solution (0.0973 N, Aldrich). The latex sample, 1.50 mL, was pipetted into a 50 mL beaker, 0.6 mL of 5 M $NaNO_3$ was added as an ionic strength adjuster, and 15 mL of water was added to cover the electrode. The mixture was adjusted to about pH 2 with 1 N HNO_3 solution. The latex was titrated with 0.0490 M $AgNO_3$ (calibrated with the standard NaCl solution described above) and millivolts of the electrode potential were recorded. Titration curves of milliliters versus millivolts were sharp and symmetrical, and end points were determined by the normal method for potentiometric titrations.[6]

Hydrolysis of tBMA Microgels. A mixture of latex (1 g, ~20 mL), PTSA (100 mol % based on tBMA), and 1,4 dioxane (2 g in 20 mL of water) was refluxed at 120 °C for 48 h. The resulting microgel was immediately sampled (10 mL) and frozen after removal from reflux. The frozen polymer was lyophilized, and DRIFTS were taken on the subsequent dried microgels to determine conversions.

Diffuse Reflectance Infrared Fourier Transform Spectroscopy. Infrared data was collected using a Nicolet Magna 750 Fourier transform infrared spectrometer (FTIR). Functionalized microgels were characterized by lypohization (12 h) and direct analysis using Spectra Tech diffuse reflectance accessory (DRIFTS). All DRIFTS spectra were obtained using 256 scans at 4 cm^{-1} resolution, a 4000-400 cm^{-1} spectral width, and Kubelka Munk processing.[7]

Conductimetric Titration of Polyampholyte Microgels. Conductimetric/pH titration was carried out on polyampholyte microgels in order to quantify carboxylic acid groups in the particles. Conductivity of the solution was measured on a Yellow Springs Instruments Model 31 analog conductivity bridge, and pH was determined on a Fisher Scientific Accumet® pH meter 25. Analytical reagent quality sodium carbonate (99.9% pure) was dried for 4 h at 200 °C and used to standardize a 0.0481 M HCl solution using methyl orange-indigo carmine indicator. Sodium carbonate was measured separately for each trial. This HCl solution was used to standardize 0.0496 M NaOH. In a three neck 75 mL beaker equipped with a magnetic stirring bar was placed 0.050 g of latex in 50 mL of deionized water. The solution was purged with nitrogen and stirred for 15 min. A

known amount of standard HCl solution (4.0 mL) was added. The mixture was titrated with standard NaOH solution and conductivity and pH measurements were taken at regular intervals of 0.1 mL every 1.5-2.0 min.

Colloidal Stability. The stability of the microgels to added electrolyte was examined by following changes in turbidity as a function of time at various concentrations of barium chloride or sodium chloride. A Hewlett Packard HP 8452A UV-visible diode array spectrophotometer, with quartz optical cells of path length 1 cm, was used for these measurements. All experiments were conducted at room temperature (20-26 °C)

Slow coagulation was measured in barium chloride solutions. Cleaned microgels were diluted so that further dilution, four fold with deionized water to ca. 0.05% w/v, gave a turbidity of about 0.7. A 2 mL aliquot of diluted latex was transferred to a clean tube, and 8 mL of barium chloride solution of known concentration was added. After initial agitation, the mixture was allowed to stand for 2 h and then lightly centrifuged using a bench top centrifuge for 10 min. The supernate was carefully removed, transferred to a cuvette, and turbidity at 546 nm was measured. This procedure was repeated over a range of barium chloride concentrations, and a plot of turbidity against electrolyte concentration was constructed. After 48 h the cuvettes were photographed.

Immediate coagulation kinetics were measured in sodium chloride solutions. In a typical coagulation kinetic experiment, 2.4 mL of a solution of known salt concentration

and 0.6 mL (0.05% w/v) of a microgel solution were quickly added and mixed. Optical turbidity at 540-550 nm was recorded continuously for 5 min. This process was repeated over a range of sodium chloride concentrations, and a plot was constructed of turbidity against time for each concentration. The initial slope of the curve is directly proportional to initial coagulation rate.

The pH coagulation kinetics were measured by adding a known amount of sodium hydroxide to the cleaned microgel solutions and following the turbidity as described above. The pH of each solution was determined after kinetic measurements were performed.

Measurement of Microgel Particle Sizes by TEM. The procedure is in Chapter II.

Measurement of Microgel Particle Sizes by DLS. Swollen sizes of microgel particles were measured by dynamic light scattering (DLS) using a Brookhaven Instruments BI-200SM Gonimeter and BI-9000AT multi-τ-digital correlator. The light source was a Coherent INNOVA-90 argon laser (488 nm). Samples were prepared by mixing a drop (15-50 μL) of latex in 25-50 mL of water or in aqueous sodium chloride of known concentration. Microgel particles were measured as a function of sodium chloride concentration at a scattering angle of 90° and a temperature of 20 °C. The hydrodynamic radius of a hard spherical particle is calculated from its diffusion coefficent by the Stokes-Einstein equation:

$$R_h = kT/6\pi\eta D \qquad (1)$$

Here k is the Boltzmann constant, T is absolute temperature, η is the viscosity of the medium, and D is the diffusion coefficient of the particle. Dynamic light scattering measures the diffusion coefficient of the particles. R_h is calculated using equation (1) and measured D, assuming no particle interaction. Plots of refractive index and viscosity against sodium chloride concentration at 20 °C are in the Appendix (Figure 6 and Figure 7).[8]

Results and Discussion

The strategy for synthesis of polyampholyte microgels is shown in Scheme 1. Initial efforts utilized methacrylic acid (MAA) or trimethylsilyl methacrylate (TMSMA) as the anionic precursor for polymerization of polyampholytes, but an excess of cationic sites could not be obtained because of instabilities of the latexes. Therefore, a protected anionic precursor (*tert*-butyl methacrylate) was employed. The *tert*-butyl protecting group was stable during emulsion polymerization. After quaternization of vinylbenzyl chloride moieties, *tert*-butyl groups were hydrolyzed to afford the desired polyampholytes. Conversions of *tert*-butyl groups were confirmed by DRIFTS and quantified by conductimetric titrations.

Polymerizations with Methacrylic Acid and Trimethylsilyl Methacrylate. Initial efforts, using MAA in an emulsifier-free copolymerization with styrene/VBC, resulted in viscous latexes probably due to formation of poly(methacrylic acid) in the water phase. For that reason, the surfactant, sodium dodecyl sulfate (SDS), was used, and the monomer content was raised to 20 wt% to increase the fraction of MAA in micelles. In those experiments only anionic stabilized latexes could be synthesized (Table 1). The latexes with equal or excess VBC units were unstable after quaternization. The reason for coagulation is probably due to the fact the latexes were neutral (equal number of anionic and cationic sites) or passed through neutrality when going from anionic to cationic stabilization during the quaternization procedure. Consequently, an ester protecting group must be employed to achieve excess cationic sites in the

polyampholytes. TMSMA was used in emulsion polymerizations, and resulted in unstable cationic latexes. These results indicate TMSMA was hydrolyzing under emulsion conditions, and MAA was being used. Observations of uniphase pre-emulsions in both MAA and TMSMA, confirms literature findings that TMSMA hydrolyzes in mild conditions,[9] and trimethylsilyl esters hydrolyze in all conditions (acidic, basic and neutral).[10] Latexes designed to encompass the mol ratios that give a anionic stabilized polyampholyte (99:1 to 60:40 / $COO^-:N^+$) were achieved by using MAA and TMSMA (Table 1).

Table 1. Compositions of the MAA and TMSMA Copolymer Microgels.[a]

	Weight of monomers, g					
Sample	Styrene	VBC	MAA	TMSMA	Precursor	After Quat.
25MAA/25VBC	2.35	1.71	0.96	--	Stable	Coagulated
30MAA/20VBC	2.40	1.40	1.20	--	Stable	Stable
20MAA/30VBC	2.37	1.92	0.73	--	Stable	Coagulated
25TMSMA/25VBC	1.99	1.49	--	1.56	Stable	Coagulated
30TMSMA/20VBC	1.93	1.20	--	1.84	Stable	Stable
20TMSMA/30VBC	1.96	1.78	--	1.23	Stable	Coagulated

[a] Sample contained 65 mL of water, 80 mg of SDS, 100 mg of DVB, 70 mg of $K_2S_2O_8$ and 27 mg $NaHSO_3$ and 45 mg of $NaHCO_3$ at 60 °C

Polymerization with Tetrahydropranyl Methacrylate and *tert*-Butyl Methacrylate. In order to achieve a cationic stabilized polyampholyte latex, which was necessary for anionic phase transfer catalysis, an ester protected carboxylate monomer was needed. This monomer must be stable under emulsion polymerization conditions, and must be hydrolyzed to the carboxylate after polymerization. Several methacrylates would be in the emulsion stability category, but most would fail in post reaction hydrolysis. After an extensive literature search, two methacrylates proved promising: THPMA and tBMA. Both of these monomers have been used in group transfer polymerizations and hydrolyzed to form the carboxylate.[11] The two monomers have not been used in an emulsion polymerization.[12] Hence, THPMA was used first because of milder acid hydrolysis conditions and stability in basic solutions.[13] A buffered batch polymerization was attempted, but the emulsion would not remain neutral even with repeated additions of $NaHCO_3$ (Each addition resulted in formation of CO_2 gas). The generation of acid during polymerization must be from hydrolysis of THPMA monomer or the polymer as shown in Scheme 2.

Scheme 2. Hydrolysis of THPMA.

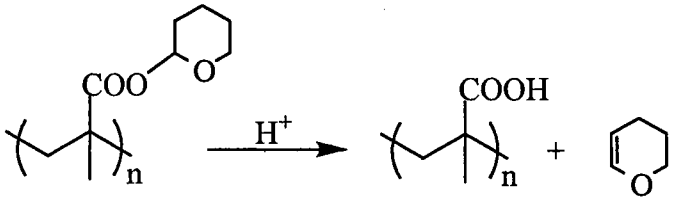

As discussed previously, tBMA has not been used in an emulsion polymerization; therefore, a batch 25 wt% tBMA styrene latex was performed as with THPMA. The pH

of the emulsion remained neutral throughout the polymerization after the first addition of $NaHCO_3$ (60 mg). Because tBMA was stable to emulsion conditions, a series of polymerizations were performed as outlined in Table 2. Sample designations indicate the theoretical mole ratio of polyampholyte microgels. For example, 25/25N represents a 1:1 mole ratio of tBMA and VBC repeat units with a theoretical mole percentage of twenty-five for each monomer. These microgels were designed so that after the quaternization and hydrolysis postreactions, charge ratios will fall into the range (60/40 to 40/60 : COO^- /N^+ sites) that has exhibited polyampholyte behavior.[14]

After forming the precursor VBC latex, benzyl chloride moieties are converted to quaternary ammonium sites with TMA, via an S_N2 mechanism. Degree of quaternization was determined by titrating chloride counter ions with a chloride ion selective electrode. Results of the chloride titrations are presented in Table 2. Conversion of benzyl chloride moieties to N^+ sites ranged from 82 to 93%. The results of the elemental analysis of the three quaternized tBMA latexes are presented in Table 3. The experimental results were high in oxygen content (O%), which is likely due to trace amounts of water. Therefore, the amount of oxygen and hydrogen corresponded to water were subtracted out of the experimental results (experimental-water, Table 3, example calculation presented in the Appendix). Conversions of the VBC moieties to quaternized sites were based on the ratio of theoretical calculated nitrogen content, and nitrogen content was determined by correction of experimental results for water content. Water content of the microgels was between 3-4 wt%. The calculations of the N^+ sites are presented in Table 2. Chloride analysis and nitrogen content (elemental analysis) agree within 5%.

Table 2. Compositions of tBMA Copolymer Microgels.

	Weight of monomers, g			Cl^- Anal.[a]		Nitrogen Anal.[b]
Sample	Styrene	VBC	tBMA	mmol/g	N^+ (mol%)[c]	N^+ (mol%)
25/25N	2.03	1.56	1.46	1.89	24.7	24.6
20/30N	2.02	1.82	1.14	2.12	28.6	29.1
30/20N	2.06	1.26	1.73	1.41	17.3	17.6

[a] Chloride-selective electrode. [b] Combustion. [c] The average repeat unit was calculated to be 126 g/mol (25/25N), 132 g/mol (20/30N), and 119 g/mol (30/20N) for determination of mol%.

Table 3. Elemental Analysis of tBMA Copolymer Microgels (wt%).

Sample	C	H	N	O[a]	Cl
25/25N					
$[C_8H_8]_{0.50}$ $[C_{12}H_{18}NCl]_{0.25}$ $[C_8H_{14}O_2]_{0.25}$	76.91	8.61	2.49	5.69	6.31
experimental	74.04	8.59	2.34	9.71	5.32
experimental-water (3.96 %)	77.55	8.47	2.45	5.96	5.57
20/30N					
$[C_8H_8]_{0.50}$ $[C_{12}H_{18}NCl]_{0.30}$ $[C_8H_{14}O_2]_{0.20}$	76.72	8.54	2.92	4.44	7.38
experimental	72.96	8.83	2.75	8.30	7.16
experimental-water (2.98 %)	76.21	8.73	2.87	4.71	7.48
30/20N					
$[C_8H_8]_{0.50}$ $[C_{12}H_{18}NCl]_{0.20}$ $[C_8H_{14}O_2]_{0.30}$	75.91	7.88	2.33	7.98	5.90
experimental	73.66	8.82	1.98	10.96	4.58
experimental-water (4.16 %)	76.21	9.13	2.05	7.87	4.74

[a] Experimental results were calculated by complement of 100%.

Hydrolysis of *tert*-Butyl Methacrylate Repeat Units. In order to get polyampholyte latexes, *t*-butyl protecting groups in quaternized latexes were cleaved to form the anionic repeat units. Methods for hydrolysis of tBMA copolymers in solution are known,[11] but the need to maintain colloidal stability made adaptation of literature conditions challenging. Both basic (aqueous NaOH) and acid (aqueous HCl) hydrolysis conditions were investigated, but because most of the *t*-butyl groups were inside the particles, the conversions were incomplete. Therefore, an organic soluble acid (PTSA) was employed along with an organic solvent (1,4-dioxane) to swell the microgels. Amounts of PTSA and dioxane, along with temperature and time, were varied to find optimum conditions. The best conditions for hydrolysis of the *t*-butyl protecting group were 120 °C for 48 h with one mole of PTSA per mole of tBMA and dioxane (10 g per 100 g of water) as shown in Scheme 3.

Scheme 3. Hydrolysis of tBMA.

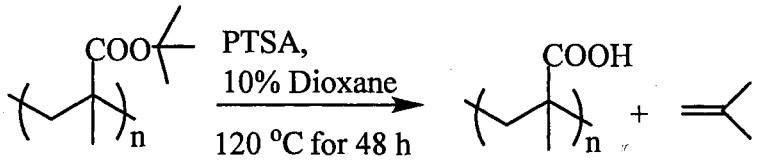

Elemental analysis of polyampholyte microgels was not useful for quantitative determination of carboxyl groups because of the large oxygen content in the experimental results (Table 4). However, a lack of chloride in the elemental analysis indicated intramolecular electrostatic attractions (Scheme 4) or the presence of

another counter anion, such as tosylate from PTSA in the hydrolysis procedure. The presence of tosylate would explain high oxygen content.

Scheme 4. Intramolecular Electrostatic Attractions of a Polyampholyte Microgel.

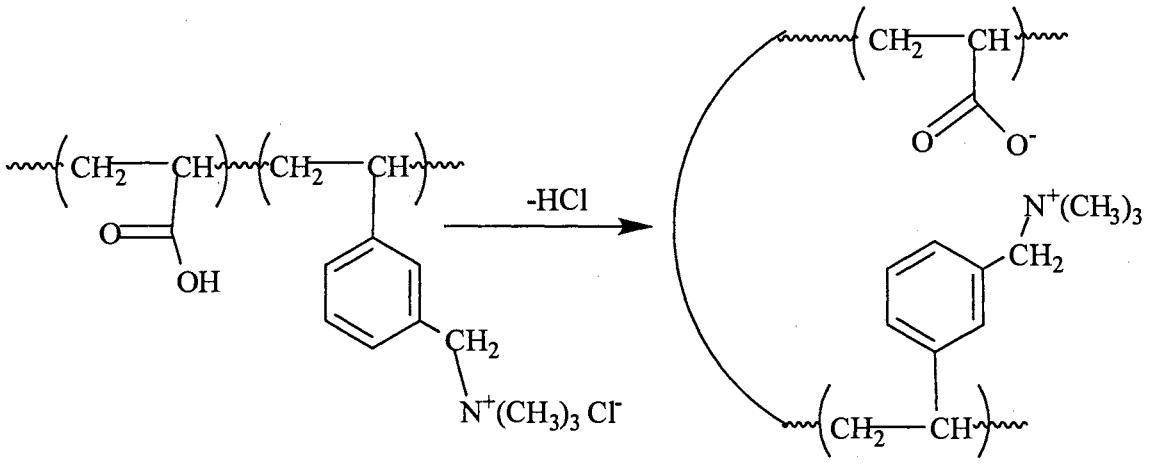

Table 4. Elemental Analysis of the Polyampholyte Microgels (wt%).

Sample	C	H	N	O[a]	Cl	other[a]
PA2525						
$[C_8H_8]_{0.50}$ $[C_{12}H_{18}NCl]_{0.25}$ $[C_4H_6O_2]_{0.25}$	75.94	7.97	2.77	6.32	7.00	--
experimental	73.36	7.94	2.60	--	0.00	16.10
PA2030						
$[C_8H_8]_{0.50}$ $[C_{12}H_{18}NCl]_{0.30}$ $[C_4H_6O_2]_{0.20}$	75.96	8.04	3.16	4.82	8.01	--
experimental	71.97	8.19	2.68	--	0.29	16.87

[a] Experimental results were calculated by difference from 100%.

DRIFTS Analysis. Broad absorptions between 3400 and 2400 cm^{-1}, characteristic of the COOH group occurred in DRIFTS spectra of hydrolyzed samples. Figure 1 shows the overlaid carbonyl region of DRIFTS spectra of 20/30N and PA2030

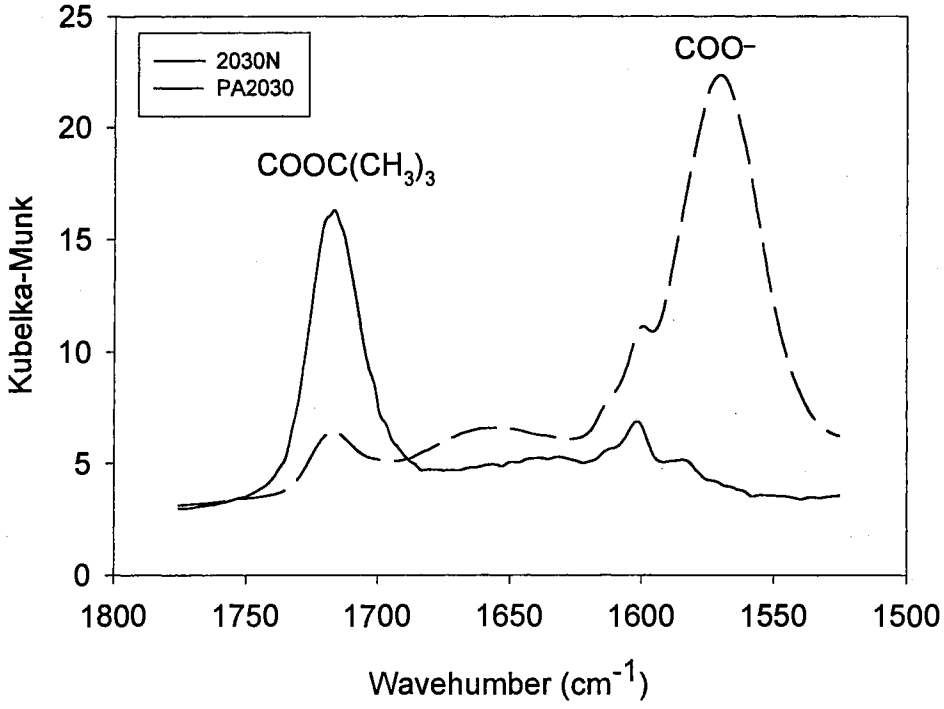

Figure 1. DRIFTS spectra of 20/30N and PA2030 microgels.

microgels. Before hydrolysis (20/30N), the C=O stretching absorption of the ester group was at 1726 cm^{-1}. After hydrolysis (PA2030), the C=O stretching absorption of the carboxylate ion occurred at 1566 cm^{-1}. Relative conversions of *t*-butyl groups were determined by normalizing the absorptions at 1495 (aromatic ring stretch of styrene) and 1454 cm^{-1} (aromatic ring + CH_2 symmetric (scissors) stretch of styrene),[15] and measuring the areas of the peaks at 1726 cm^{-1} for the two samples. Conversions of *t*-butyl groups, determined by DRIFTS, are presented in Table 5. The possible errors in DRIFTS analysis are minimized by applying the Kubelka-Munk function, which is analogous to absorbance. The Kubelka-Munk function is a mathematical simplification achieved by neglecting reflectance due to the supported materials. Other possible errors would be in the measurement of the areas under the peaks at 1726 cm^{-1}. These errors should not be greater than 2% to 3%.

Table 5. Carboxylate and *p*-Toluenesulfonate Contents of Polyampholyte Microgels.

	COOH (mol%)		PTSA (mol%)	
Sample	DRIFTS	Conductivity	Conductivity	UV-vis
PA2525	22.5	23	3.1	3.2
PA2030	17.5	19	6.5	6.8

Conductivity/pH Titrations. Quantification of carboxylate groups of the clean polyampholyte microgels was made by conductimetric/pH titrations. These microgels have varying amounts of sulfate groups (provided by the initiator), carboxyl groups (provided by the hydrolysis of tBMA), and PTSA (used in the hydrolysis procedure). PTSA and carboxylic acid groups were titrated using NaOH. PTSA groups are strong acids ($pK_a \cong 3$) than carboxylic acids ($pK_a \cong 4$). Total protonation of these weak acid groups for titration was ensured by adding a known amount of HCl solution before titrations.

Figures 2-3 shows the conductimetric/pH titration curves of PA2525 and PA2030 microgels, respectively. The conductivity titration curve presents four parts (sections) with different slopes that correspond to titration of (1) initiator sulfate groups and added HCl, (2) the weaker PTSA groups, (3) the weakest acid COOH groups, and (4) excess NaOH. Differences between slopes of a strong acid group and a weak acid group are due to the lower dissociation of the hydrogen of the weak acid.

In region (1), conductivity decreases because H^+ is replaced by Na^+ and Na^+ has a lower equivalent conductance (**7**).

$$H^+ Cl^- + Na^+ OH^- \longrightarrow Na^+ Cl^- + H_2O \quad (7)$$

In region (2), conductivity continues to decrease at a different slope because $C_7H_7SO_3H$ becomes $C_7H_7SO_3^-Na^+$ (**8**).

$$C_7H_7SO_3^- H^+ + Na^+OH^- \longrightarrow C_7H_7SO_3^- Na^+ + H_2O \quad (8)$$

In region (3), conductivity increases because polymeric COOH becomes $COO^- Na^+$ and poly(COO^-) is nonconducting (**9**).

$$RCOOH + Na^+OH^- \longrightarrow COO^- Na^+ + H_2O \quad (9)$$

In region (4), excess $Na^+ OH^-$ increases the conductivity. Conductivity measurements revealed PA2525 contained 1.59 mmol/g COOH and 0.248 mmol/g PTSA (average repeat unit was calculated to be 126 g/mol for determination mol%), and PA2030 contained 1.43 mmol/g COOH and 0.496 mmol/ g PTSA (average repeat unit was calculated to be 132.5 g/mol). In Table 5, the mol% of COOH and PTSA corresponding to PA2525 and PA2030 microgels are presented. The possible errors in determining the concentrations of COOH and PTSA come from measuring the breaking points for each conductimetric titration curve. In order to determine relative errors, several different slopes were made to determine different breaking points. The largest error from those assumptions gave <5 % error or PA2525 = 23 ± 1% and PA2030 = 18 ± 1% COOH.

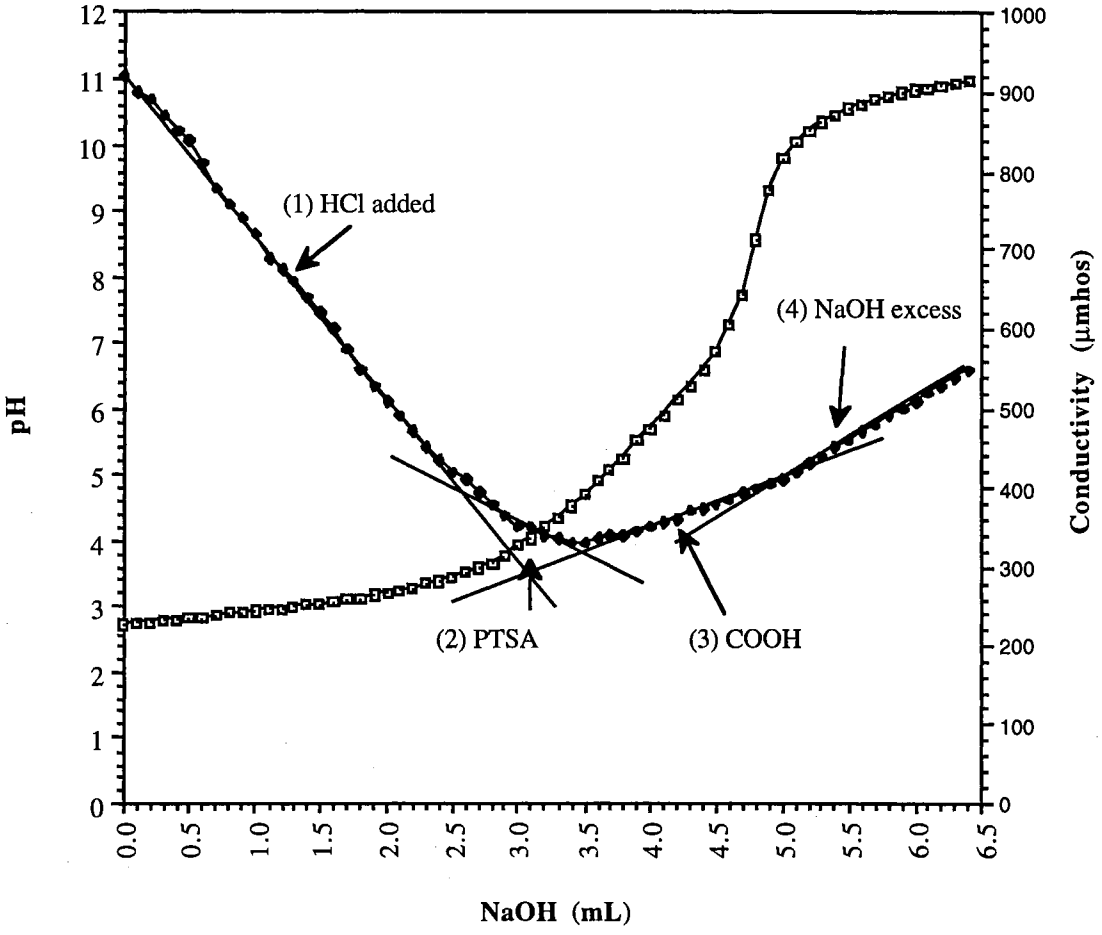

Figure 2. Conductivity/pH titration curves for PA2525 microgel.

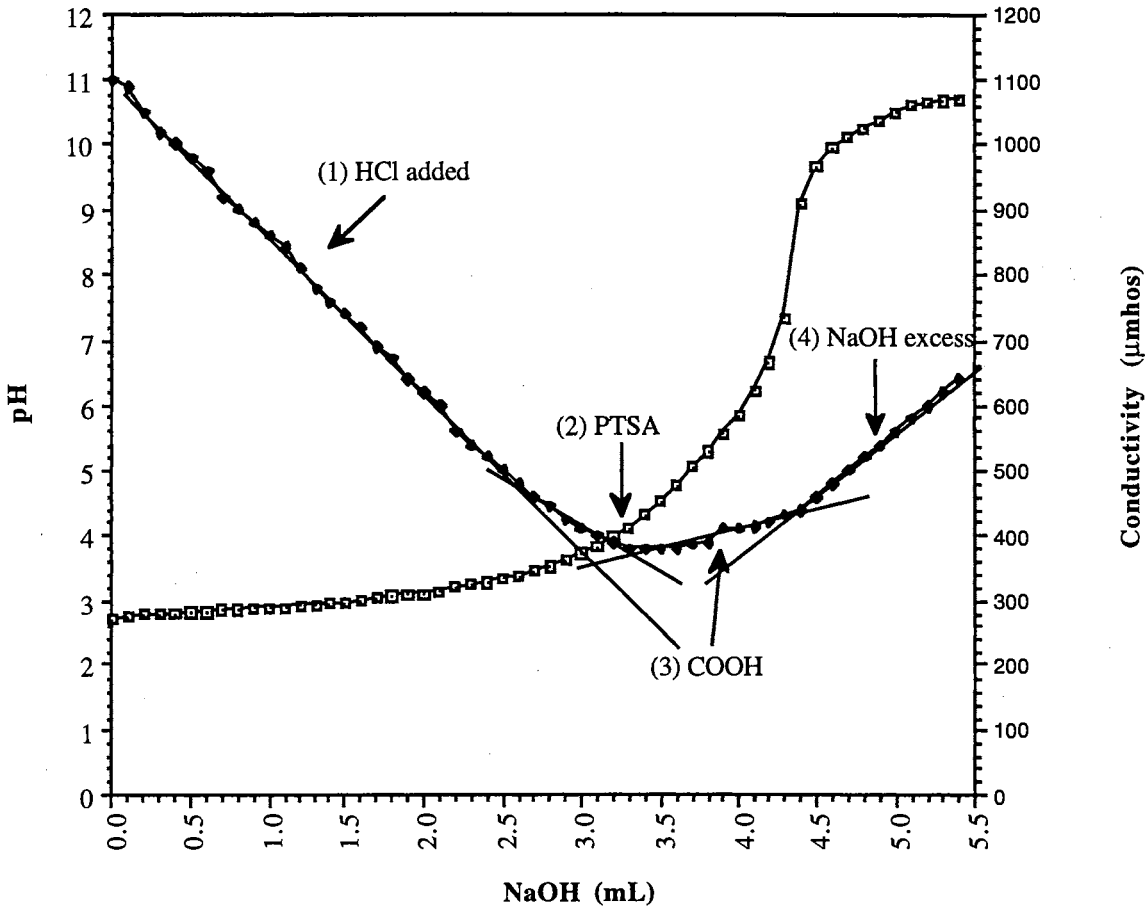

Figure 3. Conductivity/pH titration curves for PA2030 microgel.

UV Analysis of PTSA. The amount of PTSA in the latex was also determined by UV-vis spectrophotometry. Polyampholyte microgels were placed in 4 M NaCl and the pH was lowered to 2.5 with HCl. This procedure displaced PTSA from the latexes. A Beer's law plot for PTSA was constructed to determine the extinction coefficient of PTSA in water (Appendix, Figure 8). UV-vis analysis of the filtrate, collected from passing the latex through a 0.1 μm filter, revealed the concentration of PTSA in the latex. Values obtained by UV-vis are within 4.5% of those obtained by conductivity titrations (Table V). The possible error in determining the concentration of PTSA by UV-vis come from the determination of the extinction coefficient by the Beer's law plot, and the expected error is less than 2%.

Summary of Polyampholyte Microgel Compositions. The compositions of PA2525 and PA2030 microgels can be determined from Tables 2 and 5. N^+ sites were determined to be 24 mol% for PA2525 and 29 mol% for PA2030 by averaging the data obtained from chloride and elemental analysis. The COO^- sites were determined to be 23 mol% for PA2525 and 18 mol% for PA2030 by averaging the data obtained from DRIFTS analysis and conductivity titrations. Therefore, the excess N^+ sites for each microgel is $1N^+$ and $11N^+$ for PA2525 and PA2030, respectively. PA2525 contains 3 mol% PTSA and PA2030 contains 6 mol% PTSA by averaging the data obtained from conductivity titrations and UV-vis studies (Table 5). Both of these values are not consistent with excess N^+ sites; however, these microgels might not be fully dissociated and PA2030 did show some traces of chloride in the elemental analysis (Table 3). Yet,

two independent studies resulted in a concentration for PTSA that were within 2% of each other. The compositions are dipicted in Scheme 5.

Scheme 5. Compositions of PA2525 and PA2030 microgels.

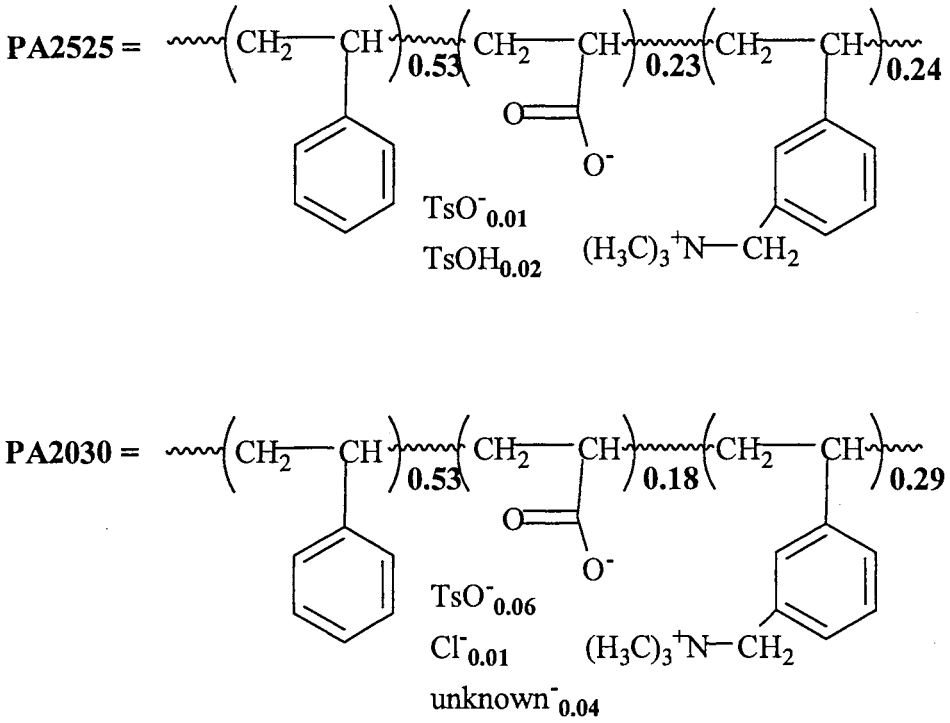

Microgel Stability. Stabilities of the quaternary ammonium chloride microgels (25/25N, 20/30N, PA2525 and PA2030) in barium chloride were examined turbidimetrically by a modifying a method of Ottewill and Satgurunathan.[16] Results are presented in Figures 4-8. The results with 25/25N and 20/30N microgels were identical, and only the results for 20/30N microgel are presented. Figure 4 revealed the typical instabilities of charge stabilized microgels: an initial increase in turbidity occurred followed by a sharp decrease. This type of initial increase in turbidity starting at $\log[BaCl_2] = -0.5$ was observed in previous studies[16] and was attributed to the presence of small aggregates from slow coagulation. The sharp fall starting at $\log[BaCl_2] = -0.2$ was attributed to more extensive coagulation occurring as a consequence of compression of the electrical double layer.[16] After 16 h, the changes of turbidity for aggregation and complete coagulation are enhanced supporting the rationale of slow coagulation. These results can also be seen photographically (Figure 5). The picture of cuvettes, in the turbidity experiment after 48 h, demonstrates that typical charge stabilized microgels are not useful in high concentrations of electrolytes. Even at concentrations of barium chloride that show small aggregates and slow coagulation, charge stabilized microgels are not useful due to phase separation.

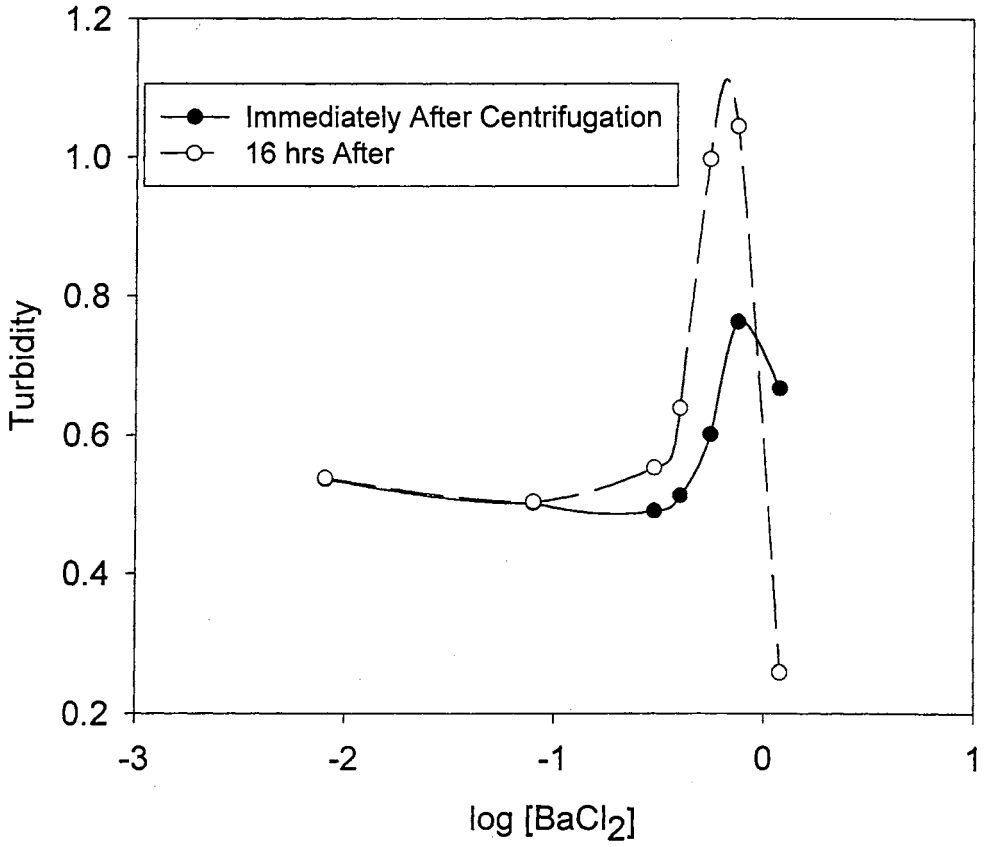

Figure 4. Turbidity of 20/30N microgel in $BaCl_2$.

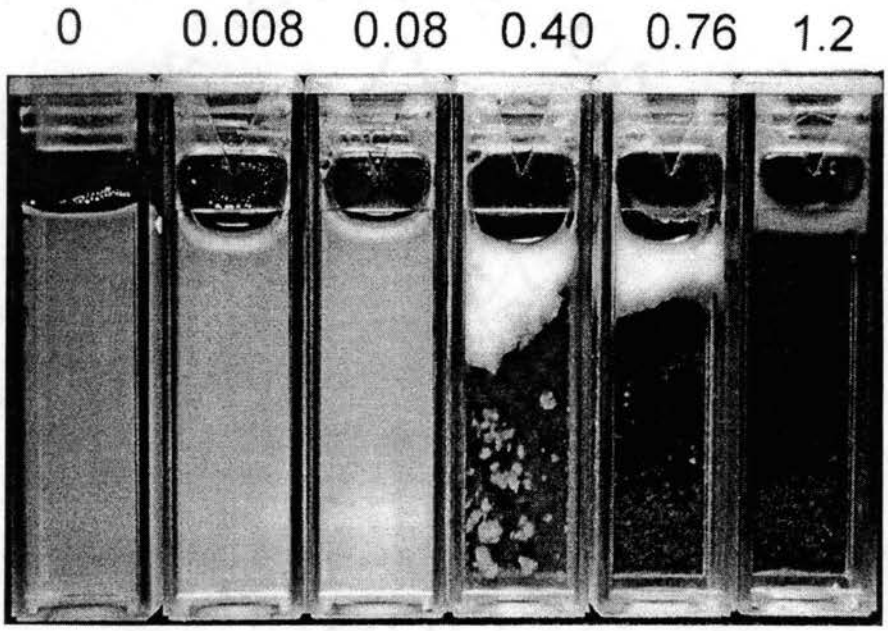

Figure 5. Effect of $BaCl_2$ concentration (M) on the 20/30N latex after 48 h.

Conversely, after hydrolysis of *tert*-butyl groups, polyampholyte latexes with both (+) and (-) moieties (PA2525 and PA2030) showed no change in turbidity to 1.2 M $BaCl_2$. Only results of the PA2030 microgel are presented (Figure 6-7), since the PA2525 results were identical. Figure 6 shows a slight decrease in turbidity with increasing barium chloride concentration. Since there is no change after 16 h, the decrease in the turbidity is not due to aggregates or coagulation, and may be attributed to decrease in the difference between the refractive indices of the solution and the polymer with increasing $BaCl_2$ concentration. These results are represented pictorially in Figure 7. The picture of cuvettes in the turbidity experiment after 48 h for the PA2030 and PA2525 microgels demonstrates that turbidity remained unchanged. Turbidity of the PA2030 and PA2525 latexes showed no change after 6 months in $BaCl_2$ concentrations up to 1.2 M.

The same trend was observed in immediate coagulation kinetics experiments. Figure 8 shows stability curves for a 20/30N microgel (20 mol% tBMA and 30 mol% quaternized VBC units). The initial slope of each of these curves is directly proportional to initial coagulation rate. These instabilities are represented pictorially (Figure 9). Both quaternized microgels (20/30N and 25/25N) showed a positive slope at 0.4 M NaCl. Stability curves for the polyampholyte microgels did not show a positive slope at 4 M NaCl (Figure 10). Therefore, the polyampholyte microgels do not form aggregates at this concentration. These results are represented pictorially in Figure 11.

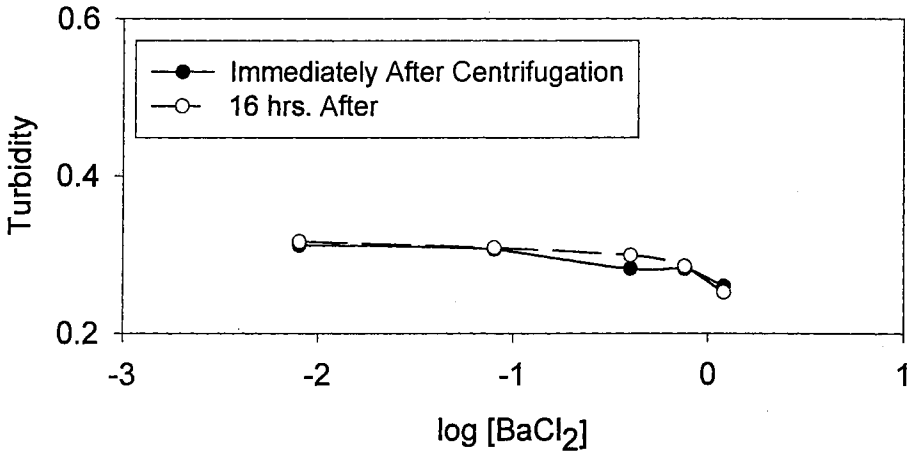

Figure 6. Turbidity of PA2030 microgel in $BaCl_2$.

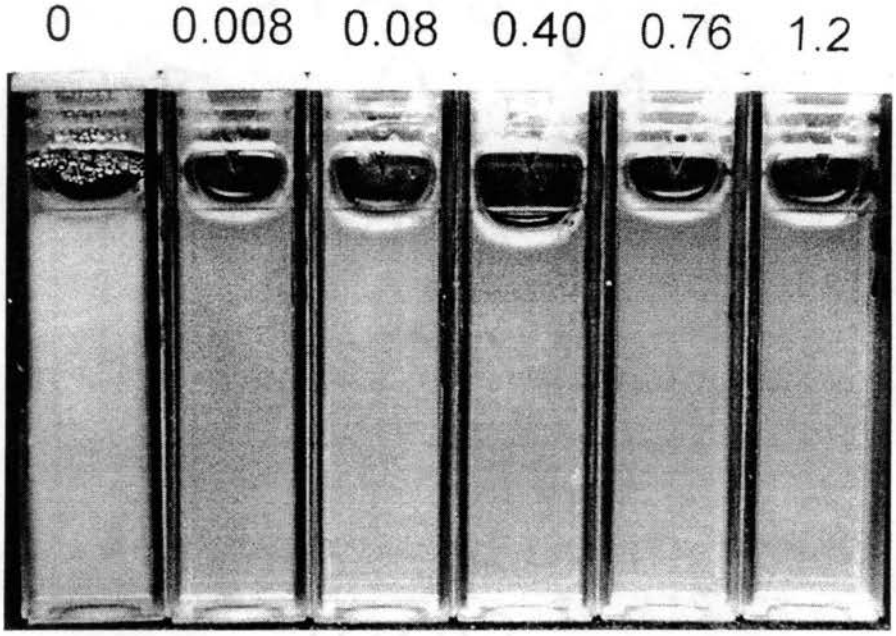

Figure 7. Effect of $BaCl_2$ concentration (M) on the PA2030 latex after 48 h.

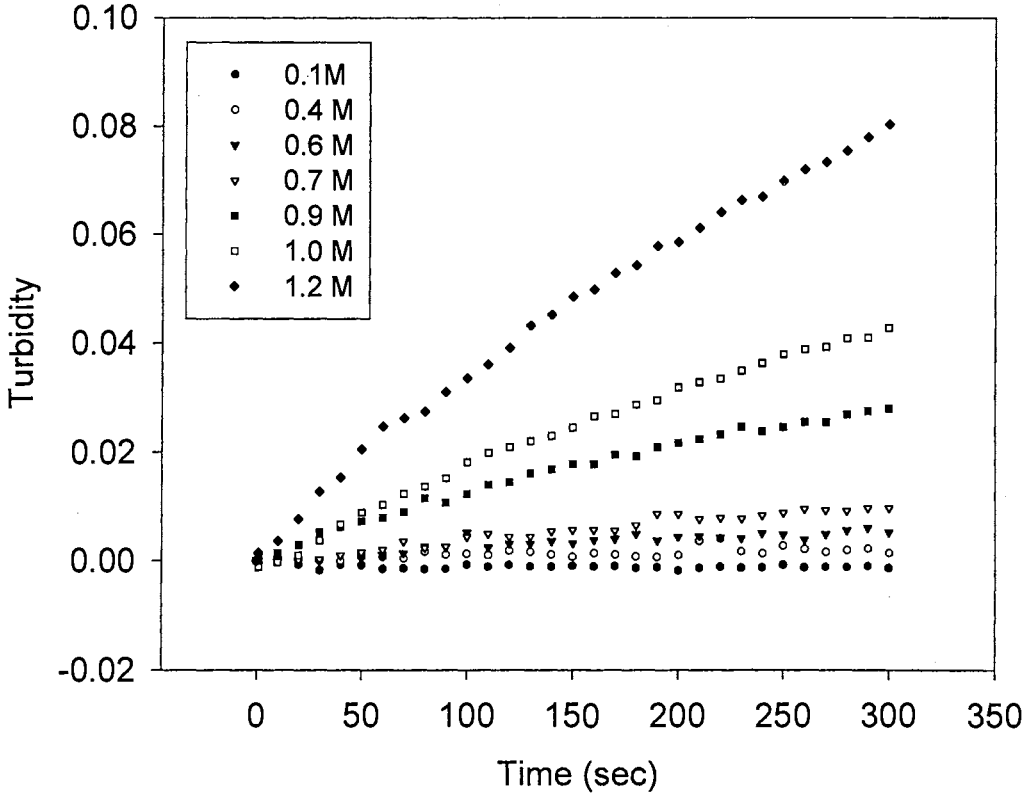

Figure 8. Coagulation kinetics of 20/30N microgel in NaCl.

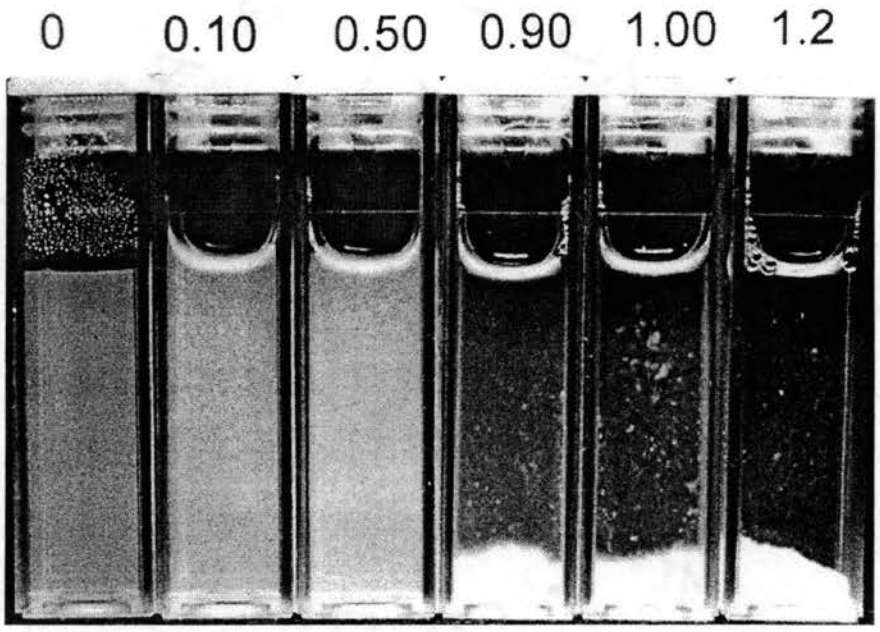

Figure 9. Effect of NaCl concentration (M) on the 20/30N latex after 48 h.

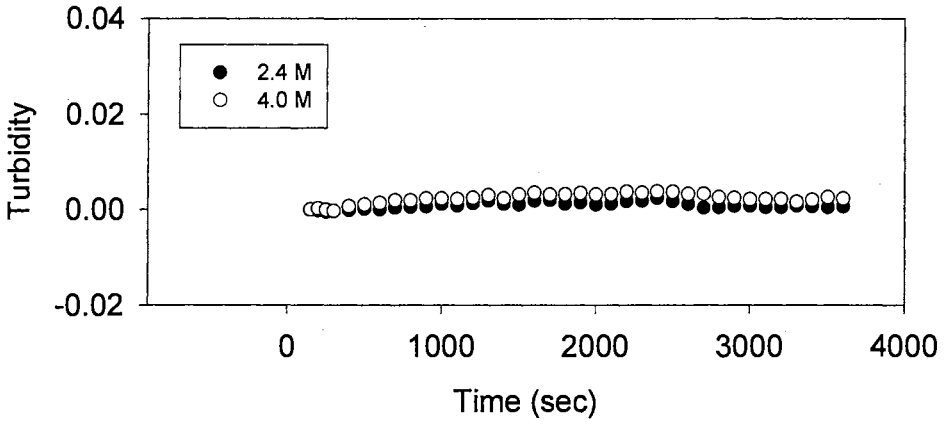

Figure 10. Coagulation kinetics of PA2030 microgel in NaCl.

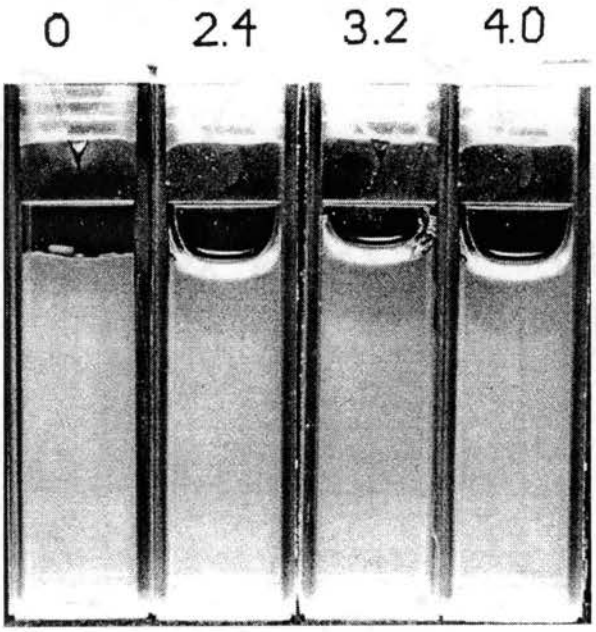

Figure 11. Effect of NaCl concentrations (M) on the PA2030 latex after 48 h.

The microgels 20/30N and 25/25N have the same stabilities in $BaCl_2$ and NaCl solutions, due to the small differences in the quaternary ammonium ion contents (30 and 25 mol% respectively). The polyampholyte latexes PA2030 and PA2525 with charge ratios of 62/38 and 51/49 (N^+/COO^-, Scheme 5) are equally stable in $BaCl_2$ and NaCl solutions. However, the stabilities of the polyampholytes do differ with respects to pH changes. The PA2030 microgel is always on the cationic side (excess N^+ sites) and its stability is unaffected by pH changes; PA2030 is stable in pH 11.3 solutions. However, increasing the pH in the PA2525 latex a different result was found (Figure 12). A positive slope can be seen at pH = 9.4, and complete aggregation is seen at pH = 9.9 in 5 min. Due to the pK_a of the carboxylic acid groups, different degrees of dissociation can occur. Referring to pH and conductivity titrations of polyampholyte microgels (Figure 2-3), the mean COOH pK_a is approximately 4, and the weakly acidic groups are fully dissociated at a pH >9. For this reason, stabilities of polyampholyte microgels differ. Within experimental error, PA2525 has equal numbers of quaternary ammonium and carboxylate groups, and therefore could have an isoelectric point. The turbidities in Figure 12 suggest that there is an isoelectric point at pH $\approx$ 9.9.

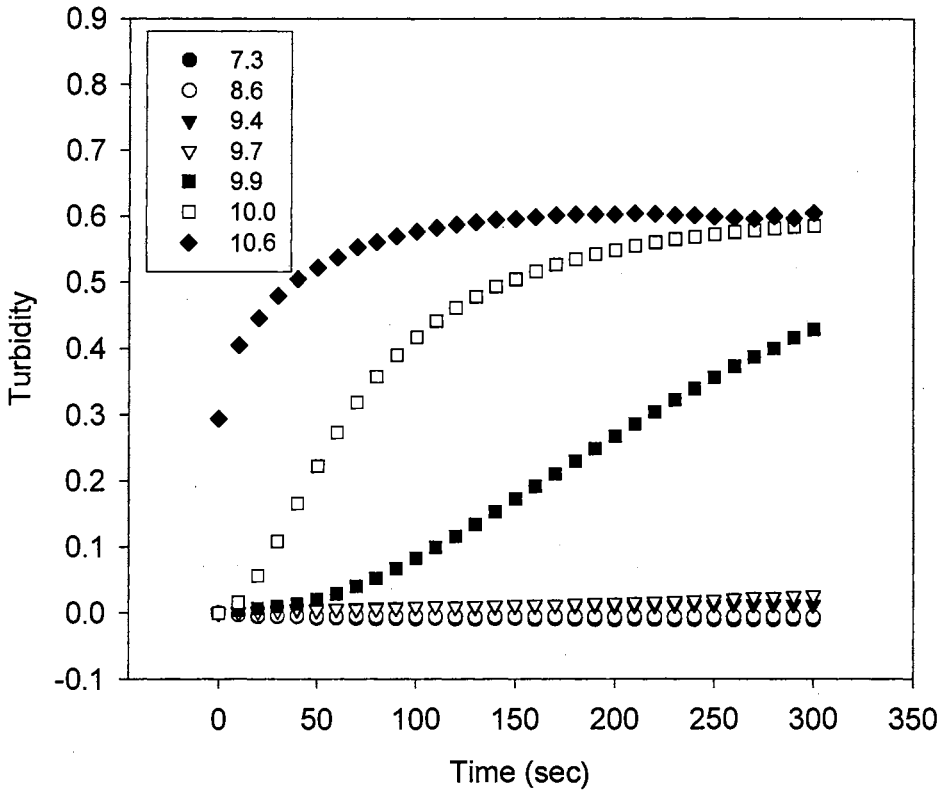

Figure 12. Coagulation kinetics of the PA2525 microgel at varied pH.

Moreover, an experiment was conducted by first placing the PA2525 latex in 4 M NaCl, which shows no aggregation, followed by addition of NaOH adjusting the pH to 10.6. In this experiment, the PA2525 microgel is stable. This suggests that the stability of polyampholyte microgels in high electrolyte solution is not due to electrostatic replusions. Therefore, the mechanism of stabilization of these microgels appears to be due to a steric mechanism. This mechanism will be further discussed when discussing the particle sizes under different conditions below.

Stability in Synthetic Seawater. Applications for stable microgels in high electrolyte solutions cover many fields including wastewater purification, lubricants, and drug delivery. Because a majority of the earth's surface is covered with oceans, a large field for exploration would be applications in seawater. Similar coagulation kinetic experiments were conducted with the microgels in synthetic seawater: Instant Ocean®. Instant Ocean's® composition is presented in the Appendix (Table 1). Immediate coagulation could not be detected in any microgel samples; however, after seven days, a noticeable change in the turbidity was observed. Charge stabilized latexes (25/25N and 20/30N) had increased turbidity while polyampholytes (PA2525 and PA2030) did not change. After one month of storage, phase separation in charge stabilized microgels was evident, and there were no changes in the polyampholyte samples. The slow coagulation of charge stabilized microgels may prevent long term seawater applications, whereas the stabilities of polyampholyte microgels could make them useful for applications in oil recovery and numerous naval applications.

Particle Sizes under Different Conditions. The measurements reported in Table 6 show that the microgels have dry particle diameters of 140-160 nm determined by TEM, and are quite monodisperse with $d_w/d_n \leq 1.04$. The swollen diameters are 190-230 nm by DLS. Swelling and deswelling of ion exchange latexes depend on their degree of cross-linking, amount of ionic groups, and affinity of fixed ionic groups and their counterions for water. This is explained via three expansion and contraction forces: (1) Fixed ionic groups and their counterions gain solvation shells due to ion-dipole attractions. (2) Electrostatic repulsion increases the distance between fixed ion groups when they dissociate in water. (3) High concentrations of ions in the particle create an osmotic pressure between the particles interior and external solution. Because the latexes are all 0.9 mol% cross-linked, the amounts of fixed ionic groups in the latexes makes them swell and deswell differently in water. Higher ion content makes latexes swell more. This trend can be seen in Table 6; where the swelling factor decreased with decreasing N^+ sites 30 > 25 > 20.

Table 6. Sizes and Swelling of Microgels in Water.[a]

	Diameters , nm			
	TEM		DLS	Swelling Factor
Sample	d_w	d_w/d_n	d_h	$(d_h/d_n)^3$
2030N	153.4	1.021	226.8	3.5
2525N	156.1	1.034	210.5	2.7
3020N	156.3	1.017	193.4	1.9
PA2030 ($18O^-/29N^+$)	149.5	1.026	220.2	3.6
PA2525 ($23O^-/24N^+$)	139.9	1.042	212.7	4.0

[a] In pure water with no added electrolytes, pH's of latexes before dilutions ranged from 6.4 to 5.5.

Hydrodynamic sizes of the cationic microgels (20/30N and 25/25N), measured by DLS in increasing concentrations of NaCl, are shown in Figure 13. The sizes of the microgels decrease when a small amount of salt is added (0.01 M NaCl). Added NaCl screens the charges on the particles and decreases the degree of dissociation of the counterions from the particles; therefore, interparticle electrostatic repulsion is reduced. Moreover, NaCl ions cause an osmotic pressure difference between the interior of particles and the external solution resulting in decreasing the counter-ion cloud surrounding the particles. A "snail effect' reduces the water volume in the electrical double layer and changes the diffusion coefficient D in equation 1. The term "snail effect" refers to the elimination of water in a snail or slug when salt is placed on it. This 'snail effect' continues with increasing salt concentrations (0.01 to 0.50 M NaCl). Just beyond 0.50 M NaCl, the barrier between individual particles is collapsed and van der Waals attractions form aggregates. These aggregates are observed around 0.5 M NaCl in the coagulation kinetic experiments (Figure 8). In DLS experiments, an increase in the average diameter is evident >0.5 M NaCl, and is due to these same aggregates. When the 20/30N and 25/25N samples stood for 8 h, DLS measurements were irreproducible at concentrations higher than 0.5 M NaCl due to formation of aggregates.

Hydrodynamic sizes of polyampholyte microgels (PA2030 and PA2525), measured by DLS in increasing concentrations of sodium chloride, are shown in Figure 14. An initial decrease in particle diameters was observed as in the cationic microgel experiments. However, turbidity experiments indicate that the polyampholyte latexes are

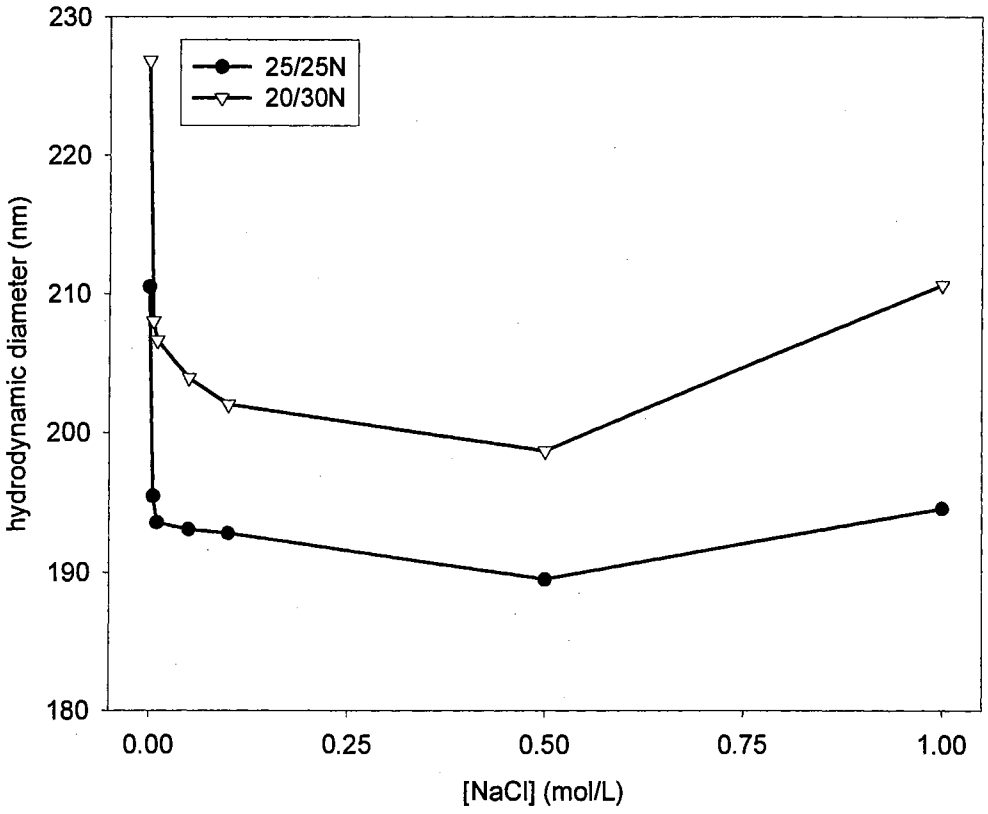

Figure 13. NaCl effect on the hydrodynamic diameter of 25/25N and 20/30N latexes.

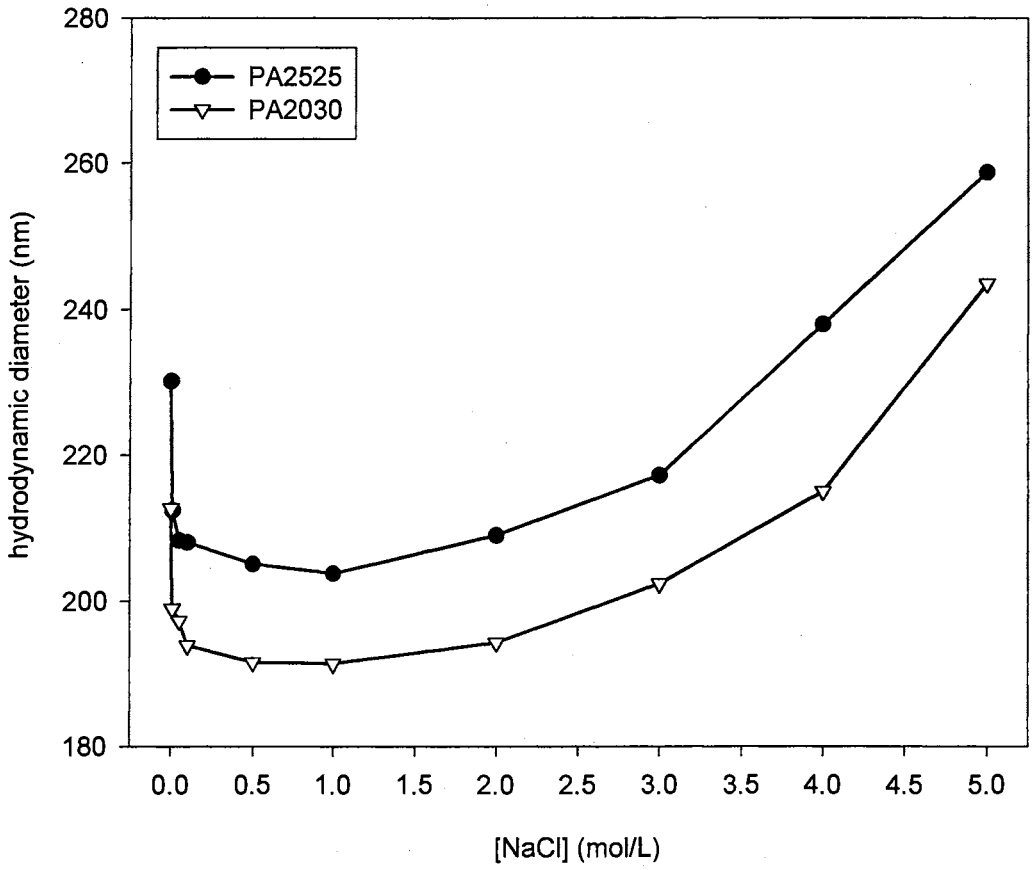

Figure 14. NaCl effect on the hydrodynamic diameter of PA2525 and PA2030 latexes.

stable and do not form aggregates in high concentrations of salts; therefore, increases in hydrodynamic diameters in high salt concentrations can only be due to swelling of the particles. Thus, polyampholyte microgels are stable in high concentrations of salts due to an "anti-polyelectrolyte effect" causing the latex to swell and become stabilized by steric interactions.

Explanation of the Polyampholyte Effect. Polyampholyte microgels are 'hairy particles' that maintain a charge balance on the latex surface with small ions of opposite sign in the solution phase (counter-ion cloud). This forms the electrical double layer (Figure 15, A). When polyampholyte microgels are in dispersions of high electrolyte concentrations the electrical double layer is disturbed due to shielding of surface groups. Concurrently, the increase in electrolyte concentration in the medium causes an osmotic effect resulting in reduction of the solvent (water) in the counter-ion cloud (Figure 15, B). The polymer chains contract due to loss of water (Figure 15, C). However, turbidity experiments proved polyampholyte microgels do not aggregate in NaCl solutions. Moreover, at concentrations ≥0.5 M NaCl, DLS measurements revealed an increase in hydrodynamic diameters. At these concentrations of sodium chloride the intrapolymer electrostatic attractions are shielded and the microgel begins to swell (Figure 15, D). This swelling extends the polymer chains into the medium giving stability to the microgels. As the concentration of NaCl increased inside the particles, more intrapolymer attractions broke apart and the hydrated ions transferred solvent (water) back into the particle (Figure 15, E). This reverse osmotic effect swells the polyampholytes increasing the steric stablization. The final measurement (4.0 M NaCl)

shows hydrodynamic diameters that are larger than the original measured diameters in pure water (Figure 15, F).

Conclusions

Polyampholyte microgels with varied functional group content, and swollen diameters of 210 and 220 nm (swelling factors of 3 and 4 respectively) were prepared. Treatment of a precursor latex with TMA, followed by hydrolysis with PTSA in two steps, produced polyampholyte microgels containing quaternary ammonium (N^+) and carboxylate (COO^-) ion repeat units. These repeat units were confirmed by chloride selective potentiometric titration and quantitative carbonyl determination by DRIFTS analysis. Polyampholyte microgels are stable in high concentrations of salt (1.2 M $BaCl_2$ and 4 M NaCl) and light scattering studies confirm a "polyampholyte effect". Unexpectedly, the microgels contained small amounts of PTSA that were not removed by dialysis of ultrafiltration after the hydrolysis experiment. The properties of the polyampholyte microgels were not affected by the PTSA at high sodium chloride concentrations.

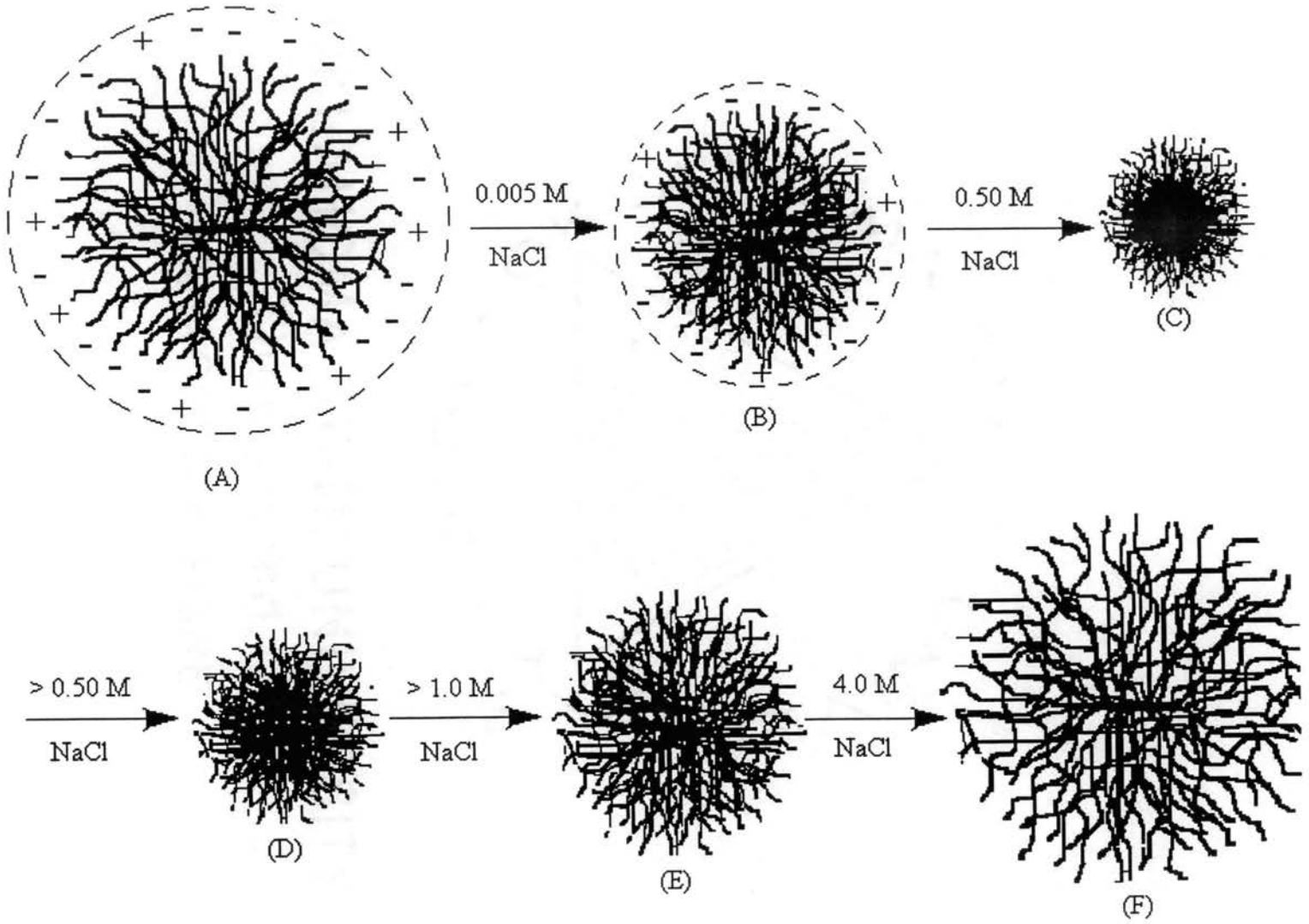

Figure 15. Effect of NaCl on polyampholyte microgels.

References

1. Alfrey, T., Jr.; Morawetz, H. M. *J. Am. Chem. Soc.* **1952**, *74*, 436-438.

2. Bekturov, E. A.; Kudaibergenov, S. E.; Rafikov, S. R. *Rev. Macromol. Chem. Phys.* **1990**, *30*, 233-303.

3. Lowe, A. B.; Billingham, N. C.; Armes, S. P. *Macromolecules* **1998**, *31*, 5991-5998.

4. Kathmann, E. E.; White, L. A.; McCormick, C. L. *Polymer* **1997**, *38*, 871-878.

5. Ruckenstein, E.; Kim, K. J. *J. Polym. Sci: Part A: Polym. Chem.*, **1989**, *27*, 4375-4388.

6. Skoog, D. A.; West, D. M.; Holler, F. J. *Fundamentals of Analytical Chemistry* ; Saunders College Publishing: New York, 1988, pp 385-387.

7. White, R. L. *Anal. Chem.*, **1992**, *64*, 2010-2013.

8. Timmermans, J. *The Physico-chemical Constants of Binary Systems in Concentrated Solutions*; Interscience Publishers, Inc.: New York, 1960, pp 303-341.

9. Mykytiuk, J.; Armes, S. P.; Billingham, N. C. *Polymer Bulletin* **1992**, *29*, 139-145.

10. Green, T. W. *Protective Groups in Organic Synthesis*; Wiley: New York, 1981, pp 154-180.

11. Patrickios, C. S.; Hertler, W. R.; Abbott, N. L.; Hatton, T. A. *Macromolecules* **1994**, *27*, 930-937.

12. No references were found when searching for THPMA or tBMA that dealt with emulsions in Chemical Abstract from 1966 to 1998 using Sci-Finder.

13. Lowe, A. B.; Billingham, N. C.; Armes, S. P. *Macromolecules* **1998**, *31*, 5991-5998.

14. Corpart, J.; Selb, J.; Candau, F. *Polymer* **1993**, *34*, 3873-3886.

15. Mark, J. E. *Physical Properties of Polymers Handbook*; AIP Press: New York, 1996, p 295.

16. Ottewill, R. H.; Satgurunathan, R. I *Colloid Polym Sci.* **1988**, *266*, 547-553.

CHAPTER IV

DECARBOXYLATION OF 6-NITROBENZISOXAZOLE-3-CARBOXYLATE IN POLYAMPHOLYTE MICROGELS

Abstract

Polyampholyte microgels with quaternary ammonium and carboxylate ion exchange sites catalyze the decarboxylation of 6-nitrobenzisoxazole-3-carboxylate (6-NBIC) in aqueous salt dispersions. A catalytic rate constant of 115-60 times the rate constant in water was achieved in particles containing 18/29 and 23/24 mol percent of (-) and (+) repeat units. Decarboxylation kinetics fit an enzyme model of micellar catalysis. Added electrolyte decreases the rate of decarboxylation but increases the intrinsic catalytic rate constants in more highly swollen microgels. Because of colloidal stability in high concentrations of electrolytes, reactions in polyampholyte microgels can be carried out at > 0.5 M NaCl.

Introduction

Unimolecular decarboxylation of 6-nitrobenzisoxazole-3-carboxylate anion (6-NBIC, **1**) is notable for its remarkable sensitivity to the reaction medium.[1-2] The decarboxylation rate increases by 8 orders of magnitude going from water to hexamethylphosphoramide.[3-4] Sensitivity to the medium has led to extensive use of unimolecular decarboxylation of 6-NBIC (**1**) as a probe of the microenvironment in micelles,[5-16] bilayers,[8-9] microemulsions,[17-19] polysoaps,[20-25] polymer and silica gels,[26-29] poly(crown ethers),[30-33] and catalytic antibodies.[34-35] Rate acceleration can be largely attributed to partial dehydration of the carboxylate function of the initial state in the hydrophobic microenvironment.[34]

Scheme 1. Decarboxylation of 6-Nitrobenzisoxazole-3-carboxylate (6-NBIC, 1)

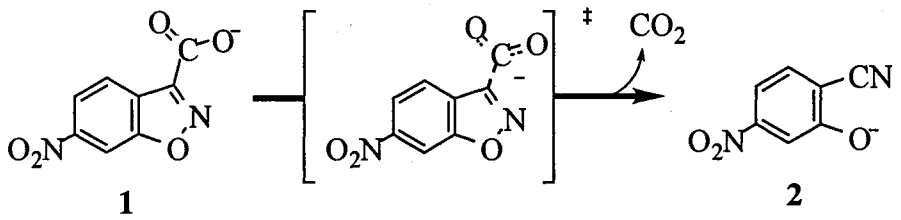

Previous work in our labs utilized cross-linked cationic polystyrene latexes to catalyze the unimolecular decarboxylation of 6-NBIC.[36] For example, the rate constant of decarboxylation of 6-NBIC is up to 21,000 times faster in polystyrene latexes containing quaternary ammonium ion sites than in water alone.[36] This is the largest rate

enhancement reported at 25 °C for the decarboxylation of 6-NBIC in any colloidal or polymeric medium.

In our previous studies, the influence of NaCl on the decarboxylation of 6-NBIC was investigated. Because the latexes are swollen microgels, an increase in intrinsic rate constants was observed at less than 0.005 M NaCl concentrations due to deswelling (water content is reduced) of the latexes. At greater than 0.005 M NaCl concentrations, rate constants decreased due to competitive ion-exchange inhibition. These experiments could not be conducted with cationic latexes at NaCl concentrations greater than 0.1 M due to colloidal instability. The effect of added electrolytes to the unimolecular reaction has been examined in cationic micelles,[6] and poly(crown ethers).[30] In general, added salts inhibit catalysis by excluding ionic reactants from the pseudophase; however, some added electrolytes enhanced the micellar-catalysis of 6-NBIC.[6]

In this chapter, we provide further insight into the relationship of colloidal stability-reactivity to rate enhancement of the unimolecular decarboxylation of 6-NBIC in aqueous salt solutions by using polyampholyte microgels.

Experimental

Materials. Methyl 6-nitrobenzisoxazole-3-carboxylate (Pfaltz & Bauer) was recrystallized from methanol to yield light yellow needles that were characterized by NMR and IR analysis and had a mp 130-131°C [lit.[37] mp = 131-132 °C]. Deionized water with conductivity of 0.65 μmhos was used in all work. Kinetic experiments were performed on a Hewlett Packard diode array UV/VIS spectrophotometer (model 8452A) equipped with a thermostated cell block and circulating water bath.

6-Nitrobenzisoxazole-3-carboxylic acid (6-NBIC, 1). 6-NBIC was prepared by heating its methyl ester in 80% aqueous sulfuric acid on a steam bath for 20 min and then pouring the reaction mixture into ice water.[6,38] The white solid, after drying in vacuo, had mp 167-169 °C [lit.[38] mp = 167-169 °C (monohydrate)]. A ^{1}H-NMR spectrum showed 90 mol% carboxylic acid and 10 mol% methyl ester. The crude product was recrystalized from a mixture of acetone and heptane to produce light yellow needles that were filtered and washed with chloroform. These crystals contained no methyl ester by ^{1}H-NMR analysis and less than 5% of the decarboxylation product, 2-cyano-5-nitrophenoxide, by ^{1}H NMR analysis, and were used for kinetic studies without further purification.

Kinetic Experiments and Calculations. A 0.0133 M stock solution of 6-nitrobenzisoxazole-3-carboxylic acid for kinetic measurements was prepared in ethanol containing 2 mM HCl. The latex samples were diluted to a solid content of 0.5 mg/mL. A 2.00 mL aliquot of latex was diluted to 50.00 mL with 2.4 mM NaOH solution (pH

11.3 ± 0.1). Using nitrogen-purged water the latex/buffer solutions were stored in an air-tight polyethylene container. In a typical kinetic run, 3.00 mL of the latex/buffer solution was pipetted into a polystyrene cuvette, stoppered, and placed in the sample chamber of a UV-vis spectrophotometer thermostated at 30.0 ± 0.1 °C. After 15 min, 30 μL of the substrate solution was added and mixed by rapid shaking for 2 s. The λ_{max} of the decarboxylation product, 2-cyano-5-nitrophenoxide, was 398 nm in water and 426 nm in latexes. A UV-vis spectrum was taken every 0.9 s, and the average Abs from 400-430 nm was plotted as a function of time. First-order rate constants (k_{obs}) for appearance of 2-cyano-5-nitrophenoxide were calculated by linear least-squares fitting of the data to the integrated form of the first-order rate equation: $\ln(A_\infty - A_t) = \ln(A_\infty - A_0) - k_{obs}t$, where A_t, A_0 and A_∞ refer to the absorbances at times t, 0, and ∞. The value of A_∞ was determined manually, and calculations were made from data over the first 20% conversion. Rate constants measured in duplicate were within 5% of the mean.

Results and Discussion

Microgels used in Decarboxylation of 6-NBIC. Latexes used for the decarboxylation study were synthesized by emulsion copolymerization of styrene, *m,p*-vinylbenzyl chloride (VBC), *tert*-butyl methacrylate (tBMA), and divinylbenzene (DVB).[39] The mol fractions of tBMA and VBC in the polymerizations were 20/30 and 25/25 for the two latexes respectively. After quaternization with trimethylamine and hydrolysis of *tert*-butyl groups, the latexes contained 18/29 and 23/24 mole ratios of carboxylate to quaternary ammonium ions. The polyampholyte latexes, PA2030 and PA2525, contained 3 and 6 mol% of PTSA, respectively. Latexes were characterized by transmission electron microscopy (TEM) and dynamic light scattering (DLS) in order to determine the sizes under dry and swollen conditions, respectively (Table 1). The polydispersity indexes d_w/d_n by TEM were less than 1.04.

In the notation 20/30N, means the copolymer is a cationic microgel, 20 refers to mol% of *tert*-butylmethacrylate and 30 to mol% of VBC in the polymerization. In the notation PA2030, PA means the copolymer is a polyampholyte, 20 refers to mol% of the carboxylate precursor monomer and 30 to mol% of the quaternary ammonium precursor monomer in the polymerization. The experimentally determined contents were 18 and 29 mol% respectively. Quaternized/hydrolyzed latexes were purified by ultrafiltration to remove possible low molar mass solutes until the filtrate reached a constant low conductivity (<2.3 μmhos).

Table 1. Sizes and Swelling of Microgels in Water.[a]

	Diameters, nm			
	TEM		DLS	Swelling Factor
Sample	d_w	d_w/d_n	d_h	$(d_h/d_n)^3$
2030N	153.4	1.021	226.8	3.5
2525N	156.1	1.034	210.5	2.7
3020N	156.3	1.017	193.4	1.9
PA2030 ($18O^-/29N^+$)	149.5	1.026	220.2	3.6
PA2525 ($23O^-/24N^+$)	139.9	1.042	212.7	4.0

[a] In pure water with no added electrolytes, pH's of latexes before dilutions ranged from 6.4 to 5.5.

Decarboxylation Kinetics. Decarboxylation of **1** in aqueous solution accelerated upon addition of polyampholyte and cationic latexes as evidenced by rapid appearance of the yellow product, 5-nitro-2-cyanophenoxide (**2**). Typical plots of the first-order rate constant (k_{obs}) for decarboxylation as a function of quaternary ammonium ion concentration in the latex are shown in Figures 1-4. First-order rate constants (k_{obs}) increase with latex concentration as substrate is incorporated into the latex and should become constant when the substrate is fully bound. We were unable to reach the fully bound limit because the turbidity of dispersions with larger amounts of particles prevented measurement of product absorbance.

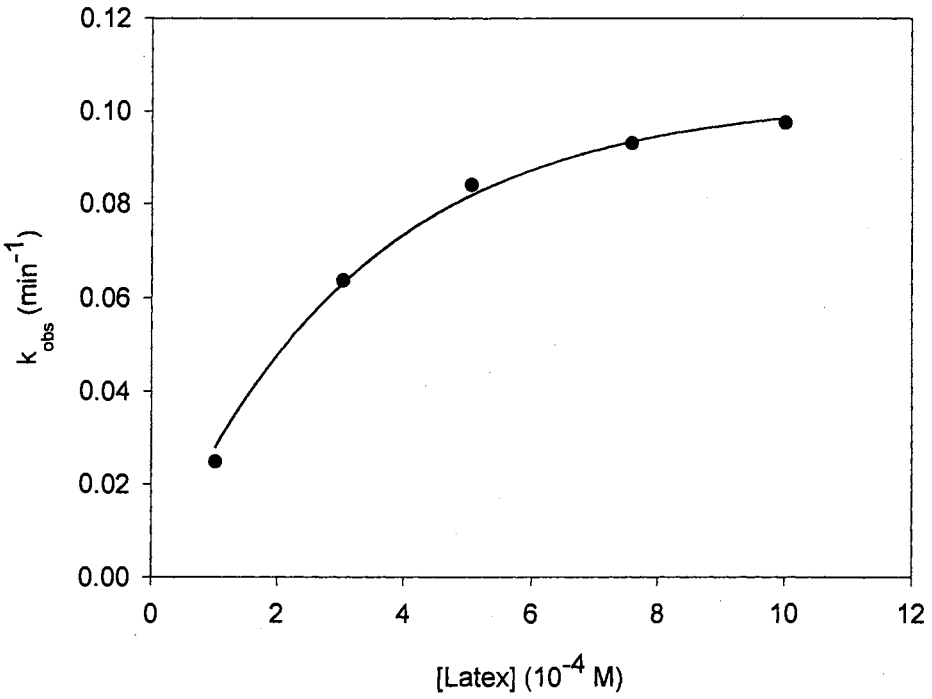

Figure 1. Pseudo-first order rate constants for decarboxylation of 6-NBIC as a function of the concentration of quaternary ammonium groups of 20/30N in 2 mM NaOH solution at 30.0 °C.

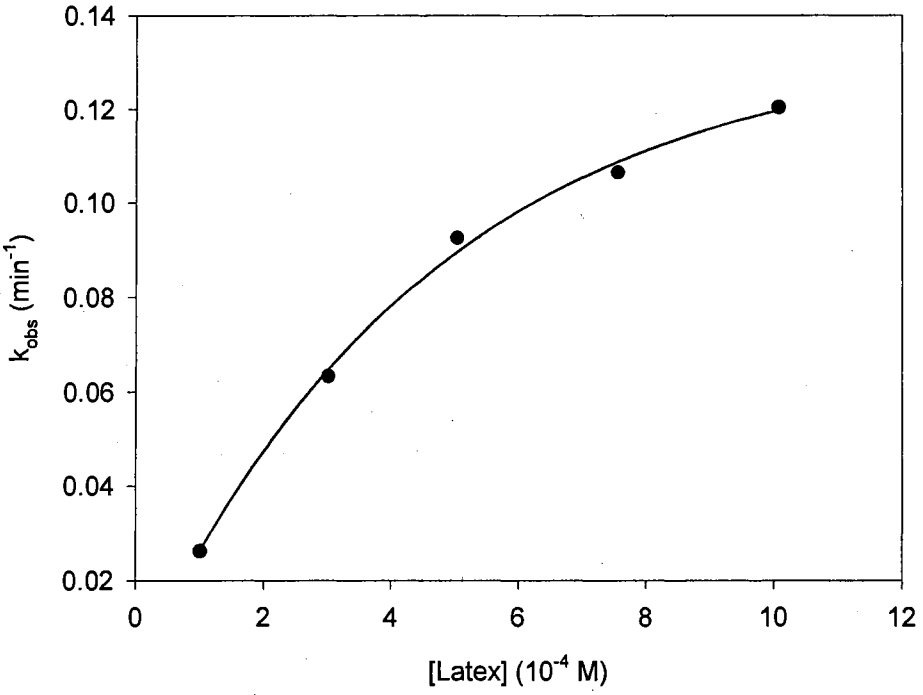

Figure 2. Pseudo-first order rate constants for decarboxylation of 6-NBIC as a function of the concentration of quaternary ammonium groups of 25/25N in 2 mM NaOH solution at 30.0 °C.

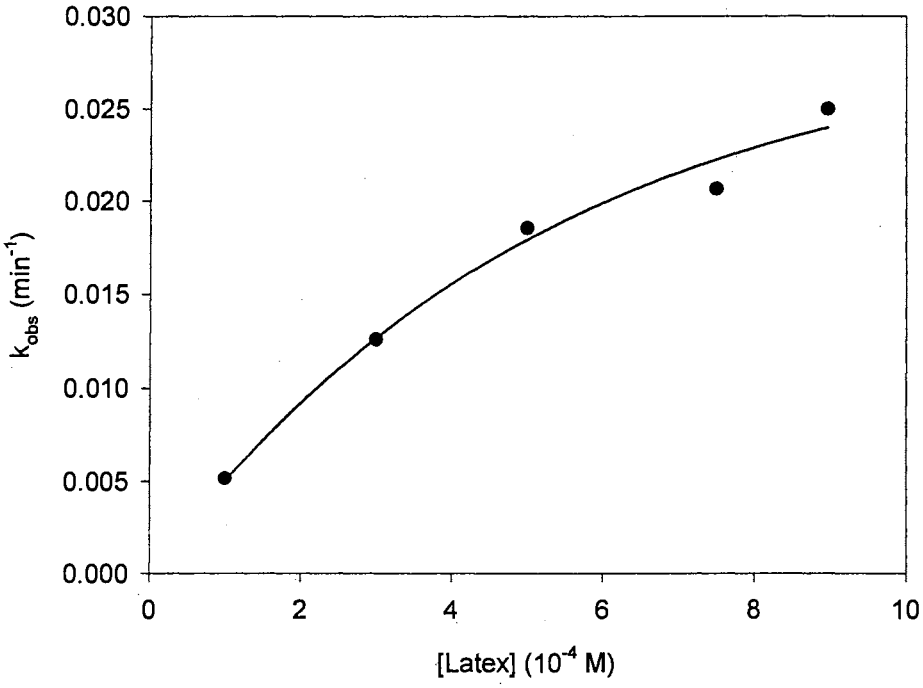

Figure 3. Pseudo-first order rate constants for decarboxylation of 6-NBIC as a function of the concentration of quaternary ammonium groups of PA2030 in 2 mM NaOH solution at 30.0 °C.

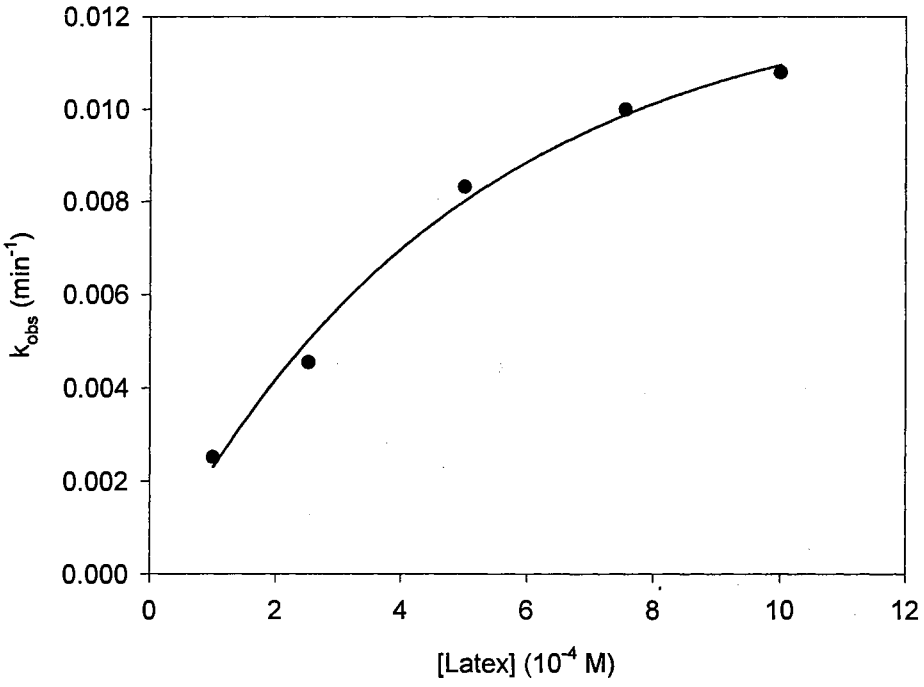

Figure 4. Pseudo-first order rate constants for decarboxylation of 6-NBIC as a function of the concentration of quaternary ammonium groups of PA2525 in 2 mM borate buffer (pH = 9.3) at 30.0 °C.

Pseudo-First Order Intraparticle Rate Constants and Equilibrium Constants. We applied the Menger-Portnoy model for pseudophase catalysis in molecular aggregates to the rate data.[40-41] Using this model, we assume substrate is distributed between the aqueous and polymer phase according to an equilibrium constant, K (Scheme 2), where [S] is the concentration of substrate in the aqueous phase, [L] is the latex concentration, and [SL] is the concentration of the substrate in the latex and all concentrations are based on total volume of the dispersion. Decarboxylation can occur either in the aqueous phase with a rate constant k_w, or inside the latex particle with a constant k_c. K is an equilibrium constant based on the total volume of the reaction mixture and does not adequately describe the concentration of substrate in the latex particle itself. Rate constants in each type of latex were measured at five different particle concentrations. Data graphed using equation (1) and examples of such plots are shown in Figures 1-4. Pseudo-first order intraparticle rate constants (k_C), and equilibrium constants (K) were obtained by regression analysis of the data from applying equation (1) to Figure 1. The independently measured rate constant k_W for hydrolysis in absence of latex was 1.84×10^{-4} min^{-1}. The decarboxylation rate constants, k_{obs}, were measured at constant initial substrate concentration and varied excess of latex.

Scheme 2. Menger-Portnoy Model for Pseudophase Catalysis.

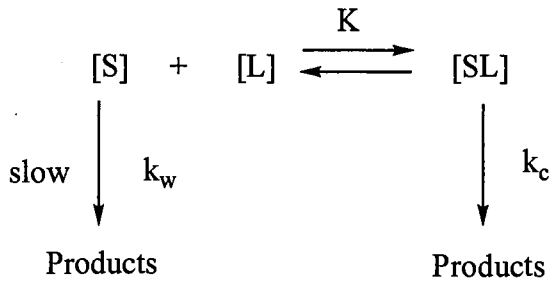

$$k_{obsd} = (k_w(1/K) + k_c\ [N^+]) / ((1/K) + [N^+]) \quad (1)$$

Similar data using latexes 20/30N, PA2030 and PA2525 are in Figures 2-4. The rate constants appear to approach a maximum as particle concentration increases. Table 2 reports pseudo-first order rate constants of decarboxylation in all of the latexes. Table 3 reports binding constants and intraparticle rate constants of decarboxylation by the latexes as well as other colloids and polymers. All latexes reported catalyze the decarboxylation in aqueous dispersions.

Table 2. Relative Rate Constants for the Decarboxylation of 6-NBIC by Microgels at 30.0 °C.[a]

	mol %				Latex[b]	k_{obs}/k_w[c]
Latex	$[N^+]$	$[Cl^-]$	$[CO_2^-]$	$[TsO^-]$	mg/mL	
2030N[d]	28	28	--	--	0.477	540
2525N[d]	24	24	--	--	0.533	670
PA2030[d]	28	1	18	6	0.423	115
PA2525[e]	24	0	23	3	0.533	60

[a] Concentration of 6-NBIC is 6.6×10^{-5} M. [b] The maximum amount of latex used. [c] The first-order rate constant in water was $k_w = 1.84 \times 10^{-4}$ min^{-1}. [d] Using 2 mM NaOH (pH = 11.3). [e] Using 2 mM borate buffer (pH = 9.3).

Table 3. Binding Constants and Relative Rate Constants for the Decarboxylation of 6-NBIC by Latexes at 30.0 °C.[a]

Latex	k_c/k_w[b]	K (M^{-1})	S_b/S_T[c]	Swelling Factor	N^+ (10^{-4} M)
2030N[d]	760	2736	0.71	3.2	10.11
2525N[d]	1070	1680	0.62	2.5	10.07
PA2030[d]	250	1320	0.46	3.9	8.97
PA2525[e]	100	1520	0.60	2.9	10.08
TMAQ39[f]	340	2600	--	--	--
Cetyltrimethylammonium bromide[g]	130	--	--	--	--

[a] Concentration of 6-NBIC is 6.6×10^{-5} M; Latex concentration (mg/mL) is given in Table 2. [b] The first-order rate constant in water was $k_w = 1.84 \times 10^{-4}$ min^{-1}. [c] Fraction of substrate bound to latex at the maximum amount used that is reported in Table 2. [d] Using 2 mM NaOH (pH = 11.3). [e] Using borate buffer (pH = 9.3). [f] Reference 36. 39 mol % of styrylmethyl(trimethyl) ammonium. [g] Reference 6.

Salt Effect on Observed Rate Constants. The decarboxylation rate in the absence of latexes is insensitive to added electrolytes.[2] However, the latex-catalyzed process is profoundly influenced by addition of electrolyte. Addition of low concentrations of NaCl to 25/25N and to 20/30N accelerates reactions until the concentrations of electrolyte and latex are approximately equal (Figure 5). At higher NaCl concentrations, the rate constants decrease to less than those in the presence of latex alone because excess chloride ions compete with carboxylate ions for binding sites in the latex thereby decreasing the observed rates. Charge-stabilized microgels (25/25N and 20/30N) were not stable at concentrations higher than 0.1 M. A_∞ could not be obtained in those experiments due to increasing light scattering from aggregate formation. Therefore, only the rate constants at concentrations ≤0.1 M NaCl are presented.

Addition of NaCl to PA2525 and to PA2030 shows a similar trend (Figure 6). However, the reaction can be carried out at higher concentrations of NaCl due to the stabilities of polyampholyte microgels. The amount of solvent (water) in the latex greatly effects the decarboxylation of 6-NBIC. The swelling ratios of the latexes in various salt concentrations can be determined from the TEM and DLS measurements in Chapter III (Table 6 and Figures 13-14) and are presented in Table 4. A initial loss of water was evident in all the microgels with the addition of 0.005 M NaCl.

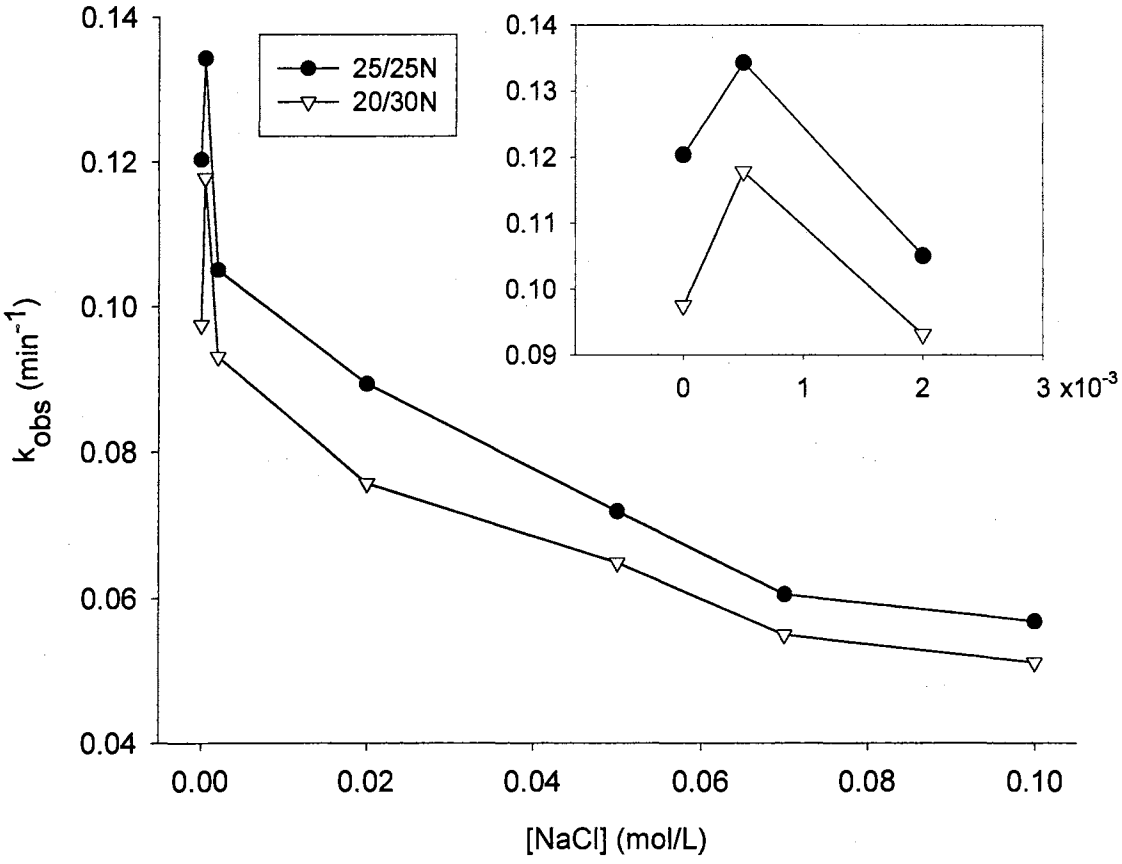

Figure 5. NaCl effect on k_{obs} for 25/25N and 20/30N latexes in 2 mM NaOH solutions (pH = 11.3) at 30.0 °C.

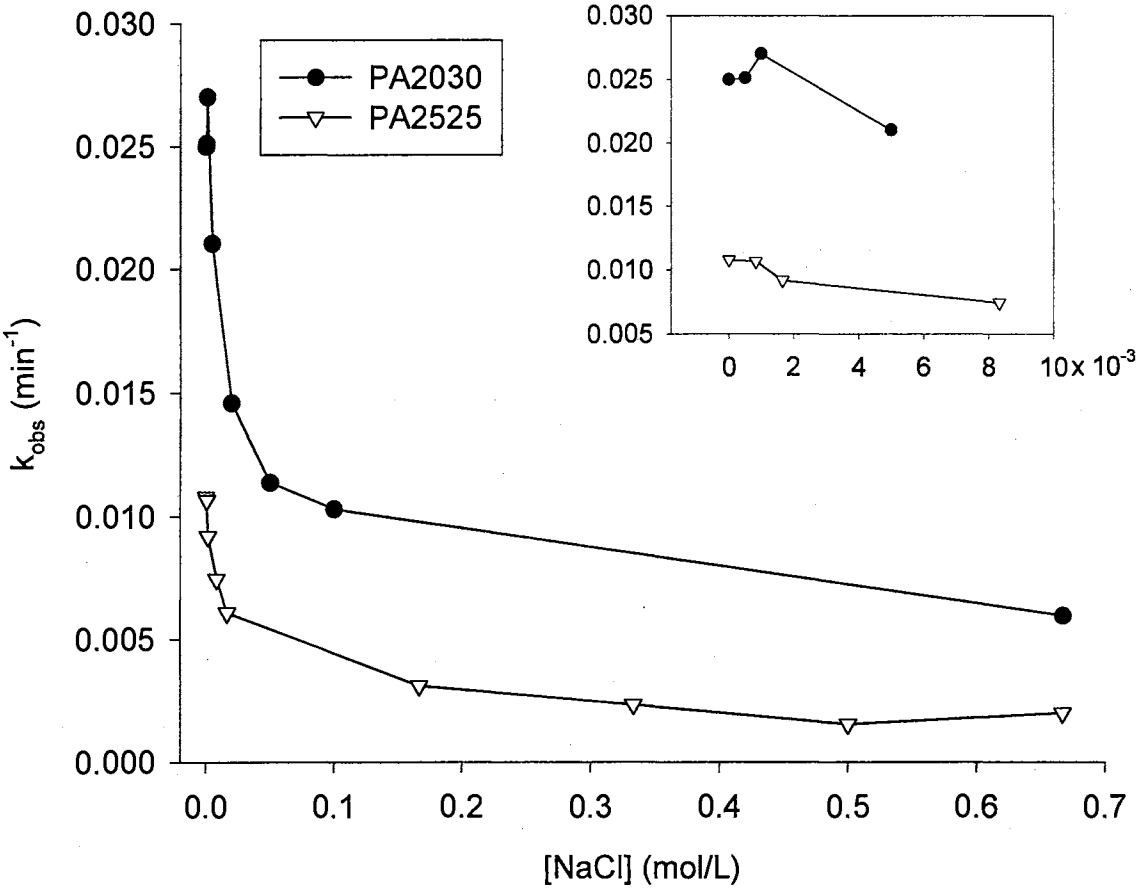

Figure 6. NaCl effect on k_{obs} for PA2525 and PA2030 latexes. PA 2525 is in 2 mM borate buffer (pH = 9.3) and PA2030 is in 2 mM NaOH solution (pH = 11.3) at 30.0 °C.

Table 4. Swelling Ratios at Different NaCl Concentrations.

	Swelling Factor $(d_h/d_n)^3$ at different [NaCl] (M)					
Sample	0	0.005	0.01	0.05	0.10	0.50
2030N	3.5	2.7	2.6	2.5	2.4	2.3
2525N	2.7	2.2	2.1	2.1	2.0	1.9
PA2030	3.6	2.7	2.6	2.5	2.4	2.4
PA2525	4.0	3.1	3.0	2.9	2.8	2.8

Ion Exchange Model. The role of latex particles in decarboxylation kinetics can be analyzed by an ion exchange model (Figure 7). This model is a modification of the pseudophase ion exchange model of micellar catalysis.[41-42] Some assumptions must be made about the ion exchange model: (1) Ion exchange is much faster than chemical reaction, (2) The degree of dissociation of counter ions from the latex is negligible, and (3) No excess substrate anions bind to the latex by nonspecific absorption. Assumptions (2) and (3) are equivalent to an assumption of stoichiometric binding; the charge of anions bound equals the charge of quaternary ammonium ions. Assumption (3) is invalid for a polyamphoyte microgel in NaCl concentrations >0.5 M. The intrapolymer ion-pairs are broken by addition of more NaCl resulting in swelling of the microgel, which indicates anion binding that is not equal to excess quaternary ammonium ions. In the ion exchange model of latex catalysis, the counterion dissociation is neglected, and the latex has a defined volume, not a pseudophase. In a pseudophase, dissociation and association of surfactants are fast compared with the rate of decarboxylation.

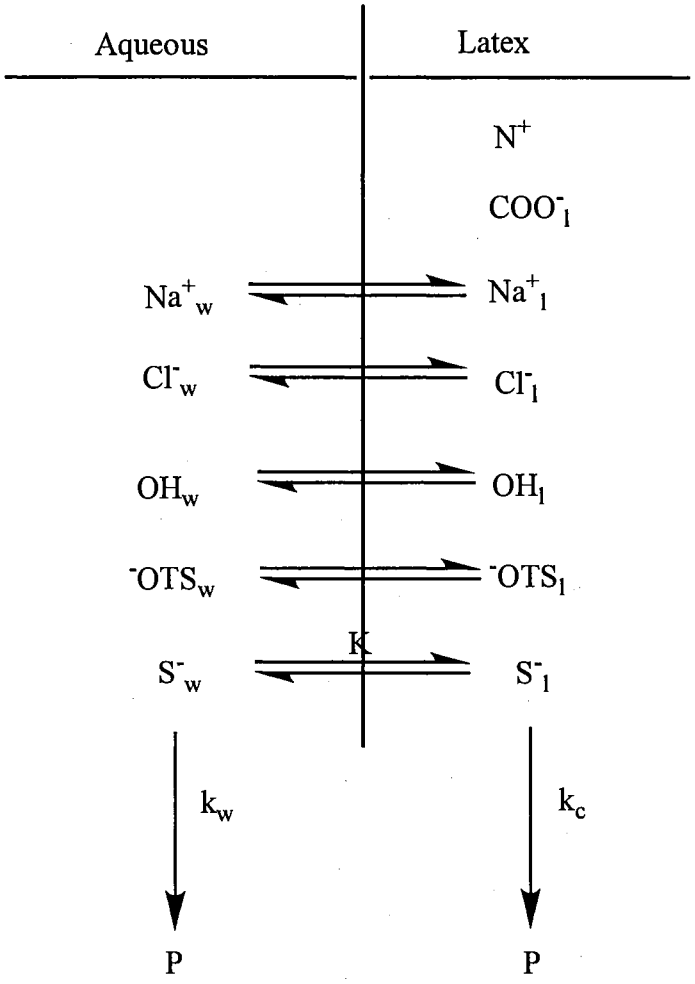

Figure 7. Ion exchange model.

The fundamental equations of the model are a rate equation (2), ion exchange selectivity coefficients $K_{S/Cl}$ (3), $K_{OH/Cl}$ (4), and $K_{S/HOTS}$ (5) and mass balance equations (6) and (8)-(10). Equation (7) is a charge balance equation. All chemical symbols such as S_w represent molar concentrations based on total volume of the dispersion, and subscripts refer to free (w) in the aqueous phase and bound (l) species in the particle phase. k_{obs} is the measured pseudo-first-order rate constant, k_w is the rate constant in the aqueous phase, k_c is the rate constant in the particle phase, and S_T is the analytical concentration of

substrate in the dispersion. This model does not consider buffered solutions but could be extended to include them with appropriate equilibria and mass balances.[40-42]

$$k_{obs} = k_w S_w/S_T + k_c S_l/S_T \quad (2)$$

$$K_{S/Cl} = S_l Cl_w/S_w Cl_l \quad (3)$$

$$K_{OH/Cl} = OH_l Cl_w/OH_w Cl_l \quad (4)$$

$$K_{OTS/Cl} = S_l^- OTS_w/S_w^- OTS_l \quad (5)$$

$$S_T = S_l + S_w \quad (6)$$

$$N^+ = Cl_l + S_l + OH_l + {}^-OTS_l + COO^-_l \quad (7)$$

$$OH_T = OH_l + OH_w \quad (8)$$

$$Cl_T = Cl_o + [NaCl] = Cl_l + Cl_w \quad (9)$$

$$Cl_T = [NaCl] \text{ for polyampholyte} \quad (10)$$

The ion exchange model is needed to understand the effects of salts on decarboxylation reactivity. First, ion exchange is much faster than chemical reaction, so that the latex always contains equilibrium amounts of anions. In ordinary ion exchange with resins >100 μm in diameter, equilibrium of small ions between aqueous and resin phases is reached on a time scale of seconds.[43] Since our particles are 200-230 nm in diameter and rate constants are 3-200 x 10^{-5} s^{-1}, slow ion exchange cannot limit rates of reaction.

The overall result of going from poly(quaternary ammonium) microgel to a polyampholyte microgels is a decrease in available N^+ sites. In previous studies, a decrease in the intraparticle concentration N^+ sites resulted in increased rates due to having a deswollen latex (less water in the particle).[36] The polyampholyte microgels should also be less hydrated due to the intraparticle attractions, which would result in collapsing the particles. The collapsed microgels would provide an environment that would favor rate increases. However, the swelling factors of the two polyampholytes in water are greater than those of quaternary ammonium ion particles (Table 1). A greater water content of the polyampholyte particles decreases the intraparticle rate constant for decarboxylation, as reported in Tables 2 and 3.

The decrease in the relative rates is might be related to the ion exchange selectivity coefficient $K_{OTS/Cl}$ (5). TSO^- in the samples competes with S^-, COO^-, and Cl^- for N^+ sites. The TSO^- has a higher selectivity than Cl^-, which was evident by the lack of chloride in the elemental analysis of the polyamphoytes (Table 4, Chapter III). Furthermore, the chloride anion's selectivity coefficient is less than the substrate anion;[36] therefore, the relative selectivity coefficients are $K_{OTS/Cl} > K_{S/Cl} >> K_{OH/Cl}$. Evaluation of equation (2) shows that the k_{obs} depends on $k_c S_I/S_T$, and comparisons of mol % of anions in Table 2 to S_I/S_T in Table 3 reveals some small trends. The fraction of substrate bound, 0.5 for PA2030 and 0.6 for PA2525, is slightly affected by the amount of PTSA (6 mol% of PTSA for PA2030 compared to 3 mol% for PA2525.

The amount of PTSA in the microgels was within experimental error of the excess amount of N^+ sites (Table 5, Chapter III). This could only mean the remaining N^+ sites were occupied by intramolecular carboxylate anions. Thus, the carboxylate anions have a higher selectivity for the N^+ sites than the PTSA anion. This polyampholyte behavior must account for some of the lower relative rates, and probably repel the substrate resulting in decreasing the partitioning of the substrate in to the particles. However, the fraction of substrate bound, approximately 0.6 for 25/25N and PA2525, is unaffected by the concentration of carboxylate anion (0 mol % carboxylate for 25/25N compared to 23 mol % for PA2525).

Figures 5-6 show a limitation of the ion exchange model. Increased chloride ion concentration should lead to systematic decrease of k_{obs}, as is the case at [NaCl] > 3 mM, if k_c and/or $K_{S/Cl}$ does not vary with NaCl concentration. At low concentrations of added NaCl; however, the k_{obs} actually increases. We attribute the increase in k_{obs} to deswelling of the latexes by the added electrolyte (Table 4). Electrolytes reduce water content of the latex interior and consequently increase k_c. Deswelling is due to osmotic forces and to replacement of the more hydrated hydroxide ion by the less hydrated electrolyte anion in the polymer.[43] Rate maxima with added salts in cationic micelles have also been reported.[6]

Conclusion

Polyampholyte microgels with quaternary ammonium and carboxylate ion exchange sites catalyze the decarboxylation of 6-nitrobenzisoxazole-3-carboxylate (6-NBIC) in aqueous salt dispersions. A catalytic rate constant of 115-60 times the rate constant in water was achieved in particles containing 18/29 and 23/24 mol percent of (-) and (+) repeat units. Decarboxylation kinetics fit both the enzyme model of micellar catalysis and an ion exchange model. Added electrolyte decreases the rate of decarboxylation but increases the intrinsic catalytic rate constants in more highly swollen microgels. Because of colloidal stability of polyampholyte microgels in high concentrations of electrolytes, decarboxylation of 6-NBIC can be monitored at > 0.5 M NaCl. The relative rates of the polyampholyte microgels were lower than the precursor quaternized microgels. The decreased rates could be a polyampholyte effect (carboxylate anions repealing the substrate), but is likely due to having PTSA anions in the latex. Future studies should involve removal of PTSA from the latexes. This can be achieved by salting out the anion with NaCl followed by dialysis and ultrafiltration to remove excess salts.

References

1. Kemp, D. S.; Paul, K. G. *J. Am. Chem. Soc.* **1970**, *92*, 2553.
2. Kemp, D. S.; Paul, K. G. *J. Am. Chem. Soc.* **1975**, *97*, 7305.
3. Kemp, D. S.; Cox, D. D.; Paul, K. G. *J. Am. Chem. Soc.* **1975**, *97*, 7312.
4. Kemp, D. S.; Resczek, j.; Vellaccio, F. *Tetrahedron Lett.* **1978**, *92*, 2553.
5. Bunton, C. A.; Minch, M. J. *Tetrahedron Lett.* **1970**, 3881.
6. Bunton, C. A.; Minch, M. J.; Hidalgo, J.; Sepulveda, L. *J. Am. Chem. Soc.* **1973**, *95*, 3262.
7. Bunton, C. A.; Kamego, A. A.; Minch, M. J.; Wright, J. L. *J. Org. Chem.* **1975**, *40*, 1321.
8. Kunitake, T.; Okahata, Y.; Ando, R.; Shinkai, S.; Hirakawa, S. *J. Am. Chem. Soc.* **1980**, *102*, 7877.
9. Germani, R.; Ponti, P. P.; Savelli, G; Spreti, N.; Cipiciani, A. Cerichelli, G; Bunton, C. A. *J. Chem. Soc. Perkin Trans.* II **1989**, 1767.
10. Engberts, J. B. F. N.; Rupert, L. A. M. *J. Org. Chem.* **1982**, *47*, 5015.
11. Biresaw, G.; Bunton, C. A. *J. Phys. Chem.* **1986**, *90*, 5854.
12. Nusselder, J. J. H.; de Groot, T. J.; Trimbos, M.; Engberts, J. B. F. N. *J. Org. Chem.* **1988**, *53*, 2423.
13. Germani, R.; Ponti, P. P.; Romeo, T.; Savelli, G.; Spreti, N.; Cerichelli, G.; Luchetti, L.; Mancini, G.; Bunton, C. A. *J. Phys. Org. Chem.* **1989**, *2*, 533.
14. Bunton, C. A.; Cowell, C. P.; Nome, F.; Romsted, L. S. *J. Phys. Org. Chem.* **1990**, *3*, 239.
15. Cerichelli, G.; Mancini, G.; Luchetti, L.; Savelli, G.; Bunton, C. A. *J. Phys. Org. Chem.* **1991**, *4*, 71.

16. Nusselder, J. J. H.; Engberts, J. B. F. N. *Langmuir* **1991**, *7*, 2089.

17. Sunamoto, J.; Iwamoto, K.; Nagamatsu, S.; Kondo, H. *Bull. Chem. Soc. Jpn.* **1983**, *56*, 2469.

18. Germani, R.; Ponti, P. P.; Spreti, N.; Savelli, G; Cipiciani, A.; Cerichelli, G; Bunton, C. A. *J. Coll. Interface Sci.* **1990**, *138*, 443.

19. Germani, R.; Savelli, G; Cerichelli, G; Mancini, G.; Luchetti, L.; Ponti, P. P.; Spreti, N.; Bunton, C. A. *J. Coll. Interface Sci.* **1991**, *147*, 152.

20. Suh, J.; Scarpa, I. S.; Klotz, I. M. *J. Am. Chem. Soc.* **1976**, *98*, 7060.

21. Kunitake, T.; Shinkai, S.; Hirotsu, S. *J. Org. Chem.* **1977**, *42*, 306. (c) Suh, J.; Klotz, I. M. *Bioorg. Chem.* **1979**, *8*, 283.

22. Shinkai, S.; Hirakawa, S.; Shimonmura, M.; Kunitake, T. *J. Org. Chem.* **1981**, *46*, 868.

23. Koyama, N.; Ueno, Y.; Sekiyama, Y.; Ikeda, K.; Sekine, Y. *Polymer* **1986**, *27*, 293.

24. Zheng, Y. L.; Knoesel, R.; Galin, J. C. *Polymer* **1987**, *28*, 2297.

25. Yang, Y. J.; Engberts, J. B. F. N.; *J. Org. Chem.* **1991**, *56*, 4300.

26. Yamazaki, N.; Nakahama, S.; Hirao, A.; Kawabata, J.; Noguchi, H.; Uchida, Y. *Polym. Bull.* **1980**, *2*, 269.

27. Tundo, P.; Venturello, P. *Tetrahedron Lett.* **1980**, *21*, 2581.

28. Ueno, Y.; Koyama, N.; Sekine, Y. *Polym. Commun.* **1983**, *24*, 185.

29. Yamazaki, N.; Nakahama, S.; Hirao, A.; Kawabata, J. *Polym. J.*, **1980**, *12*, 231.

30. Shah, S. C.; Smid, J. *J. Am. Chem. Soc.* **1978**, 100, 1426.

31. Smid, J.; Shah, S. C.; Varma, A. J.; Wong, L. *J. Polym. Sci., Polym. Symp.* **1978**, *64*, 267.

32. Smid, J.; Varma, A. J.; Shah, S. C. *J. Am. Chem. Soc.* **1979**, *101*, 5764.

33. Shirai, M.; Smid, J. *J. Polym. Sci., Polym. Lett. Ed.* **1980**, *18*, 659.

34. Lewis, C.; Kramer, T.; Robinson, S.; Hilvert, D. *Science* **1991**, *253*, 1019.

35. Lewis, C.; Paneth, P.; O'Leary, M. H.; Hilvert, D. *J. Am. Chem. Soc.* **1993**, *115*, 1410.

36. Ford, W. T.; Lee, J. J. *J. Org. Chem.* **1993**, *58*, 4070.

37. Borche, W. *Chem. Ber.* **1909**, *42*, 1316.

38. Lindemann, H.; Cissee, H. *Liebigs. Ann. Chem.* **1929**, *469*, 44.

39. Experimental given in Chapter III.

40. Menger, F. M.; Portnoy, C. E. *J. Am. Chem. Soc.* **1967**, *89*, 4698.

41. Quina, F. H.; Chaimovich, H. J. *J. Phys. Chem.* **1979**, *83*, 1844.

42. Romsted, L. S.; *in Surfactants in Solution*, Mittal, K. L.; Lindman, B., Eds. Plenum: New York, 1984, pp 1025-1068.

43. Helfferich, F. *Ion Exchange*; McGraw-Hill: New York, 1962; pp 100-125 and 250-319.

APPENDIX

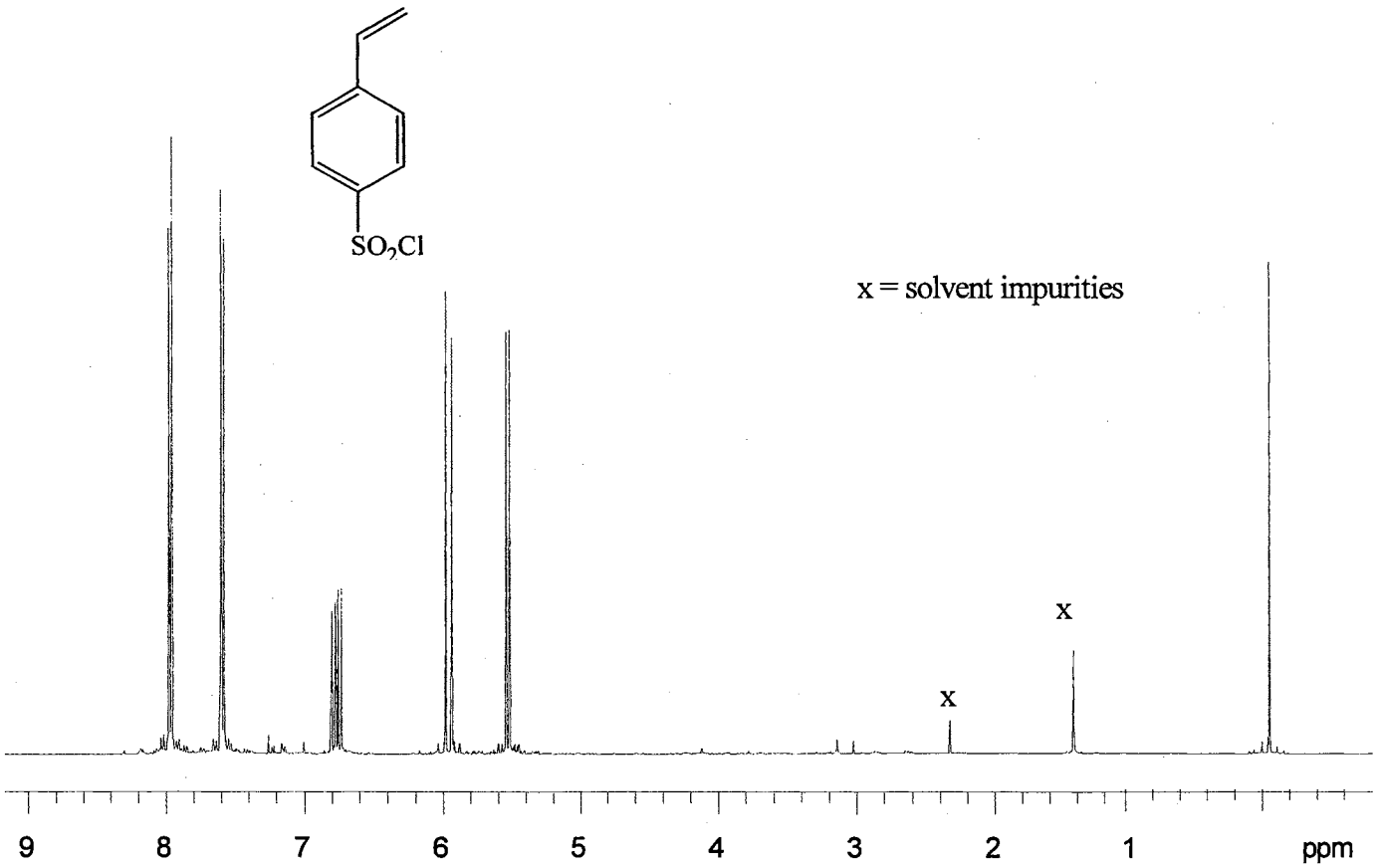

Figure 1. ^{1}H-NMR spectrum of *p*-styrenesulfonyl chloride (SSC).

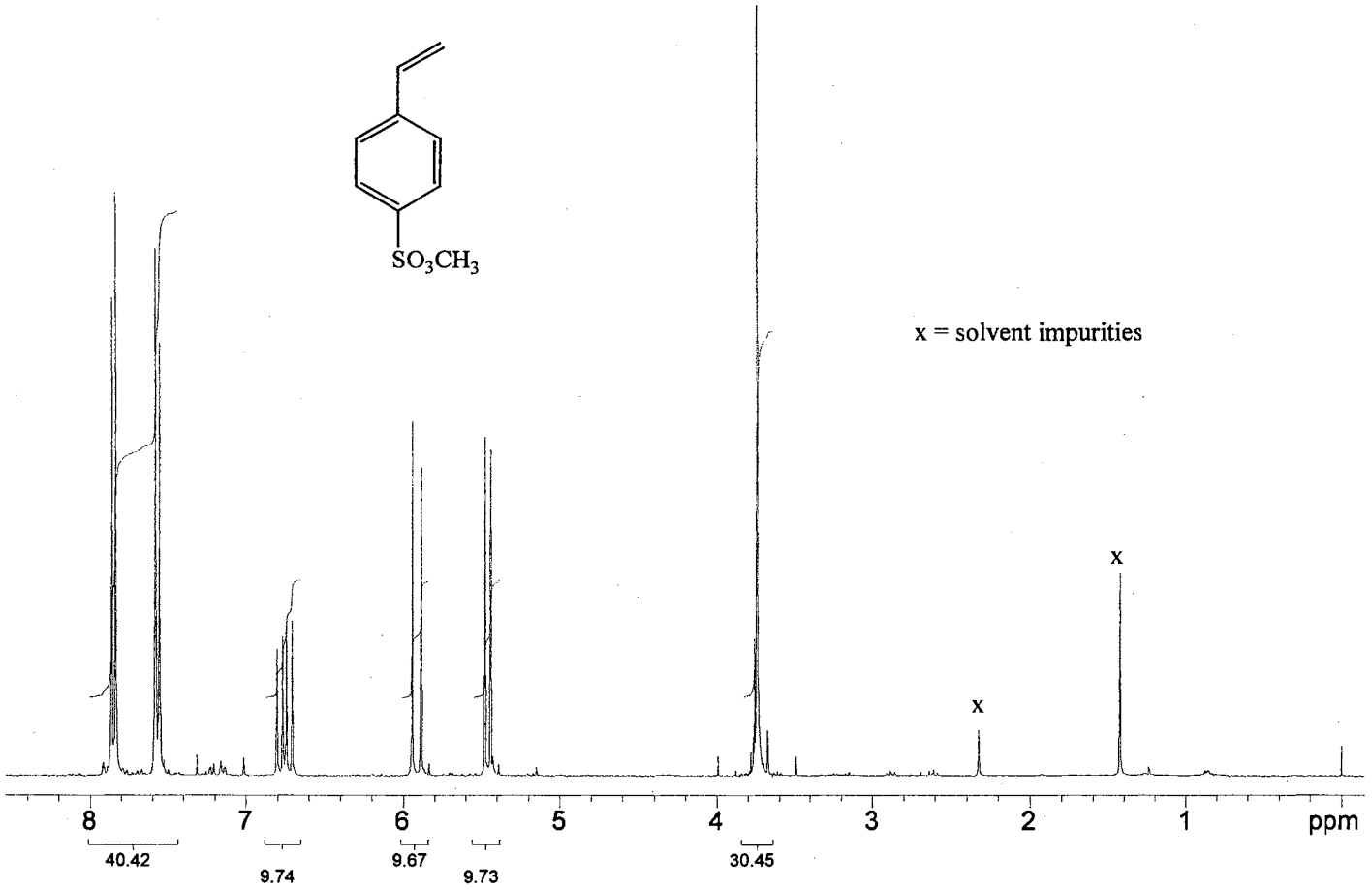

Figure 2. ^{1}H-NMR spectrum of methyl *p*-styrenesulfonate (MSS).

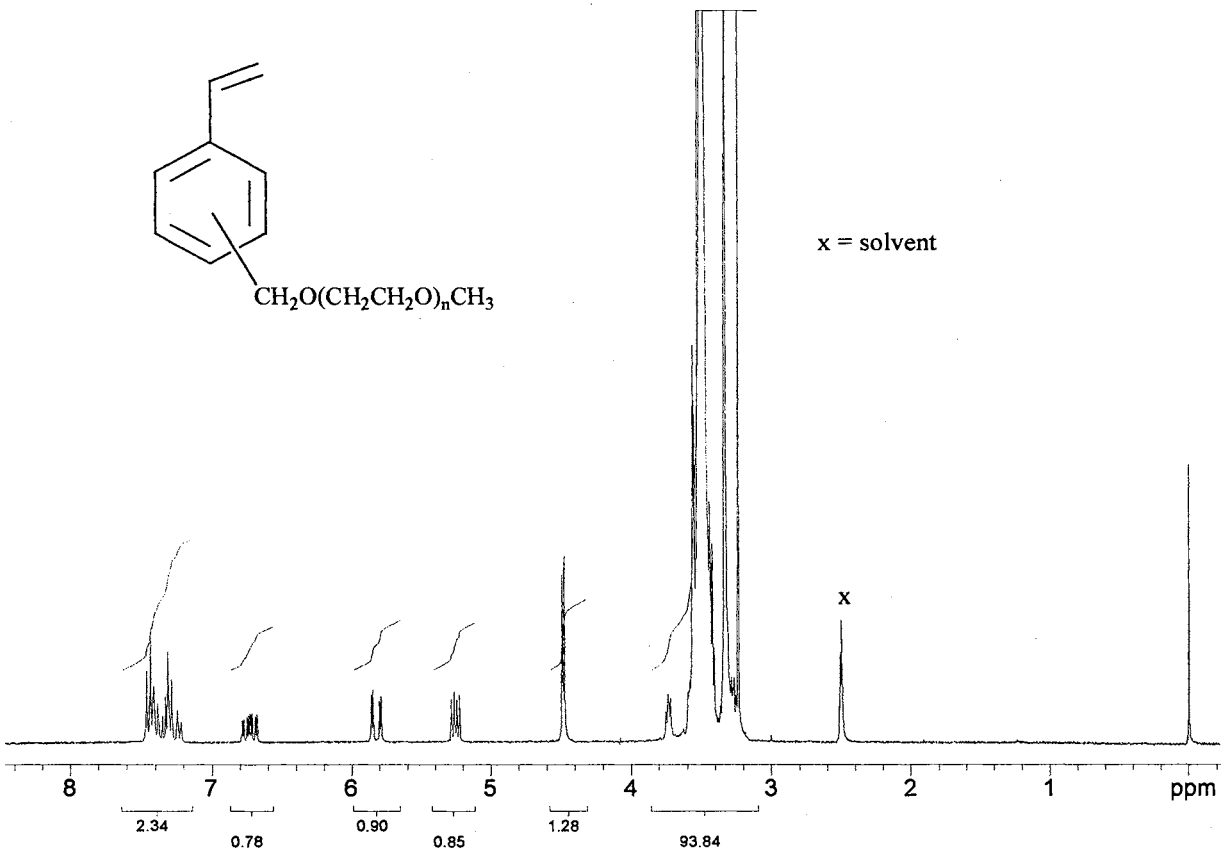

Figure 3. ^{1}H-NMR spectrum of *m,p*-vinylbenzyl methoxy poly(ethylene gycol).

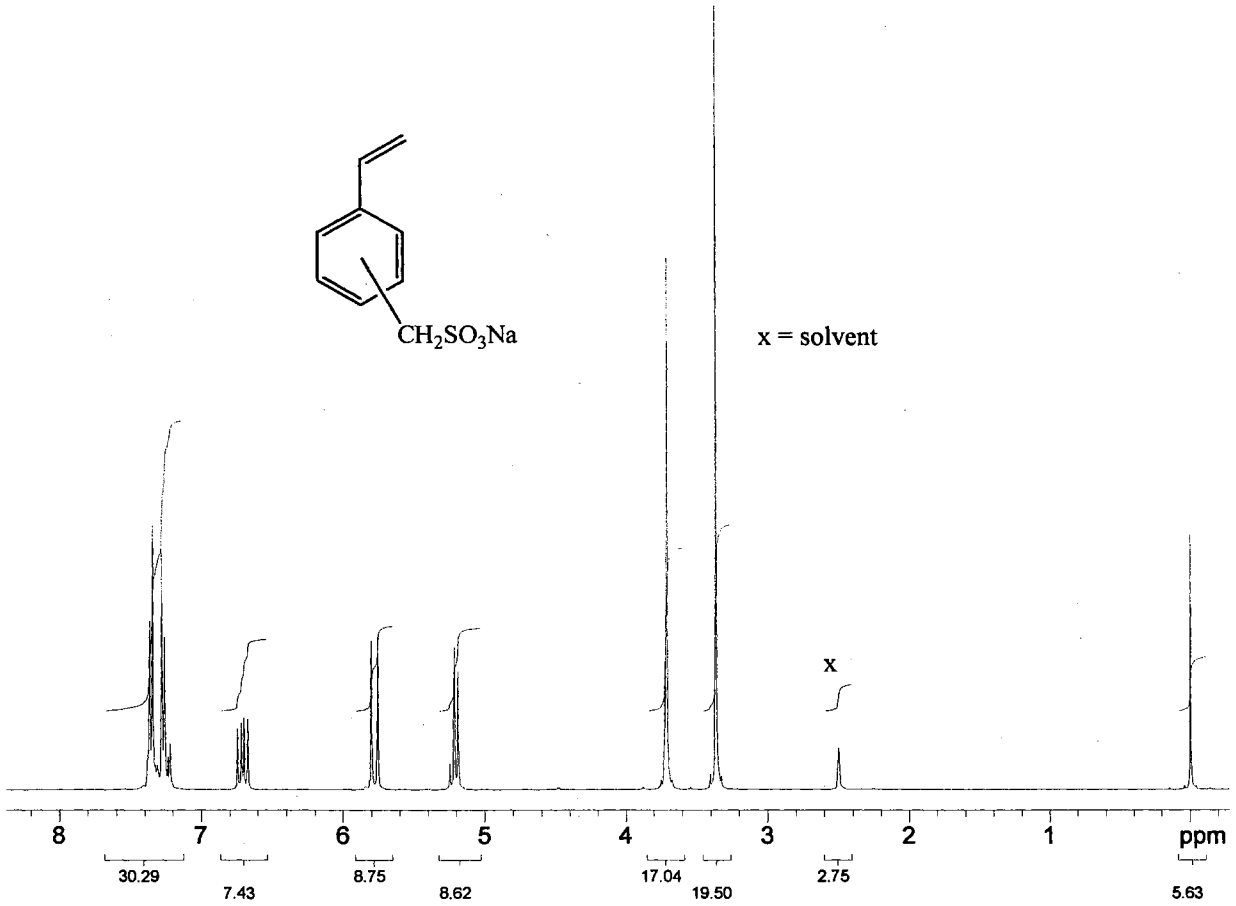

Figure 4. ^{1}H-NMR spectrum of sodium *m,p*-vinylbenzylsulfonate (NaVBS).

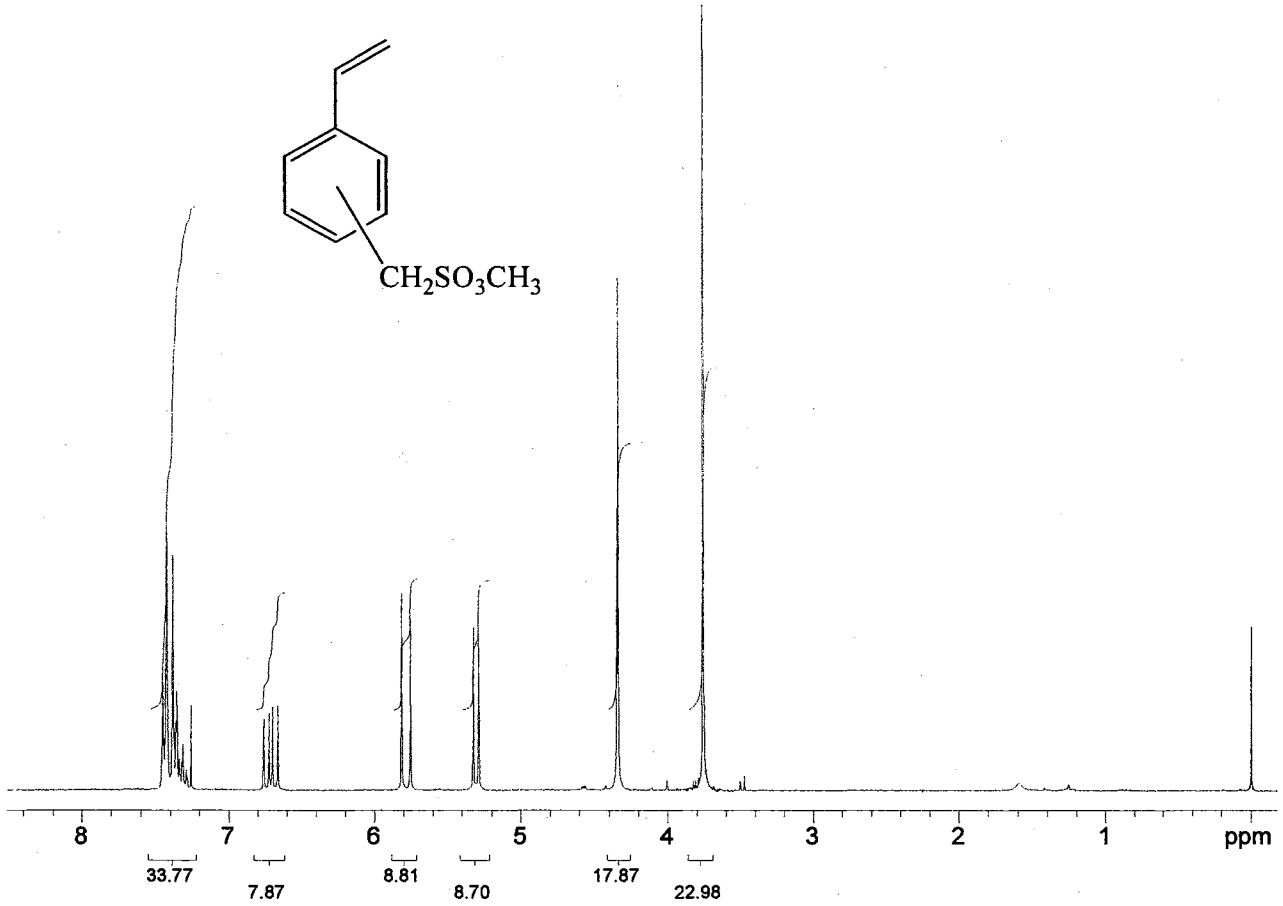

Figure 5. ^{1}H-NMR spectrum of methyl *m,p*-vinylbenzylsulfonate (MVBS).

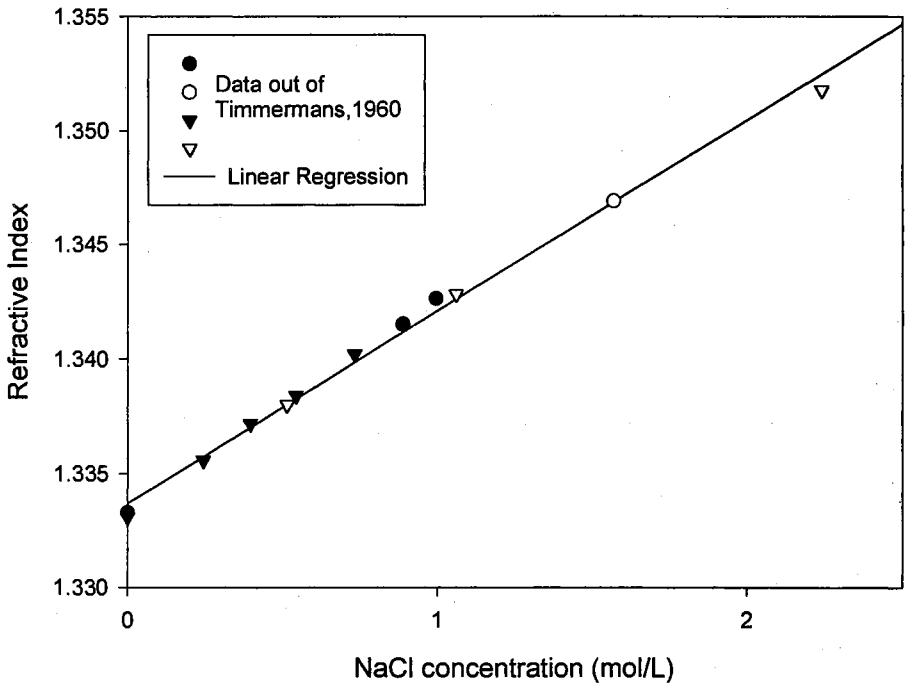

Figure 6. Refractive Index vs [NaCl] at 20.0 °C. (Timmermans, J. *The Physico-Chemical Constants of Binary Systems in Concentrated Solutions*; Interscience Publishers, Inc.; NewYork, 1960, pp303-341).

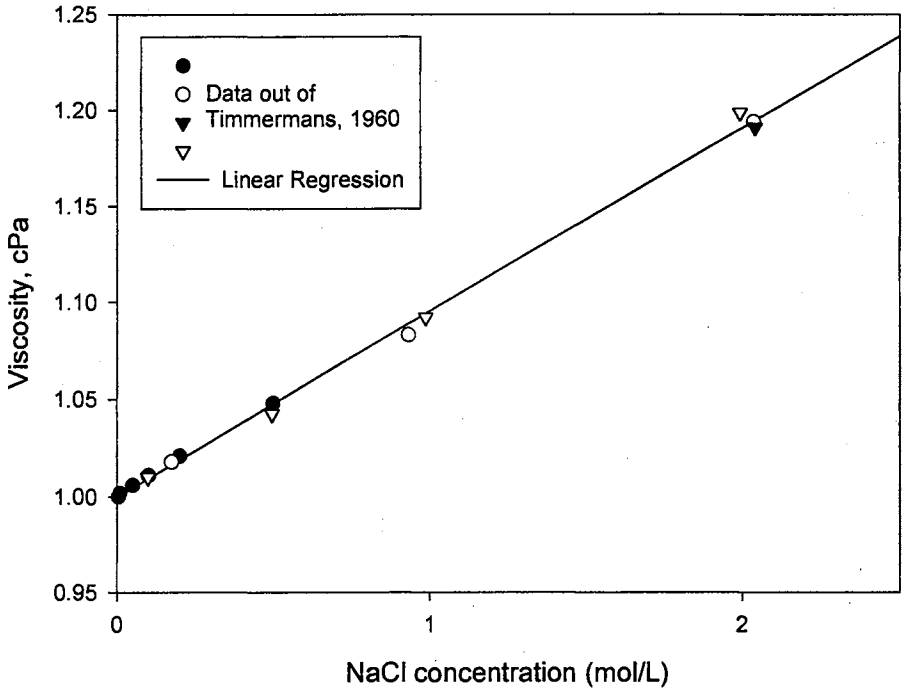

Figure 7. Viscosity vs [NaCl] at 20.0 °C.
(Timmermans, J. *The Physico-Chemical Constants of Binary Systems in Concentrated Solutions*; Interscience Publishers, Inc.; NewYork, 1960, pp303-341).

Table I. Chemical Composition supplied by AQUARIUM SYSTEMS for INSTANT OCEAN ® salt (solution at approx. salinity of 34 ppt)[a]

ION	CONCENTRATION (mg/L)
Chloride	19251
Sodium	10757
Sulfate	2659
Magnesium	1317
Potassium	402
Calcium	398
Carbonate/Bicarbonate	192
Strontium	8.6
Boron	5.6
Bromide	2.3
Iodide	0.22
Lithium	0.18

[a] Trace amounts (0.05 > 0.0002 mg/L): Copper, Iron, Nickel, Zinc, Manganese, Molybdenum, Cobalt, Vanadium, Selenium, Floride, Lead, Arsenic, Cadmium, Chromium, Aluminum, Tin, Antimony, Rubidium and Barium. Does not contain Mercury, Nitrate or Phosphate.

Sample Calculation for Elemental Analysis of 25/25N Microgel Presented in Chapter III, Table 3.

Assume excess oxygen content, in the experimental results, is off by the wt% of H_2O.

Experimental %O = 9.71
Calculated %O = 5.69

Therefore, we must account for 4.02 % of oxygen from H_2O.

%H from H_2O = 4.02 %O * 2g H/ 16 g O = 0.503%
Thus, %H= 8.59-0.503 = 8.0875%

% H_2O in sample 4.02 %O * 18 g H_2O/ 16 g O = 4.52%

% polymer in sample = 100- 4.52 = 95.48%

As a result,

Element	experimental	conversion factor (100 g/95.48 g)	experimental-water
C	74.04		77.55
H	8.09		8.47
Cl	5.32		5.57
N	2.34		2.45
O	9.71		5.96

VITA

Kenneth Wayne Hampton Jr.

Candidate for the Degree of

Doctor of Philosophy

Thesis: SYNTHESIS AND CHARACTERIZATION OF POLYAMPHOLYTE MICROGELS

Major Field: Chemistry

Biographical:

Personal Data: Born in Wynne, AR, USA, March 4, 1971, the son of Jana and Dale Wood.

Education: Graduated from Eufaula High School, Eufaula, Oklahoma, in May, 1989; received Bachelor of Science (B.S.) Degree in Chemistry from Northeastern State University, Tahlequah, Oklahoma in May, 1993; completed requirements for the Doctor of Philosophy Degree at Oklahoma State University in July, 1999.

Professional Experience: Teaching and Research Assistant, Department of Chemistry, Oklahoma State University, August, 1993, to May, 1999.

Professional Memberships: American Chemical Society, Phi Lambda Upsilon.